SIMULATING THE IMPACT OF AGRI-SILVICULTURE ON THE FUTURE CLIMATE OF WEST AFRICA

OLUSEGUN, CHRISTIANA FUNMILOLA

(MET/00/5447)

(B.Tech., M.Tech)

A THESIS

IN THE DEPARTMENT OF METEOROLOGY AND CLIMATE SCIENCE IN PARTNERSHIP WITH THE WEST AFRICAN SCIENCE SERVICE CENTRE ON CLIMATE CHANGE AND ADAPTED LAND USE (WASCAL) SUBMITTED TO THE SCHOOL OF POSTGRADUATE STUDIES, IN PARTIAL FULFILLMENT OF THE REQUIREMENT FOR THE AWARD OF THE DEGREE OF DOCTOR OF PHILOSOPHY IN METEOROLOGY AND CLIMATE SCIENCE OF THE FEDERAL UNIVERSITY OF TECHNOLOGY, AKURE, ONDO STATE IN NIGERIA

MAY, 2016

CERTIFICATION

a) By the student:

This work has not been presented elsewhere for the award of a degree, or any other purpose.

Candidate's Name: OLUSEGUN, Christiana Funmilola

Signature:……. Date:…….

b) By the Supervisor (s):

I certify that this work has been carried out by Mrs. OLUSEGUN, Christiana Funmilola under my supervision and that to the best of my knowledge, it has not been submitted elsewhere for the award of a degree.

Supervisor's Name:

Major Supervisor: Prof. P.G. Oguntunde

Signature:…… Date:……

Co-supervisor: Dr. E.O. Gbobaniyi

Signature:…… Date:……

ACKNOWLEDGEMENTS

This is to appreciate the German Ministry of Education and Research (BMBF) through the West African Science Service Centre on Climate Change and Adapted Land Use (WASCAL) for the research grant received to successfully carry out this research. I sincerely thank the Executive Director and staff of WASCAL Head Office, Accra, Ghana for their support towards the successful completion of my study.

My deepest gratitude goes to my supervisors, Prof. P.G. Oguntunde and Dr. E.O. Gbobaniyi for the invaluable guidance, patience, support and motivation received during my research. Similarly, my sincere appreciation goes to Dr. B.J. Abiodun, my host at the Climate System Analysis Group (CSAG) of the University of Cape Town (UCT) South Africa for the provision of High-Performance Computing facilities used for the numerical experiments. The technical guidance on model set-up received from Graziano Giuliani, a scientific staff at the Abdus Salam International Centre for Theoretical Physics (ICTP), contributed to the successful completion of all my numerical experiments. Similarly, Phillip Mukwenha, a member of CSAG group at UCT is highly appreciated for his technical assistance in the High Performing Computing section. My sincere appreciation goes to the ex-Director, Prof. J.A. Omotosho and incumbent Director of WASCAL, Prof. K.O. Ogunjobi for their motivation during this PhD program. Similarly, the motivation and support received from the Head of the Department of Meteorology and Climate Science, Dr. E.C. Okogbue cannot be quantified. My special thanks to Dr. V.O. Ajayi (Deputy Director, WASCAL), Prof. A.A. Balogun and the entire staff of WASCAL and Meteorology & Climate Science Department for their contributions towards the successful completion of this degree. My profound gratitude goes to Prof. A. B. Rabiu, Prof. Mrs. I. A. Fuwape, Dr. Ulrich, Dr. Mounkaila, Mira, Romaric, Mrs. Abiodun, Dr. and Mrs. K. Lawal, Mr and Mrs. Egbebiyi, Mr. and Mrs. Arowolo for their support and encouragement throughout the duration of the program.

I sincerely appreciate my parents, Elder and Evang. (Mrs.) E.A. Talabi, brother, Engr. S.I. Talabi and my in-laws Mr. and Mrs. Dare Olusegun for the understanding, support, mentorship and care received throughout each stage of my academic pursuit. Finally, special thanks to my best friend and loving husband for his understanding, motivation, support and care. His persistent encouragement has brought me this far. Thank you, sweetheart.

DEDICATION

This work is dedicated to the Almighty God and my Lord and Savior Jesus Christ. To Him be all the glory because He is Alpha and Omega, the One who was, and is, and is to come. Blessed be the name of the Lord.

ABSTRACT

The study investigated the influence of agri-silviculture on the projected future climate in West Africa using regional climate model (RegCM4). The performance of the model in the representation of surface processes over West Africa was evaluated and validated. Thereafter, the future climate change over West Africa was projected using the validated model. Investigation of the influence of different percentages cover of trees/shrubs and crops on the future climate of West Africa was also examined.

Eleven numerical agri-silviculture experiments with time-invariant vegetation and dynamic vegetation were used to simulate the historical and future climates of West Africa. The first three experiments simulated the historical climate of West Africa from 1979-2004 using time-invariant vegetation (PRES), dynamic vegetation in a smaller Africa domain (PRESd1) and dynamic vegetation in a larger Africa domain (PRESd2). The next three experiments projected the future climate from 2029-2054 with time-invariant vegetation (FUTU), dynamic vegetation in a smaller Africa domain (FUTUd1), dynamic vegetation in a larger Africa domain (FUTUd2). The next experiments were carried out using different percentages cover of trees/shrubs and crops along Guinea Savanna zone using time-invariant vegetation (GUSAG), dynamic vegetation in a smaller Africa domain (GUSAGd1) and larger Africa domain (GUSAGd2) in order to represent agri-silviculture. The last two agri-silviculture experiments were carried out along the West Africa coast using time-invariant vegetation (COAG) and dynamic vegetation (COAGd1). All future climate experiments were carried out under Representative Concentration Pathways 4.5 Scenario (RCP4.5). Model performance was evaluated by comparing historical climate simulations with gridded Climate Research Unit (CRU) datasets and Era-Interim reanalysis atmospheric data products.

Generally, the historical simulation reproduces the seasonal evolution of precipitation and temperature regimes very well with correlations greater than 0.8 but with a cold and wet bias of 1 -

2°C and 1 mm/day respectively. However, a narrow monsoon flow and weaker Jets were simulated in August. Widespread warming is projected in the near future across most parts of West Africa which range from an increase of 0.5°C along the coastal and orographic regions from June to August with an increase of more than 1.5°C over the continent in other seasons. Other parts of West Africa were projected to have positive/negative changes in precipitation not exceeding 1 mm/day during the monsoon and post monsoon seasons. The impact of the different simulated agri-silviculture experiments on the future climate of West Africa varied. The GUSAG experiment induces cooling of about 0.5 - 2°C over most areas along the agri-silviculture zone (Nigeria, Ghana, Cote d'Ivoire and Cameroon, Togo, Benin Republic and Ghana) in all seasons. However, the induced cooling does not necessarily translate to more precipitation, except over Ghana where precipitation increases by 0.5 - 1.8 mm/day during MAM and JJA seasons. On the other hand, GUSAG experiment enhances the warming over Liberia and Sierra Leone by about 2°C in all seasons, which intensifies the drying condition to about 1.8 mm/day. The GUSAG*d2* experiment induces cooling of about 2°C in areas within 8°E and 16°E along the agri-silviculture zone in all seasons but increases the warming by more than 0.5°C outside this area. Generally, agri-silviculture practice along the coast (COAG and COAG*d1*) does not necessarily have a large-scale impact on temperature and precipitation over the entire West Africa region.

The study concluded that agri-silviculture could be used to mitigate the projected future warming and drying across most West African countries except Liberia and Sierra Leone. Therefore, it is recommended that agri-silviculture practice should be adopted as a land-based strategy to combat food insecurity, deforestation due to agricultural expansion and ameliorate the impacts of climate change in West Africa.

TABLE OF CONTENTS

LIST OF TABLES

LIST OF FIGURES

LIST OF ACRONYMS

AR4	Fourth Assessment Report of IPCC
AR5	Fifth Assessment Report of IPCC
AEJ	African Easterly Jet
AEWs	African Easterly Waves
AOGCM	Atmosphere-Ocean Global Climate Model
CCM3	Community Climate Model
CDM-AR	Clean Development Mechanism for Afforestation
CLM3.5	Community Land Model version 3.5
CLM4.5	Community Land Model version 4.5
CLM4.5-DV	Community Land Model version 4.5 Dynamic Vegetation enabled
CMIP5	Fifth Phase of the Coupled Model Intercomparison Project
CORDEX	Coordinated Regional Climate Downscaling Experiment
CRU	Climate Research Unit
DJF	December, January and February
ECMWF	European Center for Medium-Range Weather Forecast
FAO	Food and Agriculture Organization of the United Nation
GCMs	Global Climate Models
HadGEM2-ES	Hadley Centre Global Environmental Model version 2- Earth System
IBRD	International Bank for Reconstruction and Development
ICRAF	International Centre for Research in Agroforestry
ICTP	International Center for Theoretical Physics
IPCC	Intergovernmental Panel on Climate Change
ITCZ	Inter-Tropical Convergence Zone
ITD	Inter-Tropical Discontinuity
JJA	June, July and August
LULCC	Land Use Land Cover Change

MAM	March, April and May
MB	Mean Bias
MCSs	Mesoscale Convective Systems
NCAR	National Center for Atmospheric Research
PFTs	Plant Functional Types
PCC	Pattern Correlation Coefficient
RCMs	Regional Climate Models
RCP	Representative Concentration Pathway
RegCM4	Regional Climate Model version 4
RF	Radiative Forcing
RMSD	Root Mean Square Difference
SON	September, October and November
SUBEX	Subgrid Explicit Moisture Scheme
TEJ	Tropical Easterly Jet
UNFCCC	United Nations Framework Convention on Climate Change
WMO	World Meteorological Organization

CHAPTER ONE

INTRODUCTION

1.1 Background

Climate is statistically described in terms of the mean and variability of relevant quantities (e.g. temperature, precipitation and wind) over a period of time ranging from months to thousands or millions of years (Le Treut *et al.*, 2007). The classical period is 30 years, as defined by the World Meteorological Organization (WMO). Major components of the climate system are the atmosphere, cryosphere, land surface and the biosphere (see Fig. 1.1). These five components interact in such a way that causes the climate system to change continually. The changes in these components can be due to natural and anthropogenic factors which causes perturbations in the Earth's radiation budget. The perturbations produce a radiative forcing (RF) which in turn affects the Earth's climate. RF is the net change in the energy balance of the Earth system due to some imposed perturbation. It is usually expressed in watts per square meter (W m^{-2}) averaged over a particular period and quantifies the energy imbalance that occurs when the imposed change takes place.

The Intergovernmental Panel on Climate Change report (IPCC, 2007a) defines climate change as a change in the state of the climate that can be identified (e.g. using statistical tests) by changes in the mean and/or the variability of its properties, and that persists for an extended period, typically decades or longer. According to the report, climate change may be due to natural internal processes (e.g. volcanic eruptions and solar variations) or external factors such as persistent changes to the atmosphere or land use. However, The United Nations Framework Convention on Climate Change (UNFCCC, 1995), refers to climate change

as a change of climate that is attributed directly or indirectly to human activity that alters the composition of

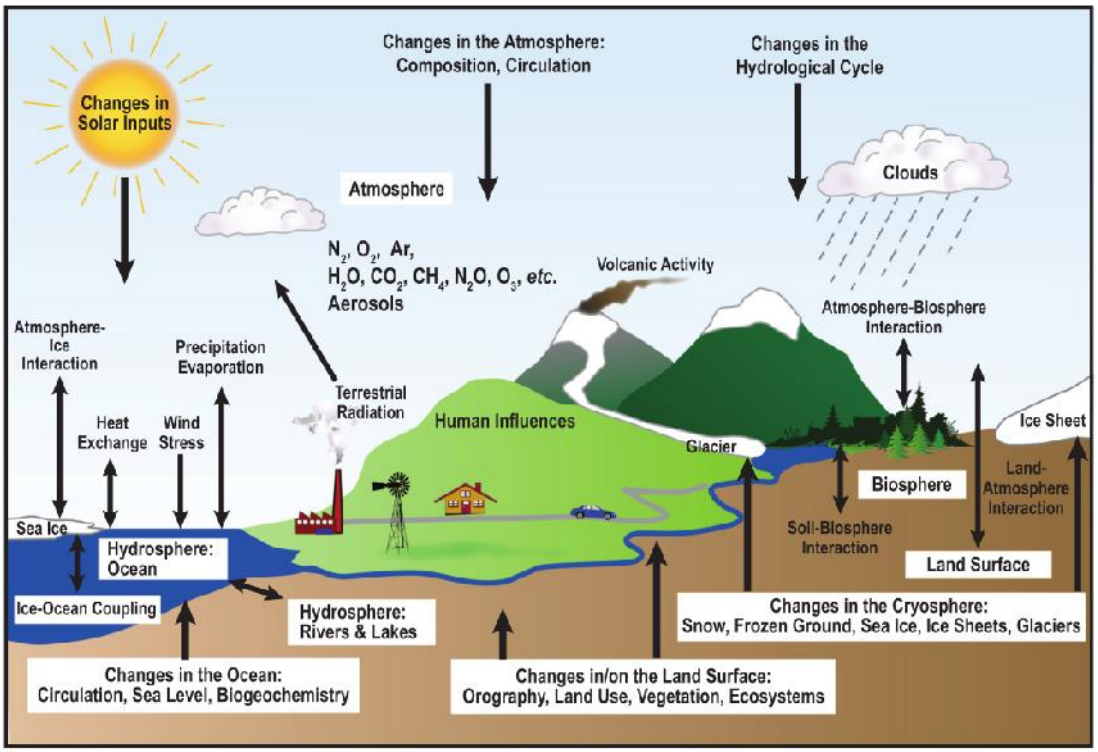

Fig. 1.1: Schematic view of the components of the climate system, their processes and interactions. (Source: Le Treut *et al.*, 2007)

the global atmosphere and that is in addition to natural climate variability observed over comparable time periods. The difference between the IPPC and UNFCCC definitions of climate change is that UNFCCC focuses only on human activity which alters the composition of the global atmosphere and excludes other human activity effects such as changes in the land surface. The increase in atmospheric concentration of greenhouse gases would result in an increase in global temperature but an increase in atmospheric aerosols would decrease global temperature. However, with changes in the land cover, there could be an increase or a decrease in local temperature.

A climate projection is a climate simulation that extends into the future based on a scenario of future external forcing (Kirtman *et al*., 2013). It differs from climate prediction or climate forecast which gives a statement about the future evolution of some aspect of the climate system encompassing both forced and internally generated components. Climate predictions do not attempt to forecast the actual day-to-day progression of the system but instead the evolution of some climate statistic such as seasonal, annual or decadal averages or extremes, which may be for a particular location, or a regional or global average. The Fifth Assessment Report (AR5) of the IPCC used four new scenarios for future emissions of important gases and aerosols referred to as Representative Concentration Pathways (RCP; Taylor *et al*., 2012; Cubasch *et al*., 2013). The four RCP scenarios which are RCP2.6, RCP 4.5, RCP6.0 and RCP 8.5 represent an approximate value of RF (in W m^{-2}) at 2100 or at stabilization after 2100 in their extensions, relative to pre-industrial (Moss *et al*., 2010) period. These scenarios describe the response of future climate to idealized greenhouse gases (GHGs) and aerosols forcing (Meinshausen *et al*., 2011) and are archived in the Climate Model Intercomparison Project (CMIP5; Van Vuuren *et al*., 2011). Listed below is a brief description of each of the four scenarios:

- RCP2.6 assumes a limit on the increase in global mean temperature. This will likely be in the 5 to 95% range of 0.3°C to 1.7°C for 2081–2100, relative to 1986–2005. The RF of this trajectory peaks at 3.0 W m^{-2} (approximately 490 ppm CO_2 equivalent) and then declines to 2.6 W m^{-2}.

- RCP4.5 assumes a limit in the 5 to 95% range of global temperature to be 1.1°C to 2.6°C for 2081–2100 relative to 1986–2005. It is a scenario of long-term, global emission of greenhouse gases, short-lived species and land-use-land-cover which stabilizes RF at 4.2 W m^{-2} (approximately 650 ppm CO_2 equivalent) after 2100.

- RCP6.0 stabilizes after 2100 at 6.0 W m^{-2} with a limit of the 5 to 95% range of global temperature to be 1.4°C to 3.1°C.

- RCP8.5 is a high greenhouse gas scenario which reaches 8.3 W m^{-2} in 2100 on a rising trajectory.

1.2 Statement of Research Problem

African forests constitute only 16 percent of the world's total but the rate of deforestation in Africa is more than six times the world's average (FAO, 2009). Increasing rates of deforestation and land degradation in West Africa has contributed immensely to increase in atmospheric concentration of greenhouse gases and food insecurity in the region. The need to address the challenge of food insecurity as well boost the economic situation of the region necessitate conversion of forests to agricultural lands for large-scale farming or for a developmental purpose such as urbanization. It is estimated that 23 percent of all land in Africa is covered by forest (FAO, 2012). Approximately ten percent of the total forest area in Africa was reported to have been converted to other uses such as agricultural purpose, wood

fuel, building and construction between 1990 and 2010 (FAO, 2012). For instance, the rate of deforestation in Nigeria increased from 2.7 % in 1990 - 2000 to about 3.3 % in 2000 - 2005, with less than 12.2 % of forested land in the country left (FAO, 2009). Similarly, Ghana loses an average of 115, 000 hectares of forest annually, which correspond to 2.0 % of the country's land. The estimated rates of deforestation in Niger is 3.7 % annually as at the year 2000 while Burkina Faso has a lower deforestation rate of 0.2 %. Generally, across West Africa, annual deforestation rate is estimated to be 1.17 % of its total land annually with about 12 million hectares of tropical forest in the last fifteen years (FAO, 2009). The estimates of deforestation rates for the period 2005-2010 in Togo, Nigeria, Ghana, Liberia, Benin, Guinea, Guinea Bissau, Liberia, Sierra Leone and Cameroon are 5.75 %, 4 %, 2.19 %, 0.68 %, 1.06 %, 0.54%, 0.49 %, 0.68 %, 0.70 % and 1.07 % respectively (FAO, 2010). However, most recent global estimates of carbon emissions from deforestation suggest a decrease of over 25 % for the period 2001 - 2010 when compared to 2011 - 2015 (FAO, 2015). On the other hand, CO_2 emissions from forest degradation have increased from 0.4 Gt CO_2 per year in the 1990s to 1.0 Gt CO_2 per year in 2011-2015 (FAO, 2015).

1.3 Aim and Objectives

The aim of the study is to investigate the influence of agri-silviculture on the projected future climate in West Africa. Therefore, the specific objectives of this study are to:

i. evaluate and compare the performance of International Centre for Theoretical Physics (ICTP) Regional Climate Model version 4 (RegCM4) in the representation of surface processes over West Africa;
ii. project the future climate change over West Africa using the validated model;

iii. investigate the proportion of deciduous trees and agricultural crops suitable for climate adaptation and mitigation purposes over West Africa; and

iv. investigate the impact of agri-silviculture on the future climate in West Africa.

1.4 Justification of the Study

Although Africa continues to have the highest net loss of forest, the net emissions from African forest are reported to have decreased over the period 1990-2015 from an average of 3.9 to an average of 2.9 Gt of CO_2 per year (FAO, 2010). This may be attributed partly to the large-scale planting of trees which increases substantially by about 5 million hectares per year during the period 2005-2010 (FAO, 2010). However, forestry projects executed in semi-arid regions like the Savanna often resulted in higher transpiration than the available precipitation. This causes the unsustainable use of groundwater and increased salinity. Therefore, re-vegetation in West Africa using agroforestry practices which utilize plant species that can adapt and mitigate against future climate disturbances in the region is highly important.

In the humid tropical region, the carbon sink potential of agroforestry is well established but little is known about agroforestry carbon stocks in the arid region (Rhodes *et al*., 2014) or how it will influence the future climate of West Africa. Benefits derived from the conversion of agricultural land to agroforestry include enhanced soil fertility, resilience to weather extremes, additional sources of income among many others (Ajayi *et al*., 2007). It has been projected that future increase in atmospheric concentration of CO_2 would favour woody plants (Ainsworth and Long, 2005) while a warming would favour herbaceous species (Epstein *et al*., 2002) in North and South America. However, the rates of photosynthesis and biomass production of C3 plants would be enhanced with increased concentration of atmos-

pheric CO_2 but C4 plants will be more abundant in the tropical region with increased temperature. Most agricultural crops such as rice, wheat, soya beans and other tree crops (e.g. oranges, grapes, coffee etc.) are C3 plants while grasses and other agriculturally important crops such as maize, sugar cane, millet and sorghum are examples of C4 plants. Deciduous trees exhibit decreased competition with crops, increased water use efficiency and enhanced stream flow when compared to the evergreens (Muthuri *et al*., 2004). Hence, during critical dry seasons of water shortages, deciduous trees consume less water than evergreens. Therefore, this study attempts to investigate the effect of changes in percentage cover of deciduous trees, C3 plants and C4 plants on West Africa future climate. This will increase our understanding of the influence of large-scale implementation of agri-silviculture practice on the projected climate of West Africa.

1.5 Contribution to Knowledge

This research has:

i. improved our understanding of the effects of agri-silviculture practices on the future climate of West Africa;
ii. established the feasibility of ameliorating the projected enhanced warming over the region; and
iii. provided decision support information to policymakers for strategic planning of West African agricultural landscape for sustainable agro-ecosystem functioning and productivity in the near future.

CHAPTER TWO

LITERATURE REVIEW

2.1 Historical Climate of Africa

The continent of Africa is one of the most vulnerable to the impacts of climate change due to its low adaptive capacity and persistent poverty (Berenter, 2012; Niang *et al*., 2014). Widespread warming has been observed over most parts of the continent (Seneviratne *et al*., 2012) and is most likely to continue to increase in future. The observed near-surface temperature has increased by 0.5°C or more during the last 5-10 decades over most parts of Africa (Collins, 2011; Nicholson *et al*., 2013). The observed warming is associated with an anthropogenic increase in greenhouse gas (Stott *et al*., 2010). Similarly, over the last 5 decades near surface temperatures have increased significantly across West Africa and the Sahel region. For instance, increase in a number of warm days and warm night between 1961 and 2000 was reported by New *et al*. (2006). Also, between 1970 and 2010, remotely sensed data shows significant warming which ranges from 0.5°C and 0.8°C over most parts of West Africa (Collins, 2011).

The rate of projected future warming over Africa is expected to be higher than the global rate in the 21st century (Sanderson *et al*., 2011; James and Washington, 2013). However, in West Africa, this is most likely to occur 1 to 2 decades earlier between the late 2030s to early 2040s (Mora *et al*., 2013). This is probably due to the natural climate variability in the region which generates narrow climate bounds that can be easily overcome by any relatively small changes in the climate system. Towards the end of the 21st-century temperature projection over West Africa using Global Climate Models and Regional Climate Models ranges

between 3°C and 6°C for both RCP4.5 and RCP8.5 scenarios (Mariotti *et al*., 2011; Diallo *et al*., 2012; Vizy *et al*., 2013).

The absence of sufficient observing stations in Africa poses a great difficulty in assessing trends in annual precipitation over the past century. Hence, there is no uniformity among the various observed precipitation data across most of the regions in the continent (Nikulin *et al*., 2012; Sylla *et al*., 2013a; Kalognomou *et al*., 2013). Nonetheless, most studies suggest a recovery of the Sahelian rainfall, from the major decline it suffers over the course of the century, towards the last 20 years of the 20th century (Lebel and Ali, 2009; Biasutti, 2013). The projected precipitation for Africa exhibits high spatial and seasonal characteristics. For instance, CMIP5 GCMs projection of West African precipitation suggests intense rainfall during the peak of the rainy season towards the end of the 21st century (Biasutti, 2013). However, with Regional Climate Models (RCMs), the projected change signal differs from what is obtained in the GCMs, especially in regions of high or complex topography (Sylla *et al*., 2013a; Cook and Vizy, 2013). Although there is a high level of uncertainty in precipitation projection over West Africa (Mertz *et al*. 2009), the number of extreme rainfall during May and July is expected to increase over West Africa and the Sahel (Vizy and Cook, 2012).

2.2 West Africa Monsoon Systems

West Africa monsoon is a large-scale meridional circulation which originates from the thermal contrast between the warm African continent and the southern Atlantic Ocean during the boreal summer (Kalapureddy *et al*., 2010). It is characterized by prevailing southwesterly wind during June-September and northeasterly winds from the Sahara during January-March of each year.

The West Africa monsoon circulation consists of the southwesterly monsoon flow at low levels, the existence of the African Easterly Jet (AEJ; Thorncroft and Blackburn, 1999; Mohr and Thorncroft, 2006) in the middle troposphere, the Tropical Easterly Jet (TEJ; Reiter, 1969) at upper levels and the Inter-Tropical Convergence Zone (ITCZ) north of the equator. The monsoon is modulated by the northward migration of the ITCZ (Hagos and Cook, 2007; Sultan and Janicot, 2003), which reaches its northernmost position in August (Hastenrath, 1991).

Other important features of the West African monsoon system are the African Easterly Waves (AEWs; Machado *et al*., 1993), South Westerly Monsoon Flow and Mesoscale Convective Systems (MCSs; Omotosho, 1984). These features play important roles in rainfall dynamics over the entire West Africa region.

2.2.1 Mesoscale convective systems

Mesoscale Convective Systems (MCSs) are well-organized cloud clusters oriented north to south and moves from east to west direction. They are characterized by rainfall, gusty wind and thunderstorm. Across West Africa region, MCSs are responsible for most of the rainfall production (Mathon *et al*., 2002; Fink *et al*. 2006). For instance, about 16% to 32% of the annual rainfall along the shore of the Gulf of Guinea (Omotosho, 1985), 50% in the Sudan zone (Omotosho, 1985) and more than 80% in the Sahelian region (Mohr *et al*. 1999; Omotosho, 1985) are caused by MCSs. Similarly, most flooding events are caused by long-lasting and slow-moving MCSs.

The lifespan of MCSs can vary from a few hours to greater than 2 days (Fink *et al*. 2006). The initiation and frequency of occurrence of the MCSs are dependent on the vertical wind shear below the African Easterly Jet (Omotosho, 1992). MCSs are usually embedded in the

African Easterly Waves (AEWs) which are organized along the African Easterly Jet. However, MCSs in West Africa usually move faster than AEW troughs (Fink *et al*. 2006), by transporting momentum (Moncrieff, 1992) and moisture (Lafore *et al.* 1988). Thereby strengthening cyclonic rotation when embedded in an AEW trough (Barthe *et al*., 2010).

2.2.2 African easterly waves

The African Easterly Waves (AEWs) are essential in local climate variability over West Africa (Ward *et al*., 2004). They are characterized by a period of 3-5 days (Diedhiou *et al*., 1999), with wavelengths between 2000-4000 km and mean speed of approximately 8 m s^{-1}. They are westward-travelling waves which originate over northern Africa between June and October (Riehl, 1945). They are usually found in the vicinity of the African Easterly Jet or formed due to the breakdown of the ITCZ. For instance, over the Sahel zone, most of the seasonal rainfall associated with organized mesoscale convective systems are found within the AEWs (Landsea and Gray, 1992). Hence, AEWs may provide a large-scale favourable condition for rainfall through the organization of MCSs.

It has been reported that in areas east of the AEW troughs inland and in the eastern Atlantic ahead of and within the AEW trough near the coast, deep convection is observed (Machado *et al*., 1993; Diedhiou *et al*., 1999).

2.2.3 West Africa Jets

Africa Easterly Jet (AEJ) plays a significant role in the convection initiation and life cycle of West African monsoon systems (Diedhiou *et al*., 1999) while Tropical Easterly Jet (TEJ) is responsible for the inter-annual variability of rainfall (Nicholson and Webster, 2007). AEJ is

characterized by the strong zonal wind between 700 and 500 hPa centred around 15°N while TEJ centred around 10°N is usually found around 200 hPa (Nicholson *et al*., 2007). The horizontal temperature gradient which exists between the Gulf of Guinea and the Sahara Desert leads to the formation of AEJ (Thorncroft and Blackburn, 1999). AEJ aids in the organization of mesoscale convective systems associated with synoptic-scale Africa Easterly Waves (Diedhiou *et al*., 1999). On the other hand, TEJ is linked to the meridional thermal gradient which exists between the Tibetan highlands and the Indian Ocean during the southwest Asiatic monsoon circulation (Koteswaram, 1958). The core of the TEJ is positioned at about 10°N between the months of June to September. The pronounced variations in the strengths of the two jets are associated with the fluctuations in rainfall amount during the summer period over West Africa (Nicholson, 1981). For instance, stronger AEJ, weaker TEJ and weaker southwesterly monsoon flow produce drier monsoon over the Sahel while weaker AEJ, stronger TEJ and southwesterly monsoon flow result in wetter monsoon (Grist and Nicholson, 2001). The moisture content of the monsoon depends on the strength of the jets so that the distribution of monsoon precipitation over West Africa is dependent on both the Africa Easterly Jet and Tropical Easterly Jet. Similarly, Omotosho (1992) shows that deep convection systems and the onset of rainfall depend on AEJ.

2.2.4 Inter-tropical convergence zone

The ITCZ is characterized by low pressure, maximum surface temperature, high cloudiness, rainfall, and trade wind convergence and confluence (Nicholson *et al*., 2009). The large-scale convective available potential energy which generates deep convection is produced by the ITCZ. It is often referred to as inter-tropical discontinuity (ITD) when it occurs over land. The continental ITCZ, occur due to the convergence of continental northerly flow with

the southwesterly flow which transport moisture further inland. It is responsible for the distribution of rainfall over the entire West Africa region. The onset of the West African monsoon is associated with an abrupt shift of the ITCZ from 5°N to 10°N in June (Le Barbe´ *et al*. 2002; Sultan and Janicot, 2003). The inland movement of the Inter-tropical convergence zone is responsible for rainfall over the Sahel. Climatologically, the ITD reaches its northernmost position at about 20°N in August before retreating southward.

2.2.5 Southwesterly monsoon flow

Southwesterly monsoon flow is a low-level westerly associated with the humid air south of the ITCZ. It serves as a major source of water vapour for West Africa (Sylla *et al*., 2010b). West Africa summer rainfall is influenced by the depth, speed and direction of the southwesterly African monsoon flow (Nicholson, 2009b). Summer rainfall over the Guinean coast is enhanced through transportation of moisture and low vorticity air by southerly monsoon flow.

2.3 Evidence and Consequences of Global Warming

Multiple pieces of evidence obtained from *in situ* observations, conceptual and numerical models of the Earth's climate system, ice core records and instrumental observations of the atmosphere, land, ocean and cryosphere clearly indicate a changing climate. These indicators include changes in the surface temperature, atmospheric water vapor, precipitation, frequent occurrence of severe weather events, glaciers, ocean and land ice, sea level and concentration of important greenhouse gases (e.g. CO_2, CH_4, and N_2O; Forster *et al*., 2007). As described in the Fourth Assessment Report (AR4) of IPCC (Forster *et al*., 2007), greenhouse

gases have increased substantially by about 7.5% since 2005, with CO_2 contributing to about 80%. The increase in CO_2 is mainly from fossil fuel combustion (Tans, 2009). The increase in greenhouse gases resulted in the trapping of incoming solar radiation which is supposed to escape back into space and thereby increases the earth's temperature.

The observed patterns of surface warming, increases in ocean heat content, increases in atmospheric moisture, sea level rise, and increased melting of land and sea ice matches closely with the rising levels of CO_2 and other human-induced changes. The major cause of present-day global warming is an increase in greenhouse gases during the industrialization era in the 1900s. The IPCC Fifth Assessment Report (AR5; IPCC, 2013) attributed the observed changes in global average surface temperature from 1951 to 2010 to the anthropogenic increase in greenhouse gas concentrations. Similarly, changes in land use (e.g. agriculture, deforestation and urbanization), high rates of population growth, increase economic activity which is heavily dependent on fossil fuel are some of the other factors responsible for the increased concentration of atmospheric greenhouse gases.

The 30- year period from1983 to 2012 has been identified as the most likely warmest of the last 800 years in the Northern Hemisphere, where such assessment is possible (Hartmann *et al*., 2013). Globally averaged combined land and ocean surface temperature from 1901 to 2012 also showed an increase in earth's surface temperature. Eleven of the twelve-year period from 1995–2006 rank among the 12 warmest years in the instrumental record of global surface temperature since 1850 (IPCC, 2007a). Also, the updated 100-year linear trend for the years 1906 to 2005 is approximately 0.14°C larger than the corresponding trend for 1901 to 2000 (IPCC, 2001). Across West Africa, statistically significant warming, ranging between 0.5°C to 0.8°C was observed between 1970 and 2010 (Collins, 2011), but the projected future warming is expected to be between 3°C and 6°C (Diallo *et al*., 2012).

Some of the consequences of global warming include significant changes in precipitation patterns, changes in the frequency and intensity of some extreme events, rise in the average global sea level, with greater implications for the 50 to 70 percent of the world's population currently living in low-lying coastal areas, shrinking glaciers, poleward and altitudinal shifts of plant and animal ranges, decreasing population of some plant and animal populations, drastic reduction in agricultural and food production, impairment of human health and socio-economic well-being, spread of pests and disease vectors including malaria, cholera, typhoid, destruction of coral reefs from warmer seas among many others.

2.4 Impacts of Global Environmental Change across West Africa

West Africa economic and population growth has been on the increase since the pre-industrial era. The economic growth has led to the evolution of more industries which have contributed to the increase in anthropogenic greenhouse gas emissions of carbon dioxide, methane and nitrous oxide. The consistent increase in greenhouse gas emissions has been the major cause of the observed global warming since the mid-20th century. Population growth has also resulted in changes in land-use leading to the conversion of grassland and forests to agriculture. Hence, increased runoff and higher rates of groundwater recharge especially in the Sahel region (Favreau *et al*., 2009; LeBlanc *et al*., 2008). For instance, conversion of grassland and forests to crop production in Senegal led to decreased rainfall (Mbow *et al*., 2008) while soil erosion, bushfires and overgrazing make northern Ghana more susceptible to drought condition (Kalame *et al*., 2011). Similarly, the occurrence of flooding has been on the increase in coastal cities of West Africa which has led to land erosion and degradation, destruction of infrastructure and crops among many others (Sarr and Lona, 2009). These impacts are further exacerbated by the low adaptive capacity of the region, high rates of pov-

erty and the rising population to 306 million as at the year 2009 (World Bank, 2011). The impacts of climate change in Africa is expected to be highly variable and devastating by the end of the 2030s and towards early 2040s (Mora *et al*., 2013).

In recent decades, West African has experienced an increase in temperature that is up to 0.5°C per decade. However, the magnitude of climate change impacts on precipitation projection over West Africa is highly uncertain. For instance, an ensemble of regional climate models which participated in the Coordinated Regional Climate Downscaling Experiment (CORDEX; Giorgi *et al*., 2009) projects a larger range of uncertainty (±30%) for precipitation, which is even expected to increase in the farther future. This is partly due to the inability of the climate models to fully represent the dynamics of West African convective precipitation and also partly due to the choice of the convective scheme for the study domain in the regional climate models among many other factors. Nonetheless, it is most likely that there will be increased precipitation events during the peak of the rainy season as well as the late onset of rain at the end of the 21st century (Biasutti, 2013). Future projections on the impacts of climate change over West Africa also suggests approximately fifty percent reduction in agricultural production (IPCC, 2007b), increased extreme precipitation days in May and July (Vizy and Cook, 2012), intense and more frequent occurrences of extreme precipitation over the Guinea Highlands and Cameroun Mountains (Sylla *et al*., 2013a; Haensler *et al*., 2013) and a net decrease in woody vegetation (Ruelland *et al*., 2011; Gonzalez *et al*., 2012).

Rainfed agriculture which is the main source of livelihood in West Africa employs more than 50% of the active labor force but only contributes about 35 % of Gross Domestic Product (Jalloh *et al*., 2013). West Africa agricultural sector depends heavily on abundant monsoon rainfall. The monsoon rainfall is modulated by the northward migration of the Intertropical convergence zone (ITCZ) during the onset of the rainy season (March to May)

and the peak of the rainy season (June to August) over West Africa (Hagos and Cook, 2007). Therefore, a slight decrease in monsoon rainfall or shift in the northward migration of the ITCZ has a major influence on the socio-economic status of the region. Hence, the impacts of climate change with regards to droughts condition, extreme weather events, shifting seasons, land degradation, soil acidity, surge in population growth among many others factors pose a great threat to food security in the region. These impacts are most adverse in the Sahel.

2.5 Changes in Land-Use and Land Cover

There is an increasing demand on land resources over most parts of Africa. The desert is expanding at the expense of natural vegetation (Brink and Eva, 2009; Mayaux *et al*., 2013) with net decreases in woody vegetation across most parts of West Africa (Ruelland *et al*., 2011; Gonzalez *et al*., 2012). Charney (1975) hypothesised that increase in albedo associated with desertification due to overgrazing as well as the removal of highly reflective soil might be responsible for rainfall decline in West African Sahel. Other scientists also confirmed the feedback effect on rainfall due to changes in the surface albedo in other regions (Xue and Shukla, 1993). Similarly, Abiodun *et al*. (2008) reported that desertification increases surface temperature, decreases rainfall over the Sahel region and increases it near the coast. On the other hand, deforestation reduces surface friction and decreases rainfall over the entire West African region.

Global emissions from changes in the land-use account for the largest source of emission for eight of the largest emitters in Sub Saharan African countries (Cannadell *et al*., 2009). In the 1990s, the estimated rates of deforestation and forest degradation across Africa were reported to be at 850 000 ha/yr and 390 000 ha/yr respectively (Achard *et al*., 2004). Approximate-

ly 30% of global greenhouse gas emissions can be attributed to changes in land-use while livestock production contributes about 14.5% (Smith *et al*., 2007). Out of the 30% emissions from changes in land-use, deforestation account for about 18% while crop production account for the remaining 12%. Hence, large-scale removal of greenhouse gases can be achieved through sustained land management practices. However, changes in land management and land use have a potential to modify or moderate both the local and regional climate (Smith *et al*., 2007). This is achieved through changes in albedo, evapotranspiration, soil moisture and temperature.

Across West Africa, the changes in land-use and land cover can be attributed primarily to agriculture expansion, livestock grazing and fuelwood harvesting (Brink and Eva, 2009; Kutsch *et al*., 2011; Gonzalez *et al*., 2012). About 75 percent or more of agricultural production in West Africa is rain-fed (Molden *et al*., 2007). This makes agriculture in Africa highly vulnerable to changes in precipitation and temperature regimes. The effect of global warming and persisting extreme weather events could lead to a reduction in crop yields while the length of growing season could also change. However, most farmers in the region lack the skill and resources required to adapt to the impacts of climate change. Hence, agroforestry is commonly practised in the arid and semi-arid zones to provide a buffer against the impacts of climate change in the region.

2.6 Influence of Land-Use and Land Cover Change on the Climate System

Changes in the global land-use pattern as a result of human activities has pronounced impact on the local, regional and global climate system (IPCC, 2007c). Feddema *et al*. (2005) also conclude that changes in land cover will significantly result in different regional climates

from what it would have been, had there not been any changes in land cover. Attempt to quantitatively describe the impact of changes in land-use and land cover remains a challenging task. Most attempts to study the influence of land-use and land cover change (LULCC) on the climate system are carried out using either Global Climate Models (GCMs) or Regional Climate Models (RCMs).

Modifications of land surface characteristics alter the thermodynamic characteristics of the atmosphere producing different climate processes and patterns (Pielke and Niyogi, 2009). Numerical experiments suggest warming is induced in the tropical region due to deforestation (Bonan, 2008) while afforestation enhances cooling over the reforested region but induces warming downwind of the reforested region (Abiodun *et al*., 2012; Chen *et al*., 2012; Abiodun *et al*., 2013). According to Avila *et al*. (2012), the impacts of land cover change on indices of temperature extreme was equal to the impacts of doubling of CO_2.

Similarly, agriculture and urbanization have also been shown to influence precipitation distribution, runoff, evapotranspiration at a regional scale (Kueppers and Snyder, 2012; Wang *et al*., 2013a). Some studies also suggest that changes in land-use and land cover may also influence extremes in temperature and precipitation (Woldemichael *et al*., 2012; Wang *et al*., 2013b). These show that LULCC has different effects on the regional climate at different spatiotemporal scales.

2.7 Agriculture Intensification and Greenhouse Gas Emissions

Agricultural intensification and expansion have negative effects on climate, soil and biodiversity at the local scale (Krausmann *et al*., 2013). Agriculture contributes approximately 25% of global greenhouse gas emissions and is projected to account for at least 70% of the total greenhouse gas emissions by the year 2050 if global warming is limited to 2°C (Ong *et*

al., 2015). Sources of greenhouse gases from agriculture are primarily nitrous oxides, plant residue, and methane besides deforestation due to agricultural expansion. Hence, urgent, continuous and consistent adaptation and mitigation practices are required.

Recently, the importance of integrating trees into the agricultural landscape as a measure to improve crop and land management system has been under discussion (Gockowski and Asten, 2012; Garnett *et al*., 2013). Agroforestry is a form of climate-smart or evergreen agriculture, which has the potential to increase crop yield for the ever-increasing population while at the same time slows down the rate of new land conversion. The International Centre for Research in Agroforestry (ICRAF) summarized the term agroforestry as a collective name for land-use systems and technologies, where woody perennials (trees, shrubs, palms, bamboos etc.) are deliberately used on the same land management unit as agricultural crops and/or animals, either in some form of spatial arrangement or temporal sequence (Nair, 1993). According to Nair (1985), agroforestry is classified structurally into three main groups namely, agri-silviculture (crops and trees), silvopastoral (pasture/animals and trees), and agro-silvopastoral (crops, pasture/animals and trees). However, the focus of this study is on agri-silviculture but it can be interchangeably used as agroforestry.

2.8 Agroforestry practices in West Africa

The simultaneous growing of crops and trees on the same piece of land has long been extensively practised by farmers in the semi-arid and sub-humid zones of West Africa (Nair, 1993). The combination of woody perennials (e.g. trees) and herbaceous plants (e.g. crops) on the same piece of land arranged in a spatial mixture or temporal sequence is increasingly becoming more popular in the semi-arid and sub-humid region of West Africa. This can be attributed to its numerous benefits which include but are not limited to nutrient cycling, wa-

ter redistribution, increased water infiltration, shade, erosion control, crop yield, carbon sink, e.tc. The combine plantation of trees, crops and shrubs on agricultural lands increases the adaptability of agricultural systems and thereby ensures food security (Torquebiau, 2013). The practice of Agroforestry is well suited for the Clean Development Mechanism for Afforestation (CDM-AR). The approximately 200 M ha area of land in Africa which is most suited for CDM-AR, is characterized as grasslands or savannahs (Zomer *et al*., 2008). Small-scale Agroforestry in diverse form is practised mostly by farmers in West Africa Sahel and Savannah zone as a buffer against the impacts of climate change. However, the deliberate incorporation of trees and crops on the same piece of land is technically referred to as agri-silviculture. According to Chaudhry and Silim (1980), agri-silviculture is a production technique which combines the growing of agricultural crops with simultaneously raised and protected forest crops.

According to the report of The International Bank for Reconstruction and Development (IBRD, 2011), approximately 5 million hectares of land has been converted to productive agroforestry systems in Niger and Burkina Faso, thereby reversing the process of desertification in the country. High-resolution images showed that between the years 2003 to 2008, tree density and cover increased in about 4.8 million hectares of farmland across Maradi and Zinder regions of Niger through farmers managed natural regeneration (Reij *et al*., 2009). Similarly, about 5 million hectares of barren and degraded lands have been transformed in the past three decades at a lower cost relative to pure forestation through agroforestry practices (Reij, 2011). Therefore, African Re-Greening Initiative project proposed to establish green belt of a tree across the Sahel region due to the high success rate recorded with agroforestry in the Maradi and Zinder regions of Niger (Tougiani *et al*., 2009). The integration of trees on agricultural lands is rapidly increasing, but how this would influence West Africa

future climate system is of major concern to the climate scientist in view of the complex interactions that exist between the land and the atmosphere.

2.9 Agroforestry as a Climate Change Adaptation and Mitigation Option

Adaptation involves initiatives and measures to reduce the vulnerability of natural and human systems against actual or expected climate change effects while mitigation is an anthropogenic intervention to reduce the sources or enhance the sinks of greenhouse gases (IPCC, 2007a). The interaction between water resources and agricultural practices is expected to become increasingly important as the climate changes. Agroforestry has the potential to act as an adaptation and mitigation option to the impacts of climate change by drastically ameliorating some of the environmental problems introduced by deforestation and forest degradation. According to Kidd and Pimentel (1992), agroforestry systems is similar to pure forestation in terms of nutrient-cycling, favourable environmental influence as well as its capacity to generate additional sources of income. It has also been established that agroforestry enhances agricultural productivity (Albrecht and Kandji, 2003), reverses land degradation (Mbow *et al*., 2014a) and provides other environmental benefits (Mbow *et al*., 2014b). However, the carbon sequestration potential of agroforestry was first considered by Albrecht and Kanji (2003) and then later by Verchot *et al*. (2007). Although the cushioning effect of agroforestry to the impacts of climate change is still in its preliminary stage (Verchot *et al*., 2007), it is still important for a climate scientist to understand how large-scale agroforestry practice can influence the future climate.

The adaptation and mitigation practice is becoming more popular and acceptable in Africa (Jalloh *et al*., 2011; Majanen and Scherr, 2011). The possibility of tropical agroforestry to

serve as a climate change mitigation option was considered in the Kyoto Protocol of the United Nations Framework Convention on Climate Change (Smith *et al*., 2007; Jose and Bardhan, 2012; UNFCCC, 2014; Minang *et al*., 2014;). The Fifth Assessment Report of The Intergovernmental Panel on Climate Change estimated the potential of agroforestry to sequester carbon by the year 2040 to be very high (Smith *et al*., 2014; Verchot *et al*., 2007). Across Africa region, agroforestry accounts for the third largest carbon sink next to a primary forest and long-term fallows (Oke and Odebiyi, 2007). The adoption of agroforestry practices in the region could provide biodiversity conservation, rural employment, and soil amelioration (Tschakert, 2007).

The far-reaching impacts of climate change in West Africa coupled with the surge in population growth pose a great threat to food security. However, Agroforestry has a great potential to reduce the vulnerabilities of farmers to the impacts of climate change (Kahiluoto *et al*., 2014; Lasco *et al*., 2014; Mbow *et al*., 2014a). This is achieved by its provision of a faster recovery from extreme weather events or market failures due to its diversified temporal and spatial management options. It also serves as a climate change mitigation option by increasing carbon stock above ground via standing vegetation biomass and below ground via soil organic matter content (Albrecht and Kandji 2003; Asase *et al*., 2008; Takimoto *et al*., 2008; Nair *et al*. 2009a, b; Luedeling and Neufeldt, 2012; Mbow *et al*., 2014a; Mbow *et al*., 2014b;).

According to Food and Agriculture Organization report (FAO, 2001), the area of the world under agroforestry will increase substantially in the near future. The total land area under agroforestry is estimated to be about one billion hectares (Zomer *et al*., 2009). The potential of all agricultural lands to store carbon below ground ranges from approximately 1500 to 4300 Mt CO_2e yr^{-1} (Mbow *et al*., 2014b). It has also been projected that the conversion of approximately 630 million hectares of unproductive cropland and grassland to agroforestry

could sequester 586 000 Mg C yr-1 by the year 2040 (Smith *et al*., 2007; Verchot *et al*., 2007). For instance, the estimated carbon sequestered by agroforestry system in Senegal was 0.4t/ha/yr with a potential of 20t/ha in 50 years (Tschakert 2004). Similarly, in Ghana, although higher soil organic carbon was sequestered in shaded cocoa plantation than the unshaded, the level of productivity in the shaded was lower than the unshaded ones (Asase *et al*., 2008).

2.10 West Africa Climate and Land-Atmosphere Interactions

Changes in vegetation structure have the potential to modify the climate and hydrological processes over West Africa (Alo and Wang, 2010; Oguntunde *et al*., 2015). The transfer of energy, mass and momentum between the biosphere and atmosphere occur at the lower atmospheric boundary layer. The interaction between the biosphere and atmosphere has an effect on local, regional and global climate. Numerous studies have been conducted on land-atmosphere interactions in West Africa region (e.g., Xue and Shukla, 1993, 1996; Cook, 1997; Xue, 1997; Wang *et al*., 2004; Patricolar and Cook, 2008; Abiodun *et al*., 2012; Sylla *et al*., 2016). Most of these studies conclude that desertification, deforestation and afforestation influence local and regional climate dynamics through changes in surface albedo, heat fluxes, and changes in evaporation. These alter land surface energy balance and moisture transfer between the land surface and the atmosphere (Paeth and Thamm, 2007). For instance, Abiodun *et al.,* 2012 used a Regional Climate Model to study the potential impacts of reforestation on the future climate of West Africa by replacing the present-day vegetation along the Sahel, Savanna and Guinea zones with tropical forest. They found that reforestation induces cooling over the reforested area but produces warming outside the reforested

zone. However, the influence of the reforestation experiment on precipitation differs for each experiment.

Generally, the different modelling approaches conclude that land surface conditions for West Africa range from extremely simple with a uniform albedo of 0.10 (Cook, 1997) to more complex, realistic values depending on soil type and vegetation (Xue and Shukla, 1996). Therefore, changes in land-use are partly responsible for drought conditions in West Africa Sahel region (Abiodun *et al*., 2008). Stebbings (1935) proposed a forest band across West Africa to facilitate increased rainfall amount and bind up the blowing sand. Forestation of an area will alter the surface roughness, albedo and the amount of water recycled to the atmosphere. The feedback from these processes will result in warming of the local climate and reduction in the net value of the mitigation strategy of planting forest (Bonan, 1997). Thus influencing the climate at a variety of scales by either enhancing or counteracting the climate benefits from carbon sequestration on global mean temperature. However, if forest lands and vast areas of degraded lands were to be converted to agroforestry, it is important to investigate the effect of this conversion on West Africa regional climate.

CHAPTER THREE

RESEARCH METHODOLOGY

3.1 The Study Area

West Africa is the westernmost part of Africa consisting of 16 countries namely Benin, Burkina Faso, Cape Verde, Côte d'Ivoire, Gambia, Ghana, Guinea, Guinea-Bissau, Liberia, Mali, Mauritania, Niger, Nigeria, Senegal, Sierra Leone, and Togo (Fig. 3.1). It is a region located between the Sahara Desert to the north and the Atlantic coast to the south. The distribution of the dominant vegetation types is approximately parallel to the latitudes due to the influence of climate. The role of climate is very crucial in the distribution of vegetation while vegetation is also important in climate modification.

The highest annual rainfall (2 500 to 4 000 mm) is received mostly by coastal cities in countries such as Guinea, Sierra Leone, Liberia, and Nigeria while West African Sahel region (e.g. Senegal, Mali, Burkina Faso, Niger and northern Nigeria) receives annual rainfall ranges from 800 to 1100 mm. Mauritania and most parts of Mali and Niger are predominantly desert regions. Generally, rainfall decreases, from south to north while temperature increases northward from the southern coast (Fig. 3.2). Maximum temperatures range from 30°–33°C along the coast to 36°–39°C in the Sahel and 42 – 45°C on the desert borders. The agro-ecology of West Africa is composed of humid forest along the coast to the Guinea savanna and the Sudan savanna northward.

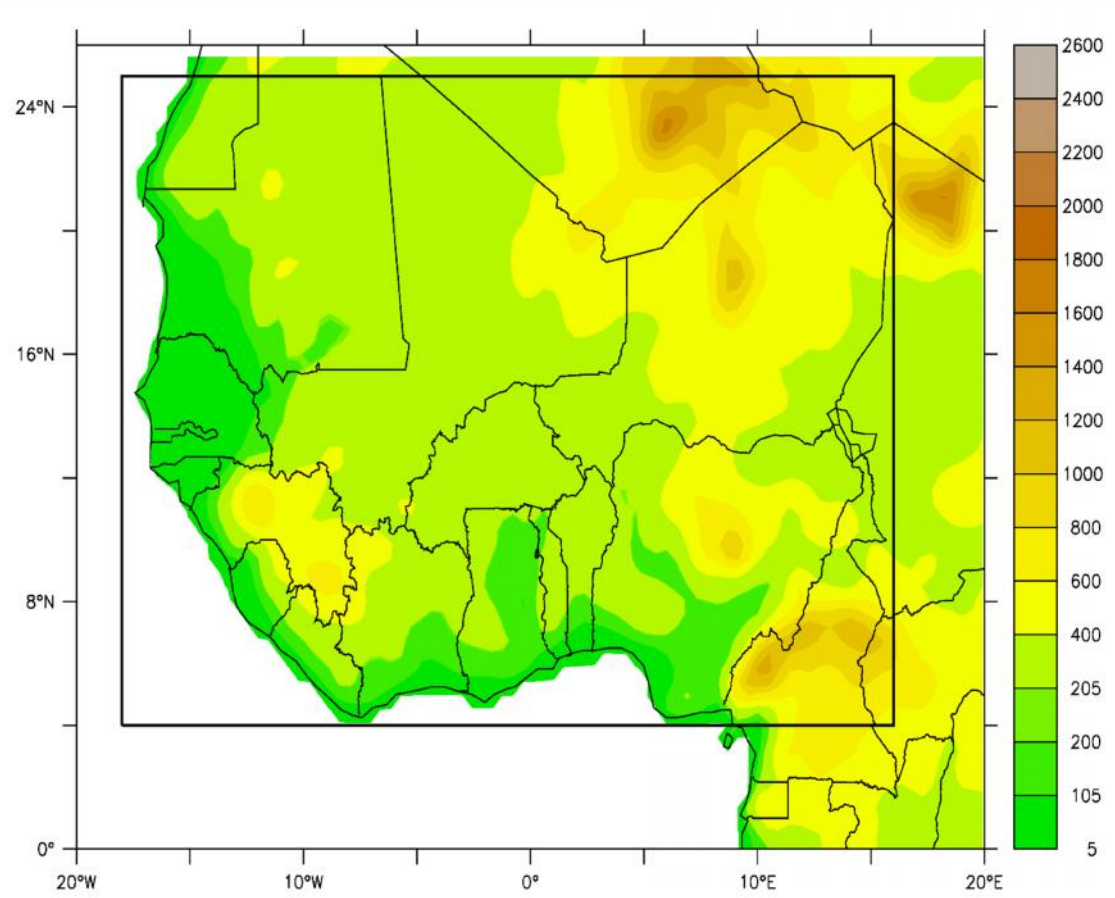

Fig. 3.1: West Africa simulation domain, and topography (in meters) for RegCM4 at 50 km resolution

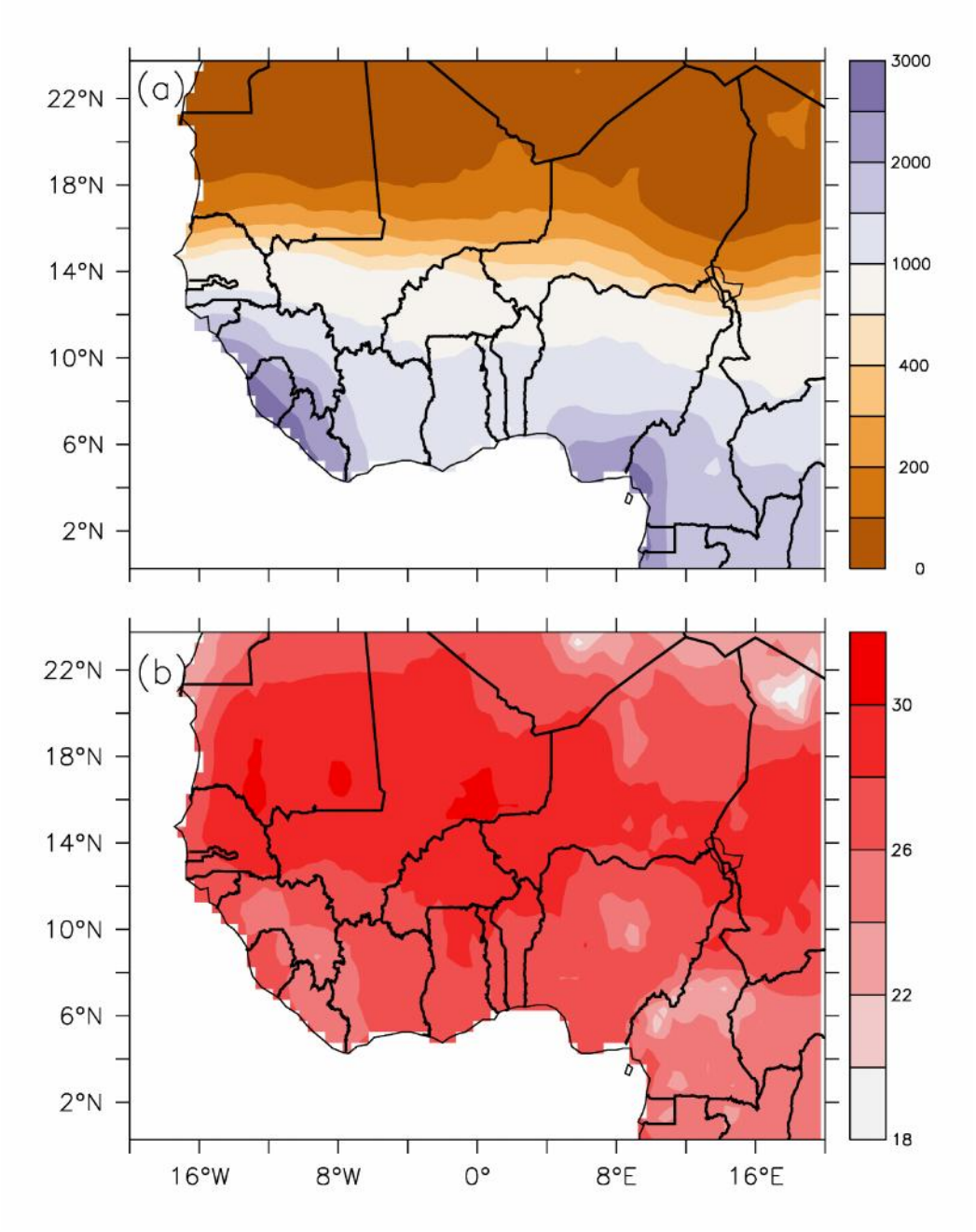

Fig. 3.2: Spatial distribution of (a) annual precipitation (mm) and (b) temperature across West Africa averaged for 1980-2004 (Data Source: CRU TS. 3.22; Harris *et al*., 2014)

3.2 RegCM4 Model Description

The International Centre for Theoretical and Applied Physics Regional Climate Model version 4 (RegCM4) is an hydrostatic, compressible, sigma-p vertical coordinate model which runs on an Arakawa B-grid in which wind and the thermo-dynamical variables are horizontally staggered (Giorgi *et al*., 2012). The model dynamics are the same with the hydrostatic version of the fifth-generation Penn State/NCAR Mesoscale Model (MM5, Grell *et al*., 1994). The model physics adopts the National Center for Atmospheric Research Community Climate Model (NCAR CCM3; Kiehl *et al*., 1996) radiative transfer scheme, implemented in Giorgi and Mearns, 1999. The planetary boundary layer process is described by Holslag *et al*. (1990) while the large-scale precipitation process is described using the sub-grid scale explicit moisture and cloud (SUBEX) scheme obtained from Pal *et al*. (2000). The parameterizations for surface ocean fluxes described in Zeng *et al*. (1998) is used in the model. RegCM4 has been successfully employed in various regional climate studies across the different region. It has the capability to realistically simulate the mean climate over a given region (Gu *et al*., 2012; Adeniyi, 2014; Oh *et al*., 2014; Wang *et al*., 2016) and therefore has been used in future climate projections and paleoclimate studies (Giorgi *et al*., 2006).

However, the choice of convective and land surface scheme has an important role in the successful simulation of the mean climate over a given region (Steiner *et al*., 2009; Patricola and Cook, 2010). The model provides five options of cumulus convection parameterization which include: Kuo-type Scheme of Anthens (1977); Grell (1993); Kain and Fritsch, 1990, Kain (2004); MIT Emanuel scheme (Emmanuel, 1991; Emanuel and Zivkovic-Rothman, 1999) and Tiedtke scheme (Tiedtke, 1989). On the other hand, three options were made available for the land surface scheme. These are Biosphere-Atmosphere Transfer Scheme (BATS; Dickson *et al*., 1993), The National Center for Atmospheric (NCAR) Community

Land Model version 3.5 (CLM3.5; Oleson *et al*., 2008) and The National Center for Atmospheric (NCAR) Community Land Model version 4.5 (CLM4.5; Oleson *et al*., 2013).

The model configurations employed in this study are summarized in Table 3.1. The simulations were carried out using two Africa domains. The first domain extends from 35°S - 35°N and 45°W - 40°E while the larger domain extends from 45°S - 45°N and 42°W - 70°E. It has a grid resolution of 50 km and 18 vertical sigma levels which extend from the surface to 50 hPa level. The cartographic projection of the domain is Normal Mercator. RegCM4 model obtains and analyzes its data on pressure surfaces which is first interpolated to the model's vertical coordinate before input to the model. The lower grid levels follow the terrain while the upper surface is flatter. A detailed description of the model can be found in the RegCM4 technical description (Elguindi *et al*., 2013).

Table 3.1: Summary of model configurations used in this study.

Model Aspects	Model Options
Radiative Transfer	Modified CCM3 (Kiehl *et al*., 1996)
Planetary Boundary Layer(PBL)	Modified Holtslag (Holtslag *et al*., 1990)
Cumulus convection	Grell with Fritsch and Chappell closure scheme over land
	MIT scheme over the ocean
Resolved scale precipitation	Subgrid Explicit Moisture Scheme (SUBEX)
Land surface scheme	BATS
	CLM3.5
	CLM4.5
	CLM4.5 Dynamic Vegetation
Ocean Fluxes	Zeng (Zeng *et al*., 1998)
Initial and boundary conditions data	HadGem2-ES
Horizontal grid	160 X 192 (Grid point resolution=50km)
	250 X 192 (CORDEX domain; Grid point resolution=50km)
Vertical layers	18 levels
Analysis period	1980-2004 (Historical climate)
	2030-2054 (Near future: RCP4.5 Scenario)

3.3 Regcm4 Model Dynamics

3.3.1 Horizontal momentum equations

$$\frac{(\partial \rho^* u)}{\partial t} = -m^2\left(\frac{\partial(\rho^* uu)/m}{\partial x} + \frac{\partial(\rho^* vu)/m}{\partial y}\right) - \frac{\partial(\rho^* u\dot{\sigma})}{\partial \dot{\sigma}} - m\rho^*\left[\frac{RT_v}{\rho^* + \frac{\rho_t}{\sigma}}\frac{\partial \emptyset}{\partial x}\right] + f\rho^* v + F_H u + F_V u \quad (3.1)$$

$$\frac{(\partial \rho^* v)}{\partial t} = -m^2\left(\frac{\frac{\partial(\rho^* uv)}{m}}{\partial x} + \frac{\frac{\partial(\rho^* vv)}{m}}{\partial y}\right) - \frac{\partial(\rho^* v\dot{\sigma})}{\partial \dot{\sigma}} - m\rho^*\left[\frac{RT_v}{\rho^* + \frac{\rho_t}{\sigma}}\frac{\partial \emptyset}{\partial x}\right] + f\rho^* u + F_H v + F_V v \quad (3.2)$$

where u = Eastward component of velocity, v =Northward component of velocity, T_v= Virtual temperature, $\emptyset$=Geopotential height, f = Coriolis parameter, F_H= Effect of horizontal diffusion, F_V= Effect of vertical diffusion, R = Gas constant for dry air, m = map scale factor for the Polar Stereographic (high latitude), Lambert Conformal (mid-latitude) or Mercator map projections). It is calculated as distance on grid / actual distance on earth, ρ* = ρs – ρt (ρs, ρt are surface and top-level pressure respectively where ρt is a constant), $\dot{\sigma}=\frac{\partial \sigma}{\partial t}$

The first, second and third term on the RHS of equation 3.1 represents the horizontal advection, vertical advection and map factor respectively. The fourth term on the other hand represents a change of coordinate.

3.3.2 Continuity and sigmadot ($\dot{\sigma}$) equations

$$\frac{(\partial \rho^*)}{\partial t} = -m^2\left(\frac{\partial(\rho^* u)/m}{\partial x} + \frac{\partial(\rho^* u)/m}{\partial y}\right) - \frac{\partial(\rho^* \dot{\sigma})}{\partial \sigma} \quad (3.3)$$

$$\frac{(\partial \rho^*)}{\partial t} = -m^2\int_0^1\left(\frac{\partial \rho^* u/m}{\partial x} + \frac{\partial \rho^* v/m}{\partial y}\right)d\sigma \quad (3.4)$$

The temporal variation of the surface pressure in the model was computed from the vertical integral of equation 3.3.

Equation 3.4 gives the surface-pressure tendency, afterwards, the vertical velocity in sigma coordinates ($\dot{\sigma}$) is computed at each level of the model using equation 3.3

$$= -\frac{1}{\rho}\int_0^{\sigma}\frac{\partial \rho^*}{\partial t} + m^2\left(\frac{\partial(\rho^* u)/m}{\partial x} + \frac{\partial(\rho^* v)/m}{\partial y}\right)d\sigma' \tag{3.5}$$

Where σ' is a dummy variable of integration and $\dot{\sigma}(\sigma = 0) = 0$

3.3.3 Thermodynamic equation and equation for omega (ω)

The thermodynamic equation is expressed as

$$\frac{(\partial \rho^* T)}{\partial t} = -m^2\left(\frac{\partial(\rho^* uT)/m}{\partial x} + \frac{\partial(\rho^* vT)/m}{\partial y}\right) - \frac{\partial(\rho^* T\dot{\sigma})}{\partial \sigma} + \frac{RT_v\omega}{C_{pm}\left(\sigma + {}^{P_T}/_{P_{ast}}\right)} + \frac{P^* Q}{C_{pm}} + F_H T + F_V T \tag{3.6}$$

Where $C_{pm} = C_p(1 + 0.8q_v)$ is the specific heat for moist air at constant pressure, C_p is the specific heat at constant pressure for dry air, q_v is the mixing ratio, Q is the diabatic heating, $F_H T$ represents the effect of horizontal diffusion, $F_V T$ represents the effect of vertical mixing and dry convective adjustment and $\omega = \rho^*\dot{\sigma} + \sigma\frac{\partial \rho}{\partial T}$ where,

$$\frac{\partial \rho^*}{\partial t} = \frac{\partial \rho^*}{\partial t} + m\left(u\frac{\partial \rho^*}{\partial x} + v\frac{\partial \rho^*}{\partial y}\right) \tag{3.7}$$

3.3.4 Hydrostatic equation

The hydrostatic equation is used to compute the geopotential heights from the virtual temperature T_v, and is expressed as

$$\frac{\partial \emptyset}{\partial ln\left(\sigma + {}^{P_t}/_{P^*}\right)} = -RT_v\left[1 + \frac{q_c + q_r}{1 + q_r}\right]^{-1} \quad (3.8)$$

where, $T_v = T(1 + 0.08q_v), q_v$, q_c, and q_r are the water vapour, cloud water or ice, and rain water or snow mixing ratios respectively.

3.4 Community Land Model (CLM4.5) Scheme

The most recent version of the National Center for Atmospheric Research Community Land Model version 4.5 coupled to RegCM4 provides a more detailed representation of land surface processes than the default Biosphere-Atmosphere Transfer Scheme. CLM4.5 provides an improvement to the unrealistically high leaf area index in the tropics in CLM3.5, as well as the inconsistencies in the observed estimate of carbon, with the transient 20th-century carbon response besides several other minor problems or biases (Oleson *et al*., 2013). The canopy conductance, gross primary production and transpiration are calculated in conformity to FLUXNET eddy-covariance flux towers (Bonan *et al*., 2011; Sun and Dickinson, 2012). Similarly, the hydrology (Swenson and Lawrence, 2012), soil biogeochemistry, soil carbon dynamics (Koven *et al*., 2013) and many other parameters were revised and updated accordingly. A detailed description of the improvements and updates on CLM4.5 with respect to its earlier version can be found in (Oleson *et al*., 2013).

CLM4.5 representation of the land surface in a grid cell is divided into three subgrid levels. These are a land unit, snow/soil columns and Plant Functional Types (PFTs). The land unit is further classified into glacier, lake, urban, vegetated and crop (when the crop model option is on). At this level, the urban unit can be further classified into density classes which accounts for the representation of tall building districts in an urban area. Hence we have, high density and medium density classes. The snow/soil column accounts for the variability of

snow and soil variables within a single land unit and is represented by fifteen layers of soil and up to five layers of snow.

Table 3.2: Plant Functional Types in CLM4.5.

Plant Functional Types				
Needleleaf evergreen temperate tree	Broadleaf Deciduous Tropical Tree	Broadleaf deciduous boreal shrub	[1]C3 irrigated	[3]Winter temperate cereal
Needleleaf evergreen boreal tree	Broadleaf Deciduous temperate tree	C3 arctic grass	Corn	[3]Irrigated winter temperate cereal
Needleleaf deciduous boreal tree	Broadleaf deciduous boreal tree	C3 non-arctic grass	[1]Irrigated corn	[2]Soybean
Broadleaf evergreen tropical tree	Broadleaf Evergreen shrub	C4 grass	[2]Spring temperate cereal	[2]Irrigated soybean
Broadleaf evergreen temperate tree	Broadleaf Deciduous temperate shrub	C3 crop	[2]Irrigated spring temperate cereal	Non-vegetated (bare ground)

[1]Available if irrigation is enabled in the model. [2]Available if crop model is enabled.
[3]Available in future implementations of crop model. (Adapted from Oleson *et al*., 2013)

Table 3.3: Heights of Plant Functional Types in CLM4.5

PFTs	Height at the top of canopy (m)	Height at the bottom of canopy (m)
Needleleaf evergreen temperate tree	17	8.5
Needleleaf evergreen boreal tree	17	8.5
Needleleaf deciduous boreal tree	14	7
Broadleaf evergreen tropical tree	35	1
Broadleaf evergreen temperate tree	35	1
Broadleaf deciduous tropical tree	18	10
Broadleaf deciduous temperate tree	20	11.5
Broadleaf deciduous boreal tree	20	11.5
Broadleaf evergreen shrub	0.5	0.1
Broadleaf deciduous boreal shrub	0.5	0.1
C3 arctic grass	0.5	0.01
C3 non arctic grass	0.5	0.01
C4 grass	0.5	0.01
C3 crop	0.5	0.01
C3 irrigated	0.5	0.01
[1]Corn	-	-
[1]Irrigated corn	-	-
[1]Spring temperate cereal	-	-
[1]Winter temperate cereal	-	-
[1]Irrigated winter temperate cereal	-	-
[1]Soybean	-	-
[1]Irrigated soybean	-	-

[1]Determined by the crop model. (Adapted from Oleson *et al*., 2013).

The PFT subgrid level accounts for the differences in the biogeophysical and biogeochemical differences between broad categories of plants. There exist up to about 25 possible PFTs on a vegetated land unit (Tables 3.2 and 3.3). The PFTs present day datasets are derived from different satellite products using the methodology of Lawrence and Chase (2007). The percentage cover of bare ground and forest cover are derived from Modis Resolution Imaging Spectroradiometer (MODIS; Hansel *et al*., 2003). However, further classification of the tree into broadleaf, needleleaf, evergreen and deciduous types are based on information derived from Advanced Very High Resolution Radiometer (AVHRR; Defries *et al*., 2000). The remaining areas of the grid cell are then assumed to be herbaceous grasses and shrubs including crops. The area occupied by crops is determined according to the methods of Ramankutty *et al*. (2008). Similarly, areas occupied by grasses and shrubs are derived from Modis land cover (Friedl *et al*., 2002).

The activation of the dynamic vegetation capability in CLM4.5 (i.e. CNDV enabled simulation; Castillo *et al*., 2012) performs an hourly carbon and nitrogen cycle calculations as well as simulation of dynamic vegetation. The plant structure begins with no PFT information per grid cell rather it evaluates the possibility of a PFT establishment or survival according to specific bioclimatic limits (Table 3.4). Therefore, in this option, there exists a two-way interaction between vegetation and climatic variables. The model updates vegetation cover once every year as it simulates unmanaged vegetation (e.g. tree, grass, shrub; Zeng *et al*., 2008) PFTs.

Table 3.4: Bioclimatic requirements for PFTs in dynamic vegetation simulation. Adapted from Table 22.1 of Oleson *et al*., 2010. Coldest minimum monthly air temperature for the survival of previously established PFTs (Tc min); Warmest minimum monthly air temperature for the establishment of new PFts (Tc Max); Minimum annual growing degree-days above 5°C for the establishment of new PFTs (GDD min).

Plant Functional Types (PFTs)	Tc min (°C)	Tc max(°C)	GDD min
Tropical broadleaf evergreen tree	15.5	No limit	0
Tropical Broadleaf deciduous tree	15.5	No limit	0
Temperate needleleaf evergreen tree	-2.0	22	900
Temperate broadleaf evergreen tree	3.0	18.8	1200
Temperate broadleaf deciduous tree	-17.0	15.5	1200
Boreal needleleaf evergreen tree	-32.5	-2.0	600
Boreal deciduous tree	No limit	-2.0	350
Temperate broadleaf deciduous shrub	-17.0	No limit	1200
Boreal broadleaf deciduous shrub	No limit	-2.0	350
C4	15.5	No limit	0
C3	-17.0	15.5	0
C3 arctic	No limit	-17.0	0

3.5 Research Data

3.5.1 Initial and boundary condition data

Six hourly initial and lateral boundary conditions (e.g. air temperature, humidity, zonal wind, meridional wind, geo-potential height and surface pressure) for RegCM4 were obtained from the Met Office Hadley Centre Global Environmental Model version 2 Earth System configuration (https://verc.enes.org/models/earthsystem-models/hadgemem2-es; HadGem2-ES; Martin *et al*., 2011). Monthly output of Sea Surface Temperature (SST) from the corresponding HadGem2-ES experiments is used as the oceanic forcing for RegCM4. The boundary conditions dataset was obtained from HadGem2-ES historical simulation (1979-2004) and HadGem2-ES scenarios (2029-2054; RCP 4.5). The first year of all the simulation experiments was discarded as model spin up to avoid the problem of initial conditions and the result of the last twenty-five years (1980-2004 and 2030-2054) of the simulations was analysed.

HadGEM2-ES is one of the models used in the Intergovernmental Panel on Climate Change (IPCC) Fifth Assessment Report (AR5) and the Fifth Phase of the Coupled Model Intercomparison Project (CMIP5; http://www.ipcc.ch/report/ar5/wg1/). It is an atmospheric ocean global climate model (AOGCM) which has an atmospheric resolution of 1.875°×1.25° and 38 vertical levels while the ocean resolution is 1o (increasing to 1/3°) at the equator and 40 vertical levels. The model represents the interaction between land and ocean carbon cycles and dynamic vegetation with an option to prescribe either atmospheric CO_2 concentrations or to prescribe anthropogenic CO_2 emissions and simulate CO_2 concentrations. The components included in HadGEM2-ES configuration are the atmosphere, land surface and hydrology, aerosols, ocean and sea ice, terrestrial carbon cycle, atmospheric chemistry, and ocean biogeochemistry. HadGEM2-ES has been employed in future climate projections studies.

3.5.2 Data for model validation and evaluation

Monthly gridded (0.5° × 0.5°) observations of 2-meter surface temperature and precipitation were obtained from the Climate Research Unit (CRU) version 3.22 (Harris *et al*., 2014). The atmospheric data (zonal, meridional and vertical winds) were obtained from European Center for Medium-Range Weather Forecast (ECMWF) 0.5° X 0.5° gridded ERA-interim reanalysis (Dee *et al*., 2011). The ERA-Interim re-analysis product combines both numerical weather prediction model forecasting and an assimilation of different observational data (Simmons *et al*., 2007).

All datasets were averaged from 1980-2004 for the seasonal and annual climatology evaluation over the entire West Africa region. The 25-year time slices employed to study the past and future climate of the region is also acceptable because shorter averaging periods (e.g. 10 years) most times performs sufficiently well as the 30-year averaging periods for most climatic parameters (WMO, 2007).

3.6 Research Methods

3.6.1 Assessment of model performance

There are quite many regional climate model validations over West Africa (e.g. Omotosho and Abiodun, 2007; Steiner *et al*., 2009; Sylla *et al*., 2009; Abiodun *et al*., 2012; Jones *et al*., 2012; Adeniyi, 2014; Gbobaniyi *et al*., 2014; Ji *et al*., 2015; Sylla *et al*., 2016;). However, none has validated for the region using the same combination of boundary conditions, domain size, land surface scheme and physical parameterization employed in this study. Since, it is generally known that regional climate models are highly sensitive to these conditions (e.g. Flaounas *et al*., 2010; Mariotti *et al*., 2011; Rauscher *et al*., 2010; Abiodun *et al*., 2012;

Gianotti *et al*., 2012), hence the importance of assessing the model's performance over West Africa with respect to the chosen configurations for this study.

RegCM4 model performance and errors were determined using three different statistical metrics expressed in equations 3.9 to 3.11. These are: pattern correlation coefficient (PCC), spatial root mean square difference (RMSD) and mean bias (MB). MB is the difference between the area-averaged value of the simulation and the observation. RMSD and PCC provide information at the grid-point level while the MB does so at the regional level.

$$PCC = \frac{1}{\sigma_s \sigma_o}\left[\frac{1}{N}\sum_{i=1}^{N}(S_i - \bar{S})(O_i - \bar{O})\right] \quad (3.9)$$

$$RMSD = \sqrt{\frac{1}{N}\sum_{i=1}^{N}(S_i - O_i)^2} \quad (3.10)$$

$$MB = \frac{\sum_{i=1}^{N}(S_i - O_i)}{N} = \bar{S} - \bar{O} \quad (3.11)$$

where, N is a number of grid points, O_i is the value of the variable to the ith grid point of observation, S_i is the value of the variable to the ith grid point of model simulations, $\bar{O}$ and $\bar{S}$ are the mean values while σ_o and σ_s are the standard deviation values.

3.6.2 Sensitivity of RegCM4 land surface schemes in simulating West Africa climate

The capability of the four different land surface schemes options in RegCM4 to simulate temperature, precipitation and wind fields over West Africa was investigated. The land surface schemes are: (i) Biosphere-Atmosphere Transfer Scheme (BATS), (ii) Community Land Model version 3.5 (CLM3.5), (iii) Community Land Model version 4.5 (CLM4.5) and (iv) Community Land Model version 4.5 Dynamic Vegetation (Dynamic CLM4.5). Five

years (1979-1983) test simulation was carried out with each of the four schemes but the results of the last four years (1980-1983) were analyzed. Therefore, the test simulation attempt to examine the sensitivity of the different land surface scheme to observed changes in precipitation, temperature and winds, to identify the most suitable option for the convective scheme, in the climate simulation of this study.

3.6.3 Experimental design with RegCM4-CLM4.5

The numerical experiments in this study use CLM4.5 land surface scheme with MIT Emanuel convective scheme applied over the ocean and Grell with Fritsch-Chappell closure scheme over the land areas. The choice of CLM4.5 in this study is based on the fact that it is the only available land surface scheme option in RegCM4 capable of simulating dynamic vegetation. Similarly, there has also been some improvements and modifications that have been incorporated into it when compared to CLM3.5. The use of either Emmanuel or Grell scheme has been recommended as appropriate for simulating tropical convection (Davis *et al*., 2009; Pal *et al*., 2007) because of its overall better performance.

In this study, eleven numerical experiments were conducted with RegCM4 (Table 3.5). The first eight experiments (***PRES***, ***PRESd1, FUTU***, **FUTU*d1, COAG***, ***COAGd1***, ***GUSAG*** and ***GUSAGd1***) were integrated over a smaller Africa domain (Fig. 3.3a) while the last three experiments (***PRESd2***, ***FUTUd2*** and ***GUSAGd2***) were integrated over the Coordinated Regional Climate Downscaling Experiment (CORDEX) recommended domain for Africa (Fig. 3.3b) so as to determine the impact of domain size on the dynamic vegetation simulations. CORDEX is an initiative by the World Climate Research Program whose principal goal is to coordinate the international effort in regional climate downscaling, thereby improving on the results from past projects (Giorgi *et al*., 2009; Jones *et al*., 2011).

The historical climate (1979-2004) was simulated and denoted as ***PRES***, ***PRESd1*** and ***PRESd2***. ***PRES*** is the output from the prescribed vegetation simulation while ***PRESd1*** and ***PRESd2*** are outputs of the dynamic vegetation simulations. Future climate (2029-2054; RCP4.5) simulations were represented as ***FUTU***, **FUTU*d1*** and ***FUTUd2***. **FUTU*d1*** and ***FUTUd2*** are the dynamic vegetation simulations output while ***FUTU*** is the output from the prescribed vegetation simulation. The historical and future climate simulations use the default prescribed plant functional types in CLM4.5 (Fig. 3.4).

The sensitivity experiments which investigate the impact of agri-silviculture on the future climate of West Africa are represented as ***COAG***, ***COAGd1***, ***GUSAG***, ***GUSAGd1*** and ***GUSAGd2***. Figures 3.5 and 3.6 compare the percentage cover of modified PFTs with the model's default PFTs over the study area in **COAG** and **GUSAG** experiments. However, with the dynamic vegetation enabled simulations (**GUSAG, GUSAG*d1* and GUSAG*d2***), the establishment or survival of a given PFT is dependent on the bioclimatic limit specified in the model (Table 3.4). The model set-up tuning for the eleven experiments is presented in Table 3.5.

Table 3.5: Summary of RegCM4 numerical experimental set-up

Experiment	Brief description	Modified PFTs	Modified zone
PRES	Prescribed vegetation simulation of historical climate (1979-2004) over a smaller domain size	None	None
PRES*d1*	Dynamic vegetation simulation of historical climate (1979-2004) over smaller Africa domain	None	None
FUTU	Prescribed vegetation simulation of future climate (2029-2054; RCP4.5 scenario) over smaller Africa domain	None	None
FUTU*d1*	Dynamic vegetation simulation of future climate (2029-2054; RCP4.5 scenario) over smaller Africa domain	None	None
COAG	Prescribed vegetation simulation of future climate (2029-2054; RCP4.5 scenario) over smaller Africa domain. The PFTs along West Africa Coastal zone is modified in this simulation.	Broadleaf deciduous tree was set to 30% C3 crop was set to 70%	4.51°N to 12.91°N; 16.60°W to 12.60°E;
COAGd1	Dynamic vegetation simulation of future climate (2029-2054; RCP4.5 scenario) over smaller Africa domain. The PFTs along West Africa Coastal zone is modified in this simulation.	Broadleaf deciduous tree was set to 30% C3 crop was set to 70%	4.51°N to 12.91°N; 16.6°W to 12.91° E
GUSAG	Prescribed vegetation simulation of future climate (2029-2054; RCP4.5 scenario) over smaller Africa domain. The PFTs along West Africa Guinea Savanna zone is modified in this simulation.	Broadleaf deciduous tree was set to 30% C4 grass was set to 60% C3 grass was set to 10%	6°N to 12°N; 15° W to 20°E
GUSAGd1	Dynamic vegetation simulation of future climate (2029-2054; RCP4.5 scenario) over smaller Africa domain. The PFTs along West Africa Guinea Savanna zone is modified in this simulation.	Broadleaf deciduous tree, C4 grass and C3 grass were set to begin at 30% , 60% and 10% respectively	6°N to 12°N; 15°W to 20°E
PRES*d2*	Dynamic vegetation simulation of historical climate (1979-2004) over CORDEX Africa domain	None	None
FUTU*d2*	Dynamic vegetation simulation of future climate (2029-2054; RCP4.5 scenario) over CORDEX Africa domain	None	None
GUSAGd2	Dynamic vegetation simulation of future climate (2029-2054; RCP4.5 scenario) over CORDEX Africa domain size. The PFTs along West Africa Guinea Savanna zone is modified in this simulation.	broadleaf deciduous tree was set to 30% C4 grass was set to 60% C3 grass was set to 10%	6° N to 12° N; 15°W to 20° E

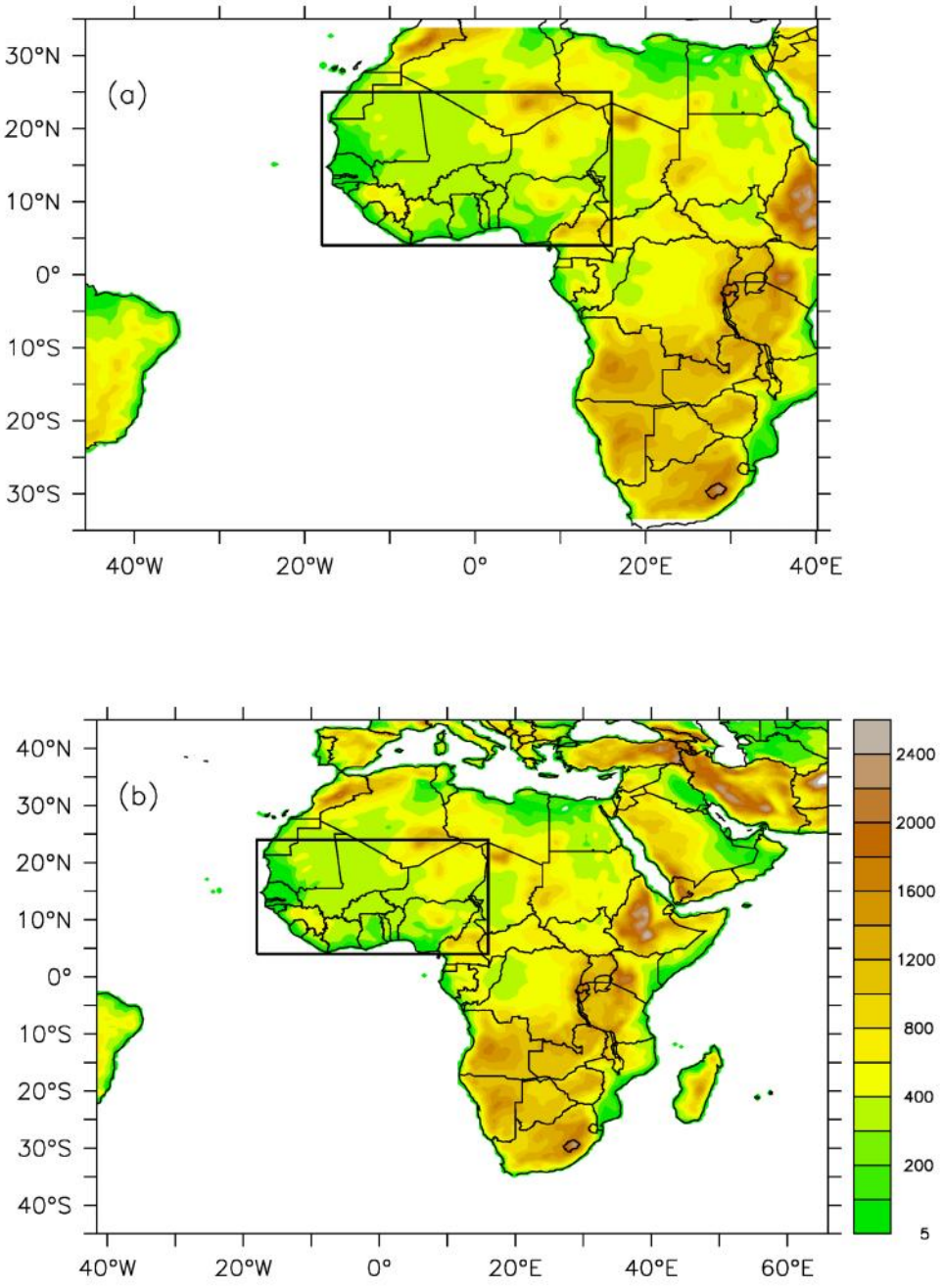

Fig. 3.3: Simulation domain and topography (m) (a) Smaller Africa domain (b) CORDEX Africa domain

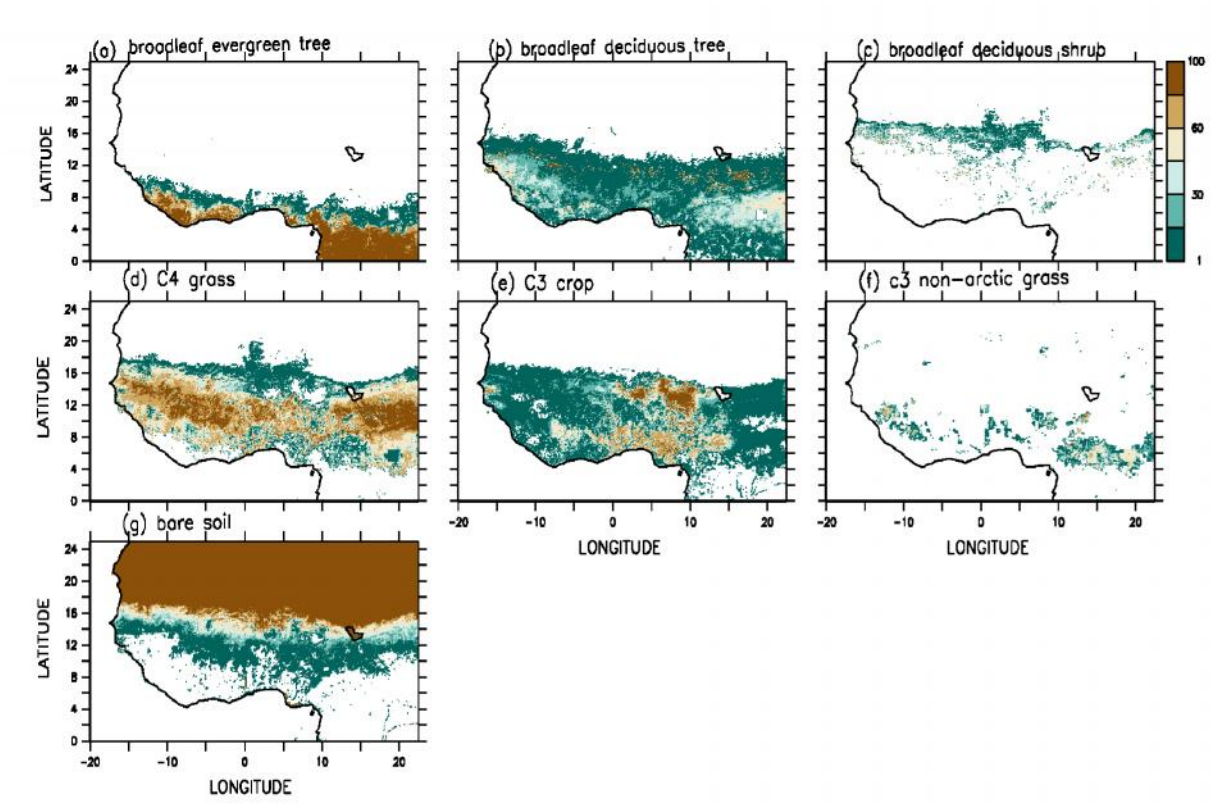

Fig. 3.4: Percentage cover of prescribed plant functional types (PFTs) over West Africa in the Community Land Model version 4.5

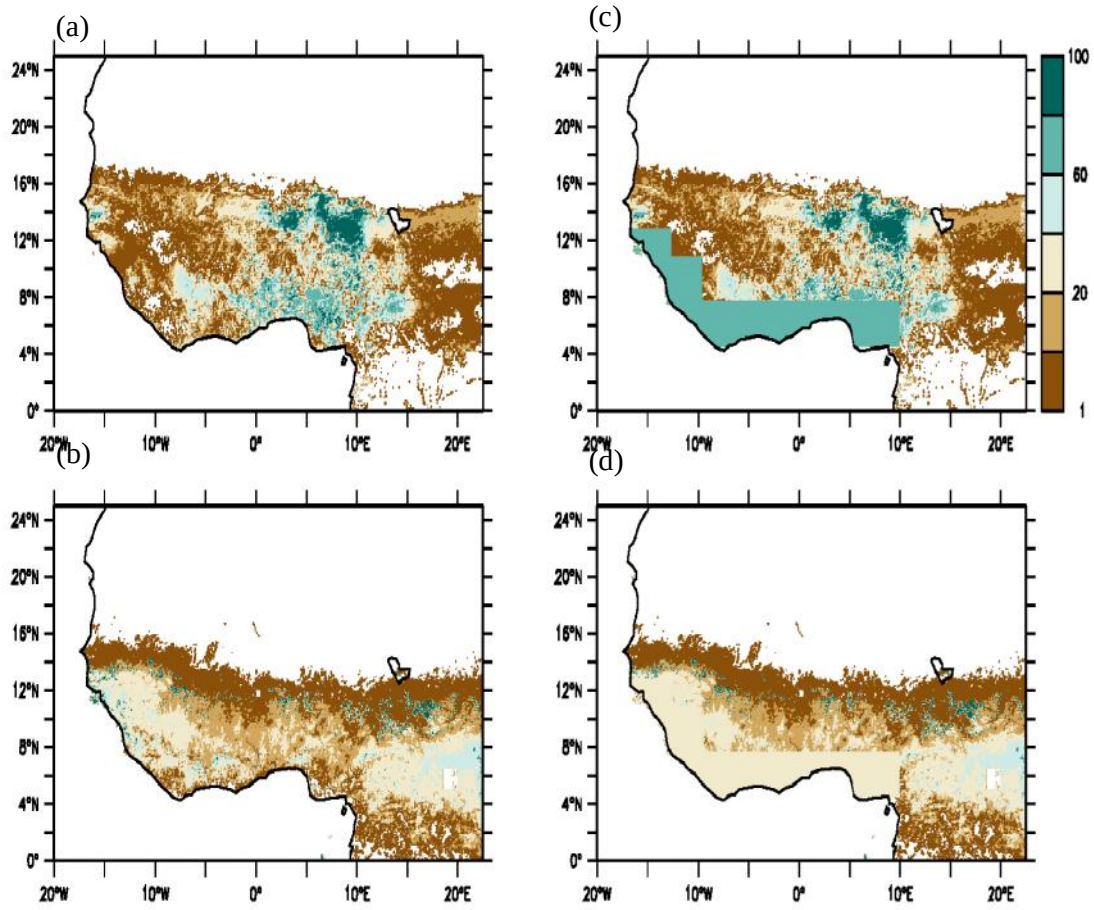

Fig. 3.5: Comparison between the model's default percentage cover of (a) C3 crop (b) broadleaf deciduous tree and the modified (c) C3 crop 70% (d) broadleaf deciduous tree 30% in COAG and COAG*d1* Experiment

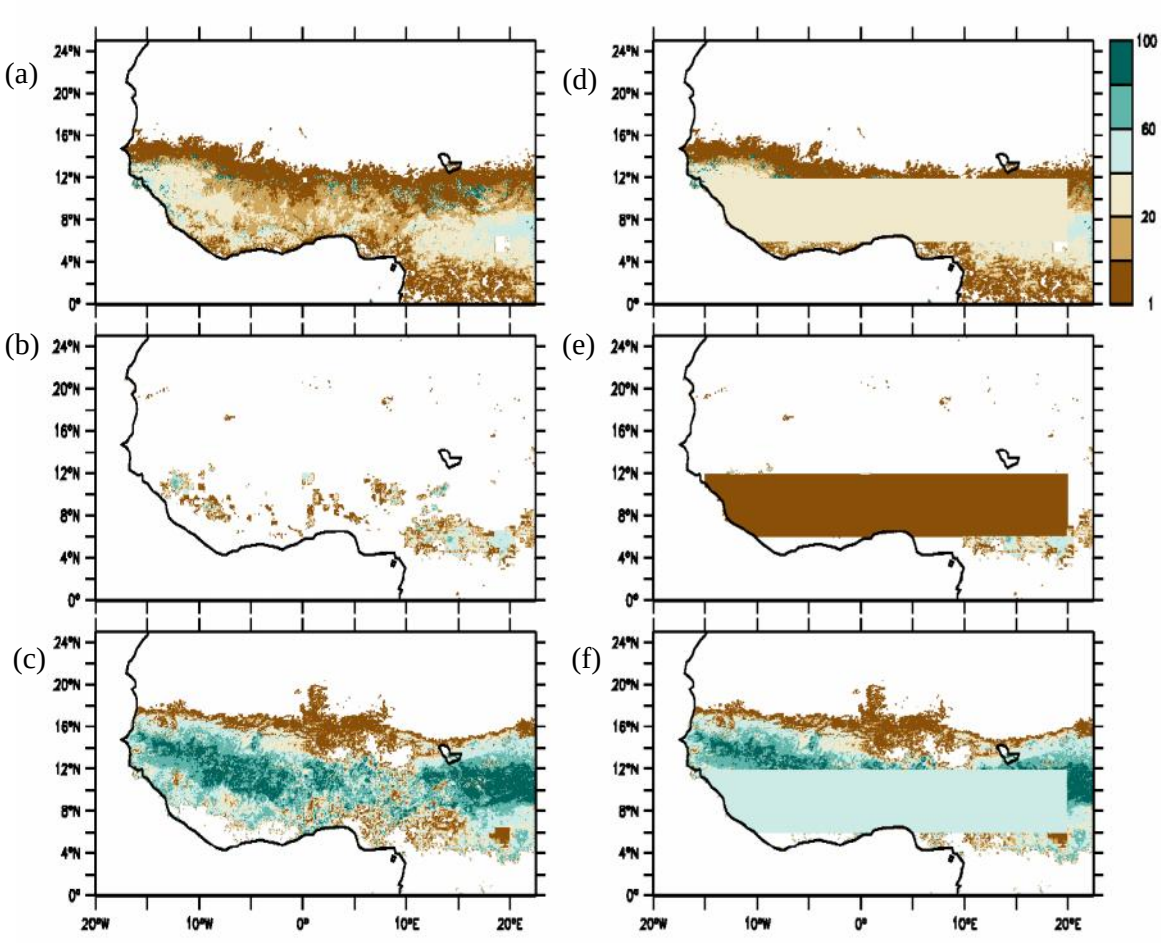

Fig. 3.6: Comparison between the model's default percentage cover of (a) broadleaf deciduous tree (b) C3 grass (c) C4 grass and the modified (d) broadleaf deciduous tree 30% (e) C3 grass 10% (f) C4 grass 60% in GUSAG, GUSAGd1 and GUSAGd2 experiment

CHAPTER FOUR

RESULTS AND DISCUSSION

4.1 Evaluation of RegCM4 Land Surface Schemes Over West Africa

The influence of four different land surface parameterizations in RegCM4 on the climate of West Africa with respect to the convective scheme and boundary forcing employed in this study is evaluated. Each of the four land surface schemes option in RegCM4 reproduces the pattern of the monthly variation of precipitation and temperature quite well (Fig. 4.1) with a strong pattern correlation coefficient (greater than 0.8), but not without some biases. Similarly, the transportation of cool moist southwesterly components of the wind from the ocean to about 16 °N in JJA was adequately represented in each of the four schemes (Fig. 4.2). This corresponds with the simulated ocean-temperature gradient simulated by the four land surface schemes.

The four land surface schemes depict the three phases (onset, peak and cessation) of West Africa monsoon reasonably well in agreement with observations and previous studies (Fig.4.1b; Abiodun *et al.,* 2012, Gbobaniyi *et al.,* 2014) although BATS grossly overestimated the magnitude of each of these phases. However, the temperature is underestimated by each of the four schemes in all months by more than 2°C (Fig. 4.1a). The differences between simulated precipitation in BATS and CLM schemes has been attributed to the characteristic drier soils and increased evapotranspiration per unit precipitation in the Community Land Model scheme (Steiner *et al.,* 2009). However, the performance of the schemes differs for each season considered.

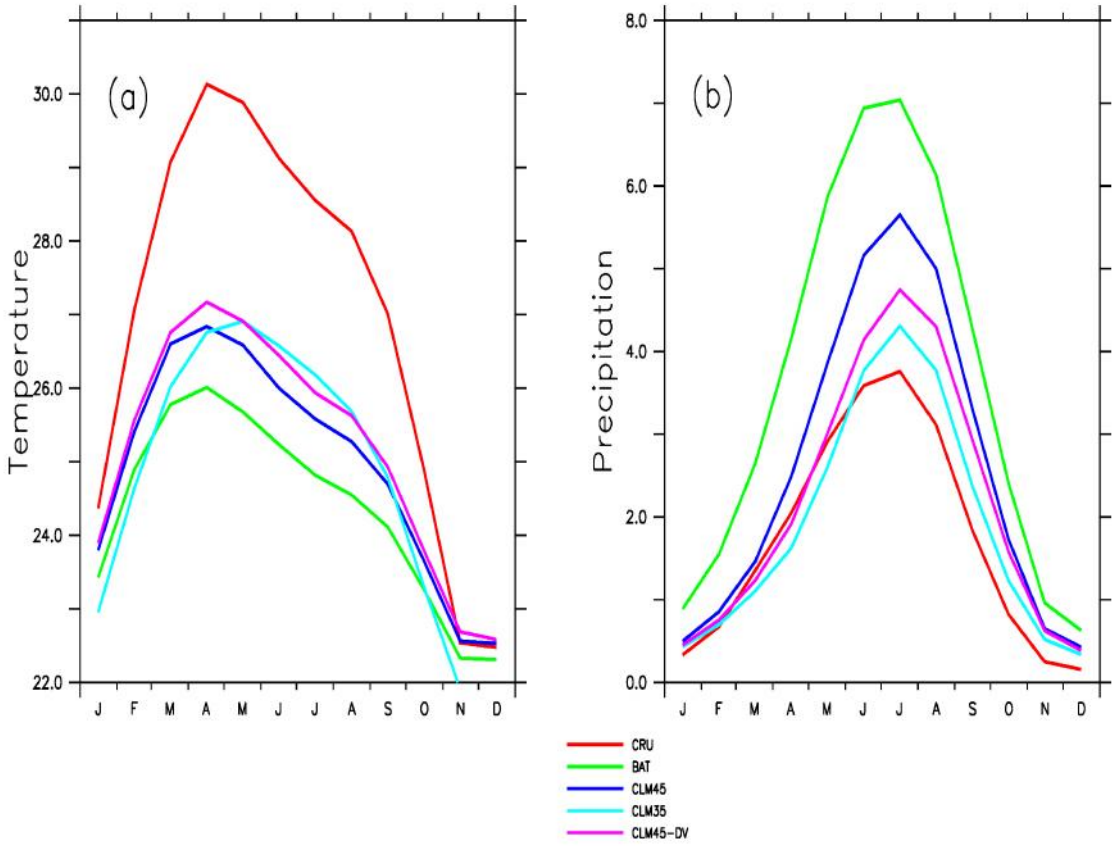

Fig. 4.1: Monthly variation in observed and simulated (a) surface 2m temperature (°C) (b) precipitation (mm/day) averaged over (2°N-24°N, 20°W-20°E) for the year 1980-1983

Tables 4.1 and 4.2 summarize the magnitude of the biases for each scheme in each season as well as the pattern correlation and root mean square difference values. For instance, model simulations result averaged for the entire West Africa region show the Community Land Model Schemes exhibits the lowest cold and wet bias in all seasons in comparison against the Biosphere-Atmosphere Transfer Scheme.

Figure 4.2 presents the spatial distribution of June to August (JJA) temperature and precipitation across West Africa while the corresponding distribution of the biases is presented in Fig. 4.3. The temperature gradient is reasonably simulated by all the schemes. Temperature increases inland from the coasts in a zonal pattern which is similar to the decrease in precipitation from the coast to the inland areas. This compares well with observation. Similarly, the four schemes were able to identify the areas of maximum precipitation along the coastal region of Guinea Republic, Guinea Bissau, Sierra Leone and Liberia. However, BAT scheme overestimates precipitation over a larger area compared to the other three schemes.

Table 4.1: Mean Bias (MB; °C), Root Mean Square Difference (RMSD; mm/day) and Pattern Correlation (PCC) between simulated temperature (BATS land surface scheme, BATS; CLM3.5 land surface scheme, CLM35; CLM4.5 land surface scheme, CLM45; CLM4.5 Dynamic vegetation; CLM4.5DV) and CRU observation averaged over 1980–1983 across West Africa region.

	DJF			MAM			JJA			SON		
Schemes	MB	RMSD	PCC	MB	RMSD	PCC	MB	RMSD	PCC	MB	RMSD	PCC
BATS	-0.15	0.10	0.98	-3.03	0.45	0.99	-3.65	0.53	0.99	-3.44	0.50	0.90
CLM35	-0.70	0.15	0.98	-2.77	0.40	0.98	-2.31	0.34	0.98	-2.34	0.34	0.94
CLM45	-0.07	0.11	0.95	-2.21	0.33	0.99	-2.84	0.42	0.99	-2.75	0.39	0.81
CLM4.5DV	-0.13	0.10	0.98	-1.94	0.29	1.00	-2.39	0.35	0.98	-2.47	0.36	0.73

Table 4.2: Mean Bias (MB; mm/day), Root Mean Square Difference (RMSD; mm/day) and Pattern Correlation (PCC) between simulated precipitation (BATS land surface scheme, BATS; CLM3.5 land surface scheme, CLM35; CLM4.5 land surface scheme, CLM45; CLM4.5 Dynamic vegetation; CLM4.5DV) and CRU observation averaged over 1980–1983 across West Africa region.

	DJF			MAM			JJA			SON		
SCHEMES	MB	RMSD	PCC	MB	RMSD	PCC	MB	RMSD	PCC	MB	RMSD	PCC
BATS	0.47	0.07	0.77	1.21	0.18	0.98	3.14	0.46	0.71	2.83	0.41	0.92
CLM35	0.18	0.07	0.73	-0.33	0.05	0.98	-0.03	0.05	0.99	0.41	0.06	0.95
CLM45	0.27	0.04	0.43	0.07	0.02	0.98	1.29	0.19	0.98	1.46	0.21	0.87
CLM4.5DV	0.23	0.04	0.43	-0.14	0.02	0.98	0.37	0.06	0.98	0.82	0.12	0.72

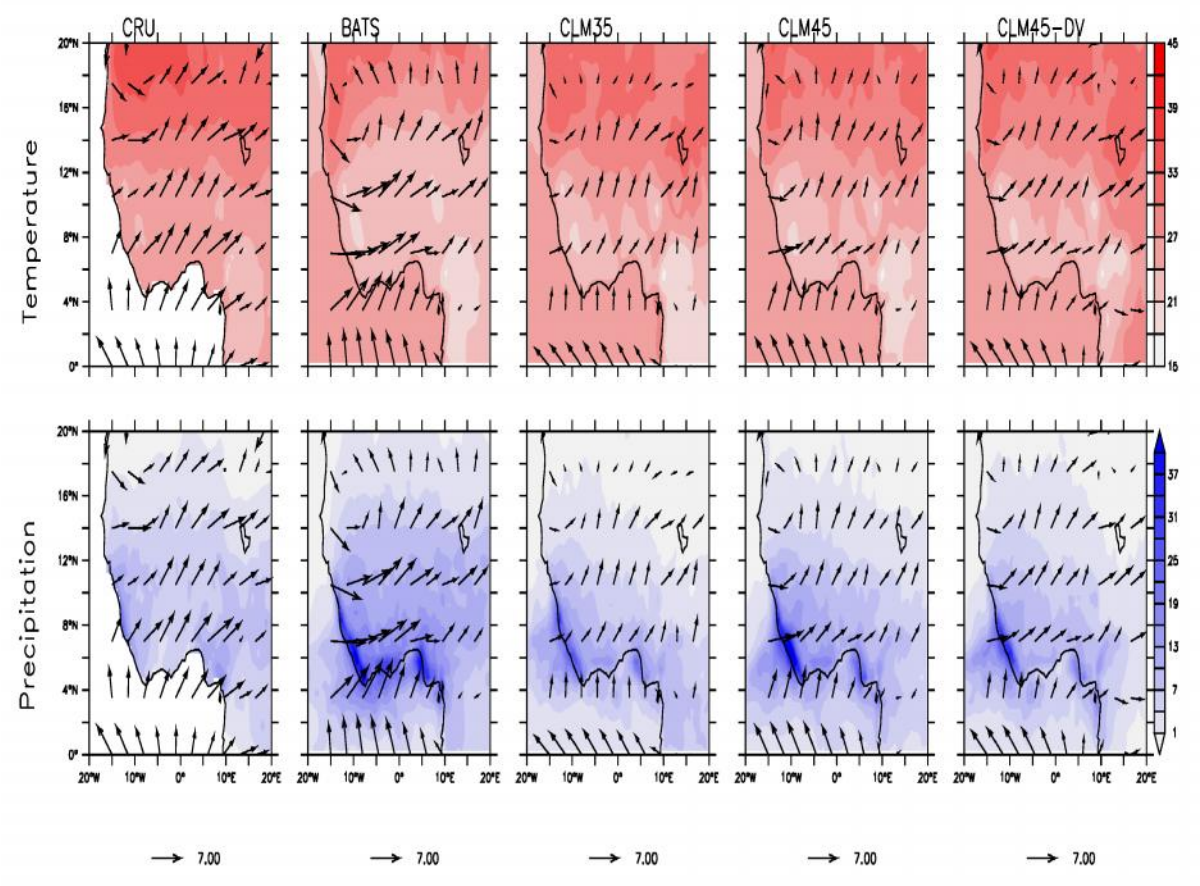

Fig. 4.2: The horizontal distribution of surface (2 m) temperature (°C) and precipitation (mm/day) over West Africa in JJA as indicated in CRU observation, and simulated in RegCM4-BATS scheme (BAT), RegCM4-CLM3.5 scheme (CLM35), RegCM4-CLM4.5 scheme (CLM45) and RegCM4-CLM4.5 dynamic vegetation (Dynamic CLM45). The arrows indicate associated wind speed (meter per second) and direction at 925 hPa level

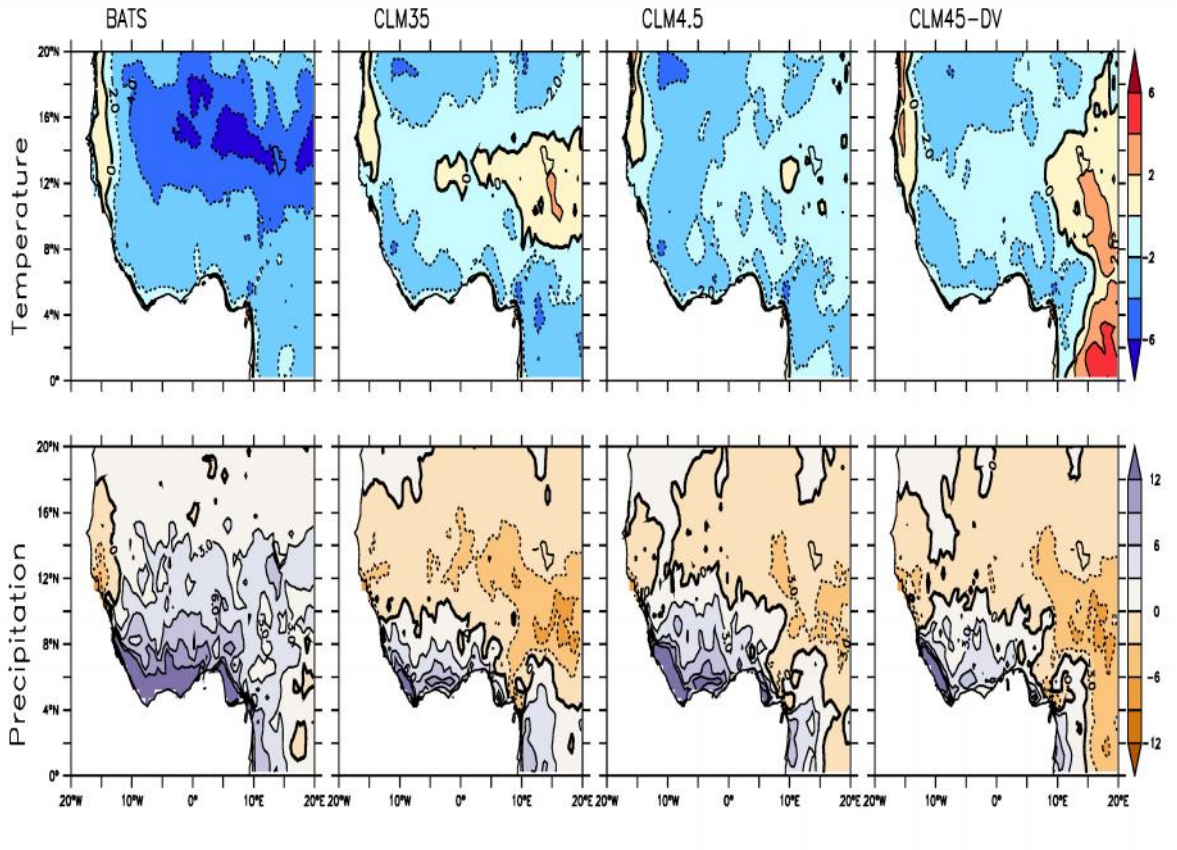

Fig. 4.3: The horizontal distribution of the mean bias in surface (2 m) temperature (°C) and precipitation (mm/day) over West Africa in JJA for RegCM4-BATS scheme (BAT), RegCM4-CLM3.5 scheme (CLM35), RegCM4-CLM4.5 scheme (CLM4.5) and RegCM4-CLM4.5 dynamic vegetation (CLM45-DV).

The essential features of the vertical structure of the monsoon during summer are well reproduced by the four schemes but not without some differences in the magnitude with observations (Fig. 4.4). For instance, BATS overestimate the strength and depth of the monsoon flow while the three versions of the Community Land Model Schemes also exhibit some differences in simulating either the depth of the magnitude of the monsoon flow (e.g. Era-Interim: below 800 hPa, 3 m/s; BATS: below 300 hPa, 7 m/s; CLM3.5: below 800 hPa, 1m/s; CLM4.5: below 500 hPa, 2 m/s; CLM4.5-DV: below 800 hPa, 2 m/s). Similarly, stronger and wider descending motion between 4 and 12°N from the surface to about 200 hPa is simulated all the schemes. However, the intensity of the descending motion is mildest in the CLM4.5-DV scheme. The strength of the Africa Easterly Jet (AEJ) between 500 and 700 hPa is underestimated in all the schemes by 2 - 4 m/s. This may be attributed to weak temperature gradient simulated between the Sahara and equatorial Africa in each of the four schemes (Abiodun *et al*., 2008; Sylla *et al*., 2010a). On the other hand, the Tropical Easterly Jet (TEJ) at 200 hPa is reasonably simulated but the three versions of the Community Land Model schemes simulate weaker TEJ while BATS simulate a stronger TEJ (e.g. Era-Interim: 13 m/s; BATS: 15 m/s; CLM3.5: 7 m/s; CLM4.5: 9 m/s; CLM4.5-DV: 8 m/s).

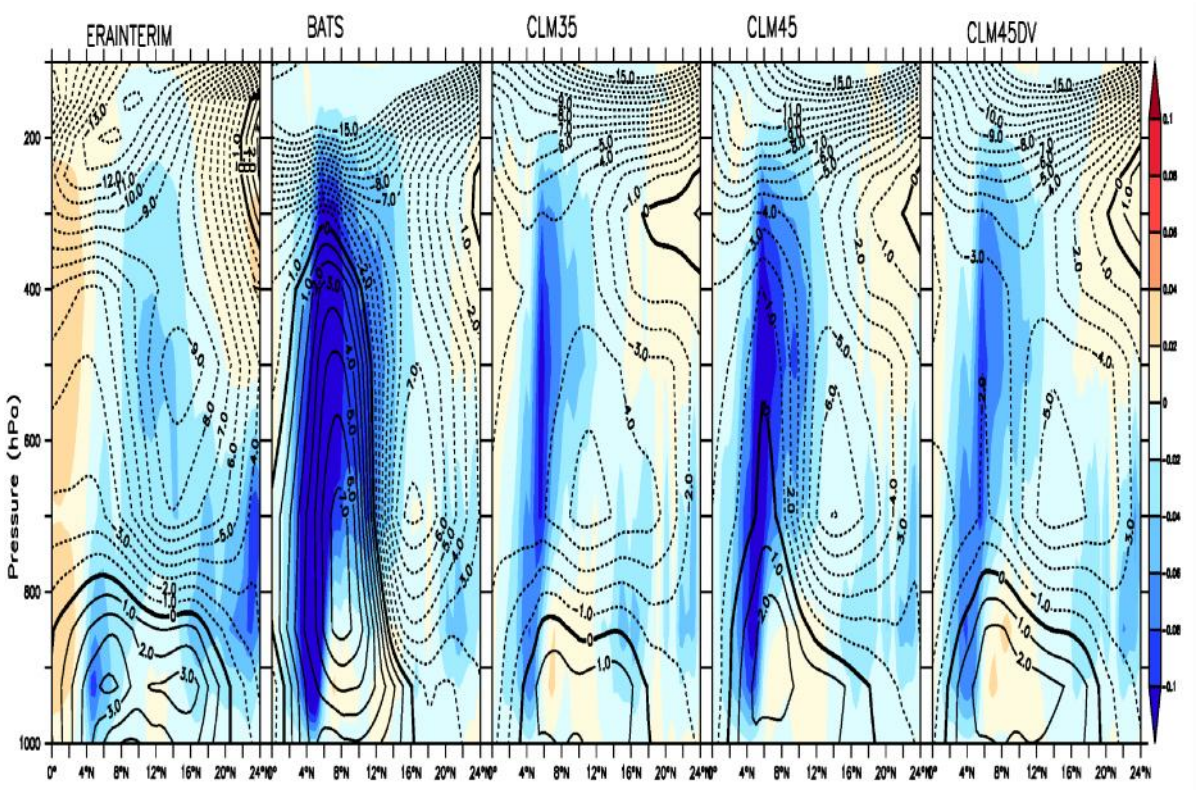

Fig. 4.4: Vertical structure of the zonal component of wind (u, m/s) averaged between 10°W and 10°E over West Africa in August as indicated in (a) Era-Interim (b) RegCM4-BATS (c) RegCM4-CLM3.5 (d) RegCM4-CLM4.5 (e) RegCM4-CLM4.5 Dynamic Vegetation. The shadings indicate the corresponding vertical wind component (ω, Pa/s).

Generally, compared to BATS, Community Land Model schemes proves to be the most suitable for the convective scheme chosen in the model configuration in terms of simulating temperature, precipitation and winds. This agrees with earlier findings which showed that Community Land Model schemes coupled with regional climate model provide an improvement on West Africa climate simulation compared to Biosphere-Atmosphere Transfer Scheme (e.g. Steiner *et al*., 2009, Wang *et al*., 2016). Therefore, for the climate simulation and experimental studies in this research, the CLM4.5 land surface scheme was preferred and integrated for all RegCM4 simulations.

4.2 Evaluation of RegCM4-CLM4.5 Model over West Africa

In this section, we evaluate both the prescribed and dynamic vegetation capabilities of CLM4.5 coupled to RegCM4 in reproducing the historical climate (1980-2004) over West Africa region using smaller Africa and CORDEX recommended Africa domain. This was carried out by comparing the spatial and annual distribution of simulated precipitation, temperature and winds with observed and reanalysis data. The observation data is available for comparison only over land, hence RegCM4 surface data output over the ocean is not used for the model validation. The capability of the model to simulate other components of the West Africa monsoon system (e.g. The Inter-Tropical Convergence Zone, African Easterly Jet and Tropical Easterly Jet) was also investigated. The surface position of the ITCZ is determined using the location of zero meridional wind (Abiodun *et al*., 2012; Flaounas *et al*., 2011). AEJ is identified as the maximum westerly zonal winds at 700 hPa while TEJ is the maximum westerly zonal winds at 200 hPa.

Figure 4.5 shows the time-latitude plots of temperature and precipitation average over West Africa region between 10°E and 10°W for CRU observations, and the three RegCM4 simulations. The pattern of simulated annual mean 2-m temperature at each latitude compares fairly well with CRU observations. **PRES**, **PRES*d1*** and **PRES*d2*** simulations reproduce the temperature regimes from the coast to 24°N well. The three phases of the West Africa monsoon precipitation characterized by onset, peak and cessation periods (Le Barbe *et al*., 2002) are well reproduced in the three simulations (Fig. 4.5) but not without some differences. CRU indicates the onset period commences from April to June and extends from the coast to about 7°N while the peak period of precipitation commences with the jump in the rain belt, a phenomenon known as the monsoon jump (Sultan and Janicot, 2003) from June to August at 9°N -14°N. Thereafter, cessation of the precipitation period begins in September resulting in the southward retreat of the rain belt to the Guinea region.

However, **PRES, PRES*d1*** and **PRES*d2*** simulated late onset and early cessation of monsoon precipitation. The onset of simulated precipitation period occurs between May and June while cessation of precipitation occurs in October. The model was unable to capture the observed monsoon jump in precipitation from June to August. The three simulations overestimate the intensity of the monsoon precipitation from June to August south of 8°N, but the migration pattern and peak position of the ITCZ over the thermal heat low at around 20°N in July/August are well represented in the simulations. The differences between observed and simulated phases of the monsoon precipitation have been attributed to the model's limited ability to adequately represent some essential features of the West African climate system such as monsoon flow, African Easterly Jet and Tropical Easterly Jet (TEJ) (Diallo *et al*., 2012). The area-averaged monthly temperature and precipitation climatology over the entire West Africa region compare the variability in the annual cycle of observations with

RegCM4 simulations (Fig. 4.6). The annual cycles of temperature for all the three simulations (Fig. 4.6a) show cold biases

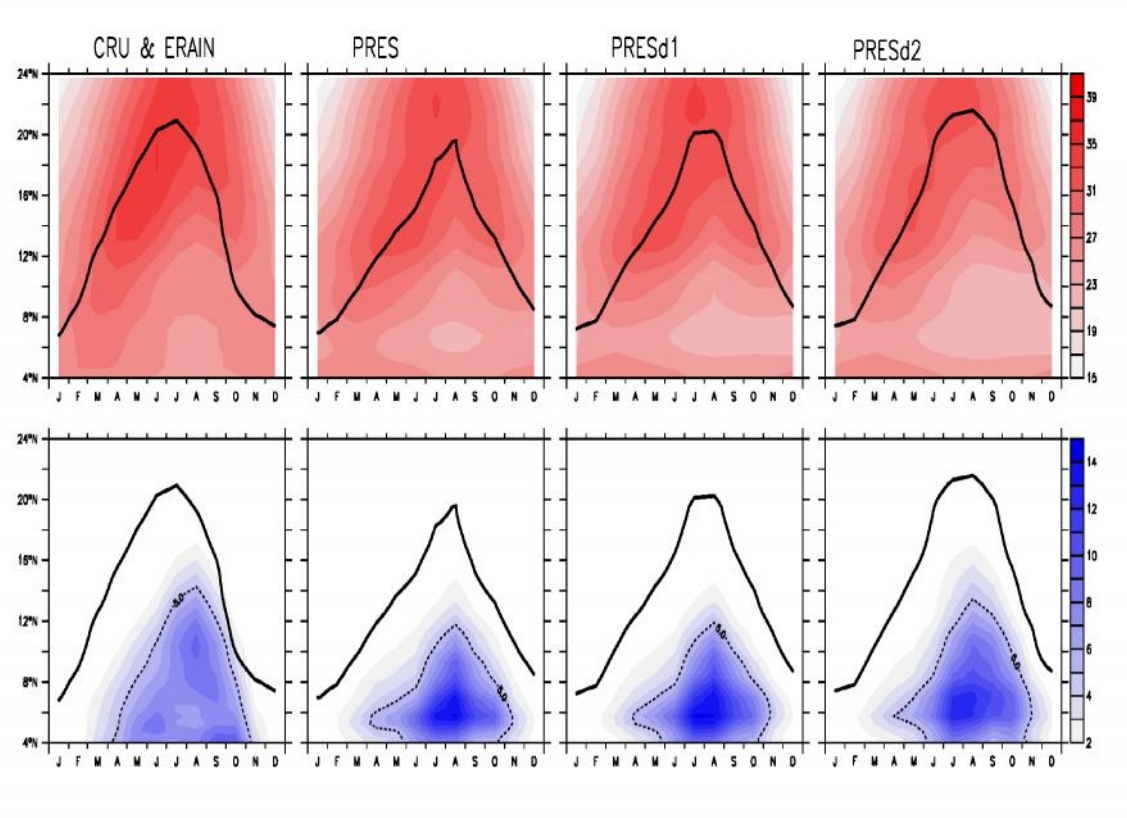

Fig. 4.5: The time–latitude cross-section of surface (2 m) temperature (°C; first row) and precipitation (mm/day; second row), averaged between 15°E to 15°W for the years (1980-2004) over West Africa as observed in CRU and ERAIM; first column) and simulated (prescribed vegetation, second column; dynamic vegetation, third column; dynamic CORDEX domain, fourth column). The corresponding surface position of ITCZ (thick continuous lines) and the onset of monsoon precipitation (i.e., isohyet of 5mm/day; thin dashed lines) are shown.

within the range of 1 to 2°C from January to October except in November and December that the three simulations appear closer to observation. **PRES*d2*** has the greatest negative bias (greater than 2°C) while **PRES** has the lowest cold bias of -0.76°C over the region (see Table 4.3). The precipitation pattern over West Africa in all the three simulations appears closer to observations from January to September with dry and wet biases less than 1 mm/day (see Table 4.7). The three simulations reproduce fairly well the peak of the precipitation in August but with some differences in magnitude for both **PRES*d1*** and **PRES** simulations. **PRES** and **PRES*d1*** underestimate the magnitude of the peak precipitation but **PRES*d2*** fully represent the magnitude of the peak precipitation when compared with observations (Fig. 4.6b).

The performance of **PRES, PRES*d1*** and **PRES*d2*** to simulate temperature and precipitation over the entire West Africa region and sub-regions is presented in Table 4.3 to 4.10. Generally, over West Africa region **PRES** performs best in simulating temperature (Table 4.3) but with precipitation, **PRES*d1*** is preferred (Table 4.7). This selection is based on simulation with the highest pattern correlation coefficient (PCC) and least root mean square difference and bias across all seasons. Similarly, over Guinea region, **PRES*d1*** performs best in simulating precipitation, but **PRES** performs best for temperature simulation over the region. However, this assessment is not applicable to West Africa subregions because each of the simulation has different capabilities in the representation of temperature and precipitation for each season across the sub-regions.

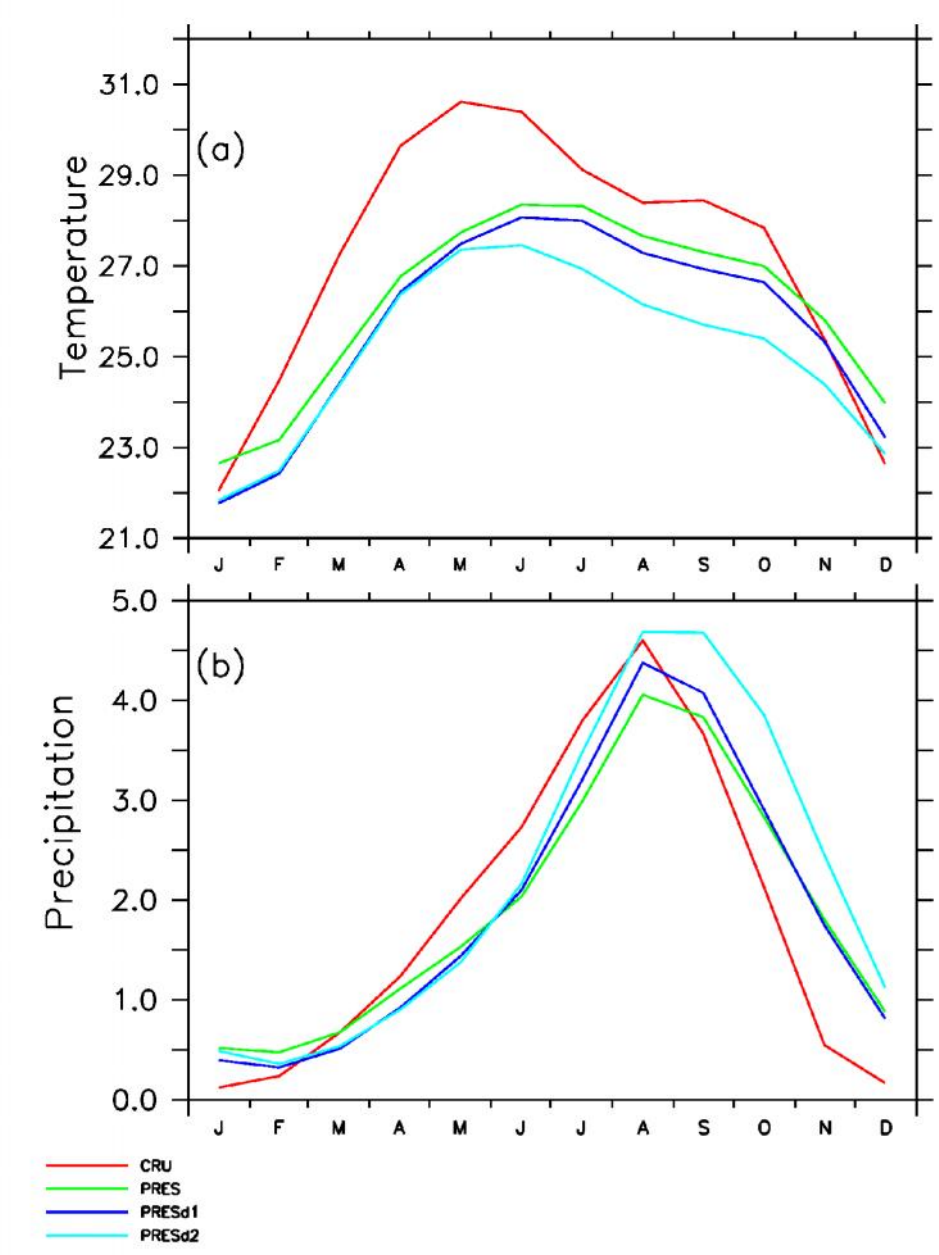

Fig. 4.6: The annual cycle of monthly (a) temperature (°C) and (b) precipitation (mm/day) averaged between 2°N to 24°N and 15°W to 20°E for the period 1980–2004**.**

Table 4.3: Mean Bias (°C), Root Mean Square Difference (RMSD; °C) and Pattern Correlation (PCC) between observed and simulated temperature over West Africa averaged for the period 1980-2004. Correlations are significant at 95% confidence interval.

Simulation	Evaluation Statistics (West Africa)														
	DJF			MAM			JJA			SON			ANNUAL		
	BIAS	RMSD	PCC	BIAS	RMSD	PCC	BIAS	RMSD	PCC	BIAS	RMSD	PCC	BIAS	RMSD	PCC
PRES	-0.42	1.53	0.93	-1.42	1.98	0.88	-0.56	1.83	0.89	-0.64	1.76	0.83	-0.76	1.78	0.92
PRES*d1*	-1.58	2.34	0.89	-1.86	2.32	0.89	-1.10	1.97	0.94	-1.24	2.25	0.86	-1.44	2.23	0.93
PRESd2	-2.07	2.29	0.86	-2.7	2.49	0.84	-3.08	2.82	0.92	-3.17	2.98	0.82	-2.75	2.66	0.91

Table 4.4: Mean Bias (°C), Root Mean Square Difference (RMSD; °C) and Pattern Correlation (PCC) between observed and simulated temperature over West Africa Sahel region for the period 1980-2004.

Simulation	Evaluation Statistics (Sahel)															
	DJF			MAM			JJA			SON			Annual			
	BIAS	RMSD	PCC	BIAS	RMSD	PCC	BIAS	RMSD	PCC	BIAS	RMSD	PCC	BIAS	RMSD	PCC	
PRES	-0.82	1.43	0.92	-1.75	2.16	0.87	-1.24	1.87	0.73	-0.92	1.35	0.90	-1.18	1.78	0.97	
PRES*d1*	-1.45	1.86	0.93	-1.58	2.04	0.87	-1.02	1.78	0.70	-0.93	1.36	0.91	-1.25	1.79	0.97	
PRES*d2*	-1.34	1.65	0.90	-1.82	1.99	0.83	-2.79	2.86	0.62	-2.00	2.03	0.83	-1.99	2.19	0.96	

Table 4.5: Mean Bias (°C), Root Mean Square Difference (RMSD; °C) and Pattern Correlation (PCC) between observed and simulated temperature over West Africa Savanna region for the period 1980-2004.

Simulation	Evaluation Statistics (Savanna)														
	DJF			MAM			JJA			SON			ANNUAL		
	BIAS	RMSD	PCC	BIAS	RMSD	PCC	BIAS	RMSD	PCC	BIAS	RMSD	PCC	BIAS	RMSD	PCC
PRES	0.43	1.11	0.87	-1.13	1.61	0.66	0.57	1.47	0.84	0.48	1.56	0.74	0.09	1.42	0.86
PRES*d1*	-0.47	1.32	0.85	-1.57	1.93	0.73	-0.06	1.13	0.89	0.09	1.33	0.79	-0.50	1.44	0.88
PRESd2	-0.95	1.28	0.70	-2.56	2.39	0.73	-2.67	2.47	0.87	-3.01	2.88	0.82	-2.30	2.315	0.86

Table 4.6: Mean Bias (°C), Root Mean Square Difference (RMSD; °C) and Pattern Correlation (PCC) between observed and simulated temperature over West Africa Guinea region for the period 1980-2004.

Simulation	Evaluation Statistics (Guinea)														
	DJF			MAM			JJA			SON			ANNUAL		
	BIAS	RMSD	PCC	BIAS	RMSD	PCC	BIAS	RMSD	PCC	BIAS	RMSD	PCC	BIAS	RMSD	PCC
PRES	-0.64	1.90	0.57	-1.09	1.99	0.85	-0.93	2.17	0.67	-1.34	2.41	0.60	-0.99	2.12	0.74
PRES*d1*	-2.83	3.45	0.59	-2.42	2.88	0.89	-2.26	2.76	0.80	-3.06	3.65	0.72	-2.63	3.21	0.79
PRESd2	-3.67	3.65	0.54	-3.48	3.24	0.84	-3.46	3.28	0.75	-4.58	4.29	0.73	-3.79	3.63	0.79

Table 4.7: Mean Bias (mm/day), Root Mean Square Difference (RMSD; mm/day) and Pattern Correlation (PCC) between observed and simulated precipitation over West Africa Guinea region for the period 1980-2004.

Simulation	Evaluation Statistics (West Africa)														
	DJF			MAM			JJA			SON			ANNUAL		
	BIAS	RMSD	PCC	BIAS	RMSD	PCC	BIAS	RMSD	PCC	BIAS	RMSD	PCC	BIAS	RMSD	PCC
PRES	0.12	0.49	0.67	-0.14	0.94	0.85	-1.02	2.37	0.76	-0.42	1.39	0.85	-0.33	1.45	0.82
PRES*d1*	0.13	0.37	0.93	-0.10	0.71	0.92	-0.61	2.05	0.82	-0.17	1.07	0.93	-0.21	1.22	0.88
PRESd2	0.16	0.49	0.78	-0.19	0.71	0.89	-0.25	1.76	0.83	0.44	1.12	0.92	0.07	1.09	0.90

Table 4.8: Mean Bias (mm/day), Root Mean Square Difference (RMSD; mm/day) and Pattern Correlation (PCC) between observed and simulated precipitation over West Africa Sahel region for the period 1980-2004.

Simulation	Evaluation Statistics (Sahel)														
	DJF			MAM			JJA			SON			ANNUAL		
	BIAS	RMSD	PCC	BIAS	RMSD	PCC	BIAS	RMSD	PCC	BIAS	RMSD	PCC	BIAS	RMSD	PCC
PRES	0.19	0.22	0.21	0.29	0.32	0.30	-0.02	0.39	0.75	0.16	0.22	0.68	0.16	0.30	0.69
PRESd1	0.06	0.11	0.04	0.15	0.18	0.39	-0.16	0.41	0.84	0.01	0.12	0.81	0.02	0.25	0.77
PRESd2	0.05	0.08	0.15	0.17	0.19	0.66	0.30	0.38	0.91	0.15	0.17	0.88	0.17	0.24	0.90

Table 4.9: Mean Bias (mm/day), Root Mean Square Difference (RMSD; mm/day)and Pattern Correlation (PCC) between observed and simulated precipitation over West Africa Savanna region for the period 1980-2004.

Simulations	Evaluation Statistics (Savanna)														
	DJF			MAM			JJA			SON			ANNUAL		
	BIAS	RMSD	PCC	BIAS	RMSD	PCC	BIAS	RMSD	PCC	BIAS	RMSD	PCC	BIAS	RMSD	PCC
PRES	0.10	0.15	0.45	-0.02	0.32	0.91	-2.37	2.54	0.91	-0.71	0.89	0.91	-0.75	1.38	0.90
PRES*d1*	0.04	0.08	0.42	-0.12	0.36	0.91	-2.23	2.39	0.93	-0.84	0.99	0.91	-0.79	1.34	0.93
PRESd2	0.02	0.06	0.47	-0.09	0.38	0.88	-1.07	1.38	0.91	0.39	0.62	0.95	-0.18	0.74	0.95

Table 4.10: Mean Bias (mm/day), Root Mean Square Difference (RMSD; mm/day) and Pattern Correlation (PCC) between observed and simulated precipitation over West Africa Guinea region for the period 1980-2004.

Simulations	Evaluation Statistics (Guinea)														
	DJF			MAM			JJA			SON			ANNUAL		
	BIAS	RMSD	PCC	BIAS	RMSD	PCC	BIAS	RMSD	PCC	BIAS	RMSD	PCC	BIAS	RMSD	PCC
PRES	0.29	0.62	0.82	-0.64	1.49	0.79	-1.00	3.62	0.56	-0.68	2.41	0.69	-0.51	2.37	0.75
PRESd1	0.28	0.56	0.90	-0.49	1.28	0.88	0.27	2.88	0.56	0.37	1.92	0.80	0.11	1.92	0.84
PRESd2	0.47	0.73	0.79	2.44	2.95	0.67	-0.07	3.05	0.46	1.56	2.19	0.75	0.33	1.99	0.81

The relative strengths of the three experiments (**PRES**, **PRES*d1*** and **PRES*d2***) to simulate the amplitude of the seasonal variation of temperature and precipitation averaged over the entire West Africa region in comparison to the observed data (CRU) can be inferred from Figures 4.7a and 4.7b. Simulated patterns that agree well with observations will lie nearest the point marked "CRU" on the x-axis. **PRES*d2*** simulation of MAM and JJA temperature over West Africa matches closely with observation with the best normalized standard deviation (SD≈ 1.0) and high correlation of 0.80 and 0.92 respectively (Fig. 4.7a). However, in DJF it underestimates the amplitude of temperature variations (SD≈0.9) but overestimates it during SON season (SD≈1.2). With **PRES and PRES*d1*** simulations, the amplitude of temperature variation is overestimated in all the seasons despite having a high correlation that is greater than 0.5. The magnitude of overestimation in DJF and MAM is similar for both **PRES and PRES*d1***. This shows that irrespective of the domain size or state of vegetation (i.e, dynamic or prescribed), the model's simulation of temperature variation over West Africa in DJF and MAM seasons is not improved upon. In contrast, during SON season, there is a marked difference in the magnitude of overestimation of temperature by **PRES** (SD≈1.9), **PRES*d1*** (SD≈1.4) and **PRES*d2*** (SD≈1.2)**.** The performance of the model with respect to the domain size and activation or deactivation of dynamic vegetation in simulating the seasonal variability of temperature averaged over the entire West Africa region varies with each season. However, the larger domain size and activation of dynamic vegetation used in **PRES*d2*** improved on the amplitude variations of temperature as simulated over West Africa in MAM and JJA.

Figure 4.7b presents the performances of the three experiments (**PRES**, **PRES*d1*** and **PRES*d2***) in the simulation of the seasonal variation of precipitation averaged over the entire West Africa region. All the three experiments overestimate precipitation in DJF, JJA and

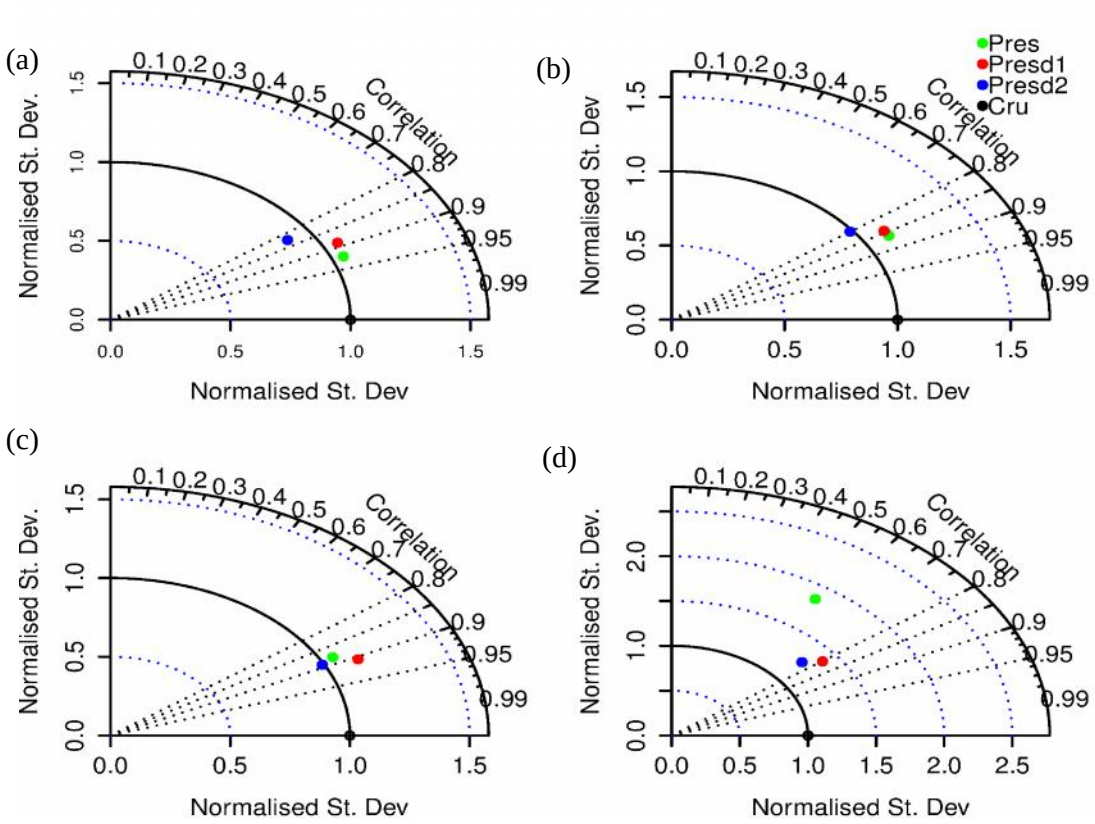

Fig. 4.7a: The Taylor diagram comparing the statistics (i.e., correlation and the normalized standard deviation) of the simulated temperature (°C) with the observation. Standard deviation and correlation are computed for (a) DJF (b) MAM (c) JJA and (d) SON seasons.

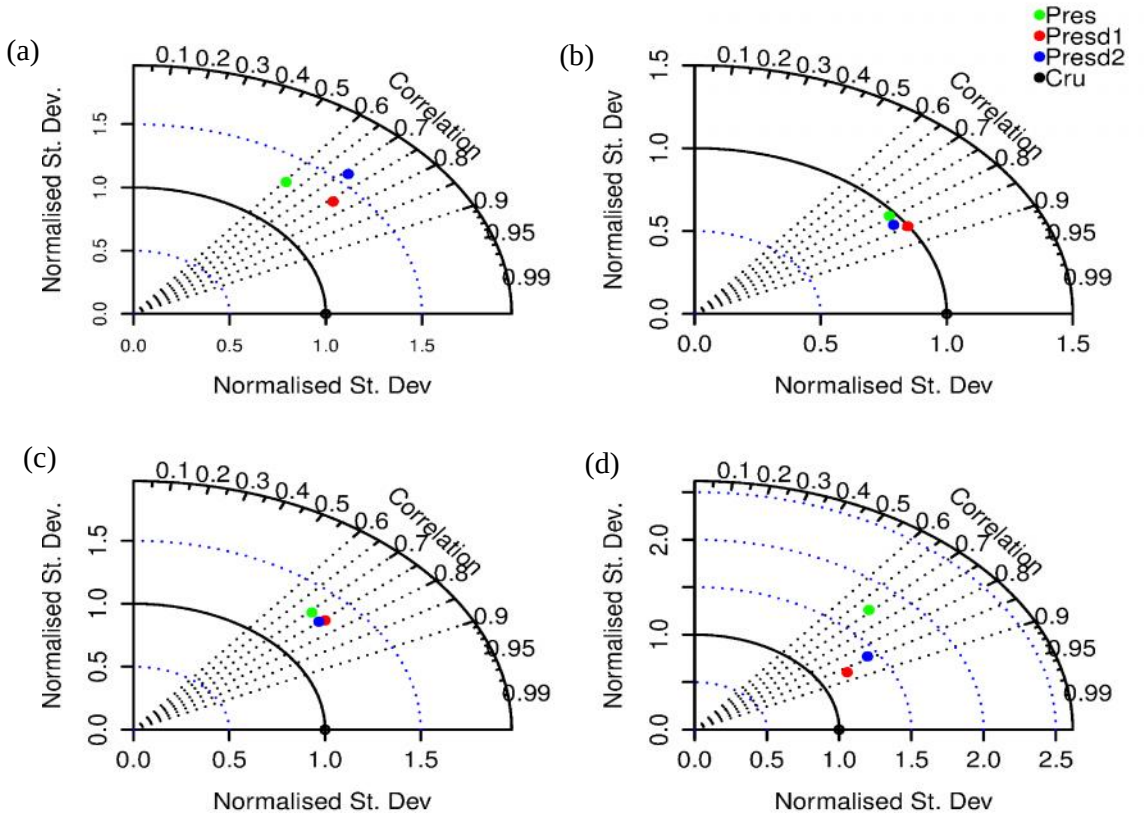

Fig. 4.7b: The Taylor diagram comparing the statistics (i.e., correlation and the normalized standard deviation) of the simulated precipitation (mm/day) with the observation. Standard deviation and correlation are computed for (a) DJF (b) MAM (c) JJA and (d) SON seasons.

SON irrespective of the domain size or state of the vegetation specified in the simulations but with a high correlation that is greater than or equal to 0.6. In JJA, **PRES**, **PRES*d1*** and **PRES*d2*** behave in a similar pattern in overestimating the magnitude of summer precipitation (SD≈1.2)**.** On the other hand, the three experiments perform well in simulating MAM precipitation with a normalized standard deviation that is approximate equal to one and correlation that is greater than 0.7. Therefore, for precipitation simulation in all the seasons, **PRESd*1*** shows the most outstanding results with a high correlation and normalized standard deviation that is closest to observation.

The spatiotemporal distribution of temperature, precipitation and wind for the prescribed and dynamic vegetation simulations in **PRES**, **PRES*d1*** and **PRES*d2*** experiments is compared to observed and reanalysis data (Fig 4.8a and 4.8b). The simulation results reproduce the seasonal evolution of wind, precipitation and temperature regimes well. The transportation of cool moist south-westerly winds from the ocean up to about 18° N during the peak of the monsoon (JJA) as well as the intensification of the north-easterly dry winds in winter compares favourably well with the reanalysis atmospheric wind data. The spatial contrast of temperature and precipitation from the coast to the continent in the three simulations matches closely with CRU observations. Similarly, the simulations capture the observed minimum temperature and maximum precipitation over the orographic region of Guinea Highlands, Jos Plateau and Cameroun Mountains during the peak of the monsoon. However, each of the model simulations exhibits cold and warm biases of about 2°C with an associated wet and dry biases of 1-4 mm/day along the coasts and over the continent (Fig. 4.9 and 4.10). Previous studies with regional climate model using different model configuration and boundary condition also reported similar biases (e.g. Alo and Wang, 2010; Sylla *et al*., 2010a; Abiodun *et al*., 2012; Nikulin *et al*., 2012; Sylla *et al*., 2013b; Gbobaniyi *et al*., 2014; Klutse *et al*., 2014).

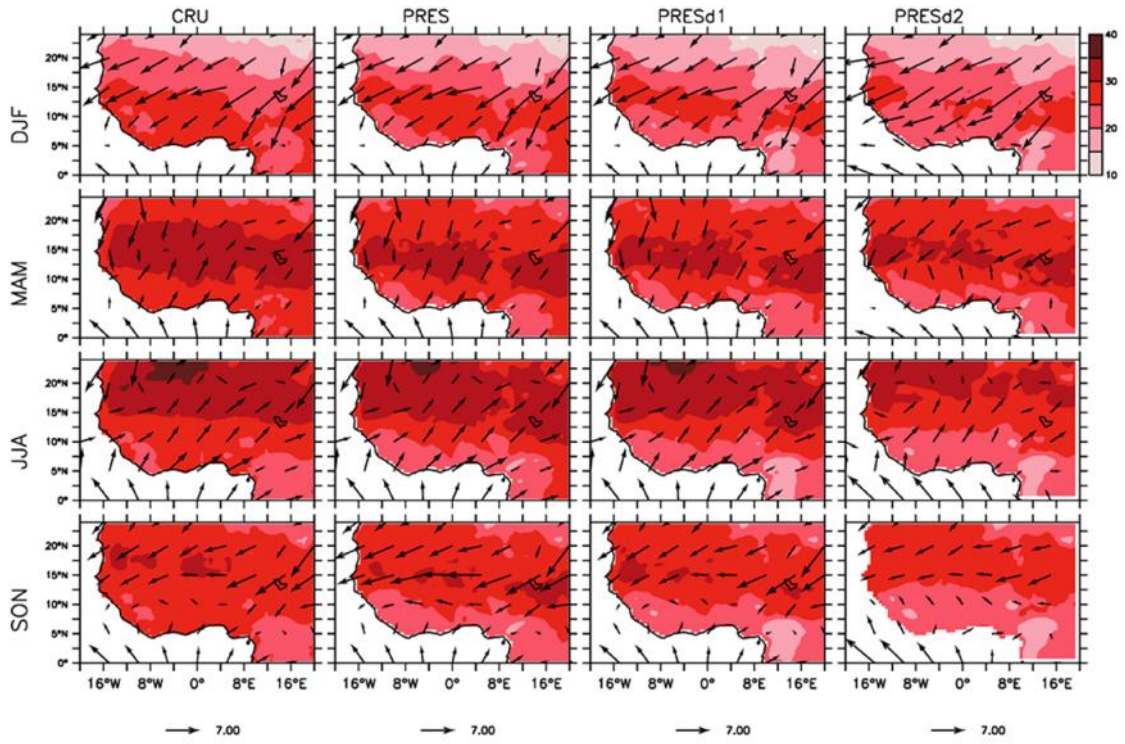

Fig. 4.8a: Spatial distribution of mean seasonal temperature (°C) and 925hpa wind (m/s) averaged for the year 1980-2004 First column; CRU and Era-Interim wind, second column; RegCM4 prescribed vegetation, third column; RegCM4 dynamic vegetation and fourth column; RegCM4 dynamic vegetation CORDEX domain

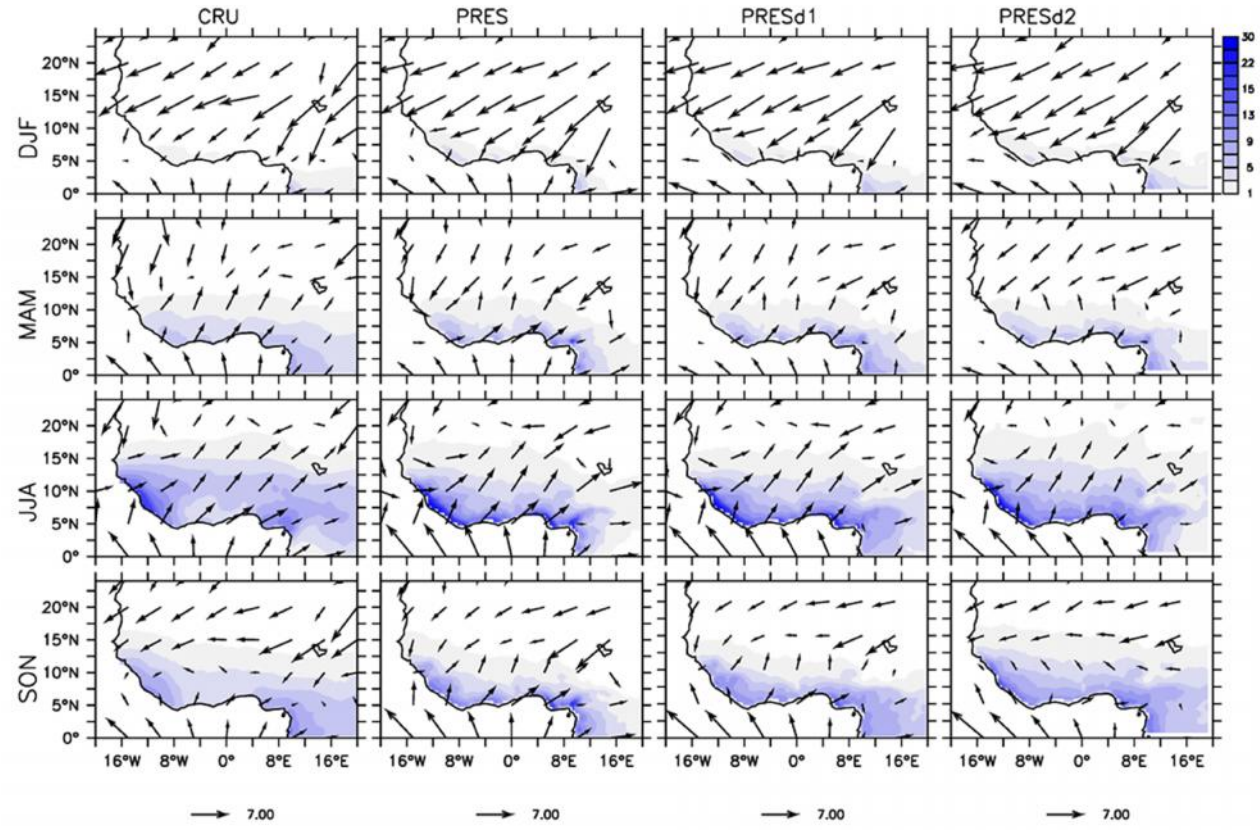

Fig. 4.8b: Spatial distribution of mean seasonal precipitation (mm/day) and 925hpa wind (m/s) averaged for the year 1980-2004. First column; CRU and Era-Interim wind, second column; RegCM4 prescribed vegetation, third column; RegCM4 dynamic vegetation and fourth column; RegCM4 dynamic vegetation CORDEX domain.

PRES simulations exhibited the largest warm bias (2-4°C) south of 14°N within 10°E and 20°E but the bias is reduced to 1°C in **PRES*d1*** (Fig. 4.9). However, the spatial distribution of **PRES*d2*** biases appears colder than the other two simulations. **PRES*d2*** underestimates temperature over most parts of West Africa but **PRES** and **PRES*d1*** underestimate temperature along the coasts, orographic region and north of 18°N.

Precipitation along West African coasts is grossly overestimated (greater than 4 mm/day) in the simulations during JJA and SON seasons but underestimated by the same magnitude over the continent (Fig. 4.10). The pattern of the dry and wet bias is consistent with the temperature biases. The seasonal dry bias in PRES (Fig. 4.10) is reduced by about 2 mm/day in **PRES*d1*** and ***PRESd2***. However, feedback from vegetation dynamics in the regional climate model improves the temperature and precipitation biases of **PRES*d1*** and **PRES*d2*** simulations. The magnitude of the temperature and precipitation biases in all the seasons is not horizontally homogeneous, but these biases are more pronounced in regions with complex terrains, such as the Guinea Highlands, Cameroon Mountains and Jos plateau in Nigeria. This may partly be a result of insufficient observing stations over these complex terrains.

The wet and dry biases along the coast and over the continent may be attributed to the choice of convective scheme employed in the model configuration. Emanuel scheme (Emanuel, 1993), which is applied over the ocean assumes quasi-equilibrium which can lead to the immediate stabilization of convective clouds in the environment as soon as large-scale processes destabilise it. This mechanism enhances more precipitation and thereby result in overestimation of precipitation. Another assumption in the scheme is that mixing within clouds is highly episodic and inhomogeneous. Thus, convective fluxes are based on an idealized model of sub cloud-scale updrafts and downdrafts.

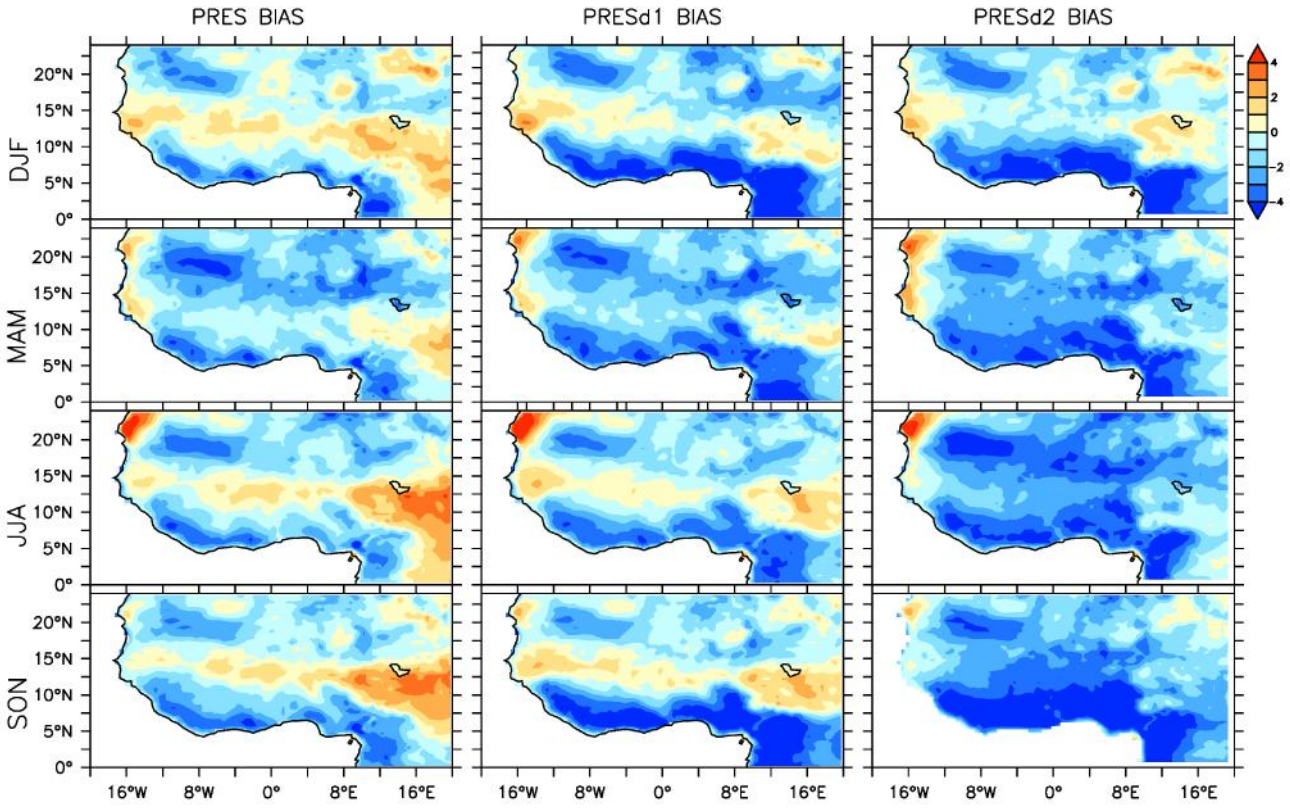

Fig. 4.9: Horizontal distribution of historical temperature biases (Model minus CRU; °C) for each season in RegCM4 prescribed vegetation (first column), dynamic vegetation (second column) and CORDEX domain dynamic vegetation (third column).

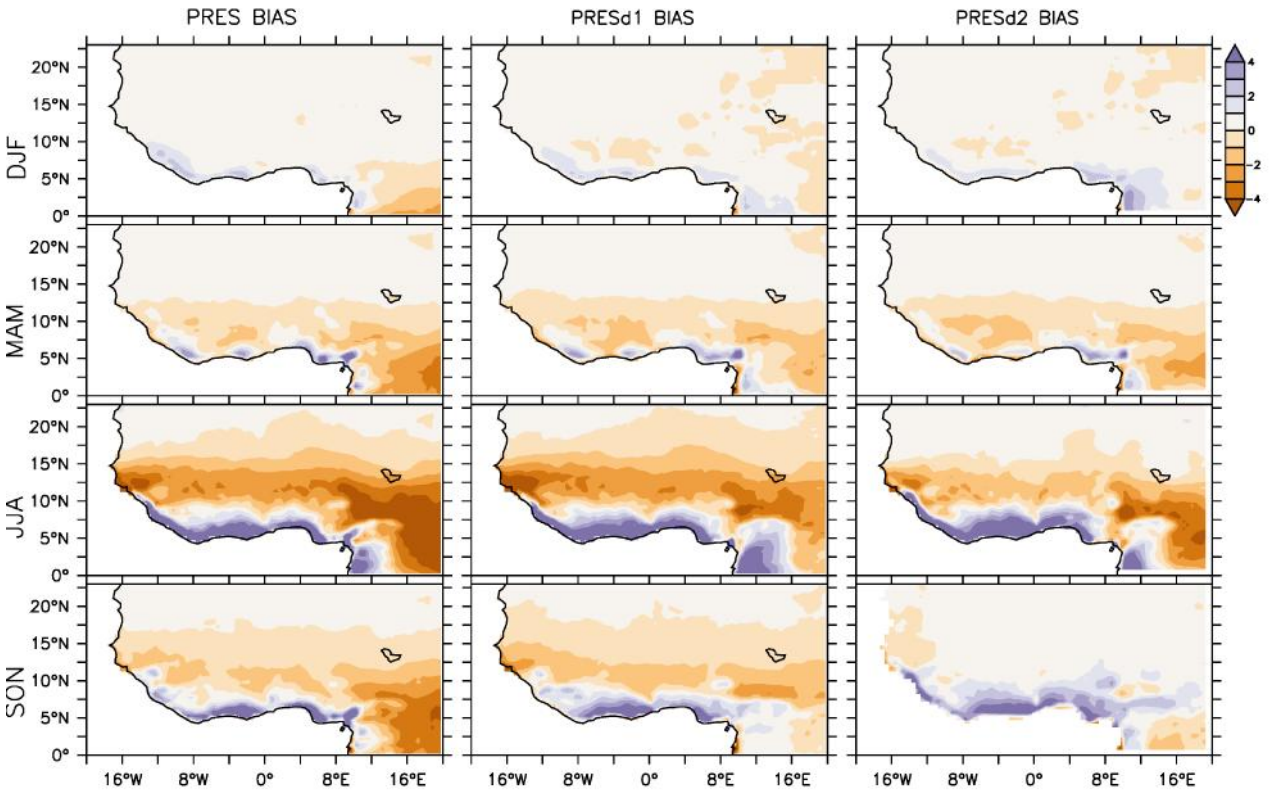

Fig. 4.10: Horizontal distribution of historical precipitation biases (Model minus CRU: mm/day) for each season in RegCM4 prescribed vegetation (first column), dynamic vegetation (second column) and CORDEX domain dynamic vegetation (third column).

On the contrary, Grell scheme which is applied to land, assumes no mixing between the cloud and the environment except at the top and bottom of the circulation, with no entrainment or detrainment along the cloud's edges.

Generally, the model biases can be associated with different factors which include: absence of sufficient observing stations in the mountainous region, influence of land/sea boundary conditions, physics configuration of the model, influence of the driving global circulation models (GCM) or the choice of cumulus convective parameterization (Bhaskaran *et al*., 1996; Bergant *et al*., 2007; Meinke *et al*., 2007; Rockel and Geyer, 2008; Lafore *et al*., 2006; Druyan *et al*., 2010; Oh *et al*., 2014, Yu *et al*., 2015). Table 4.3 to 4.10 presents the mean bias (MB), root mean square difference (RMSD) and pattern correlation coefficient (PCC) between simulated and observed temperature and precipitation over the Sahel, Savanna, Guinea and entire West Africa region. All the three simulations have a high PCC but the mean bias across each region differs with each model simulations.

The model's ability to simulate the magnitude and position of the African Easterly Jet (AEJ), Tropical Easterly Jet (TEJ) and the monsoon flow is also examined. Figure 4.11 compares the simulated vertical cross-section of the monsoon flow, African Easterly Jet (AEJ) and Tropical Easterly Jet (TEJ) in August with Era-Interim reanalysis data. At the lower levels, Era-Interim shows the monsoon flow below 800 hPa at 0 - 19°N while the Harmattan winds are observed north of 20°N. At mid-tropospheric levels of 600-700 hPa, the core of the AEJ (9 m s-1) is centred at 15°N while at 200 hPa the TEJ (15 m s^{-1}) is centred at 10°N. The existence of AEJ has been linked to the meridional surface moisture and temperature gradient between the Sahara and equatorial Africa (Thorncroft and Blackburn, 1999) while the appearance of the TEJ is linked to the upper-level outflow from the Asian monsoon.

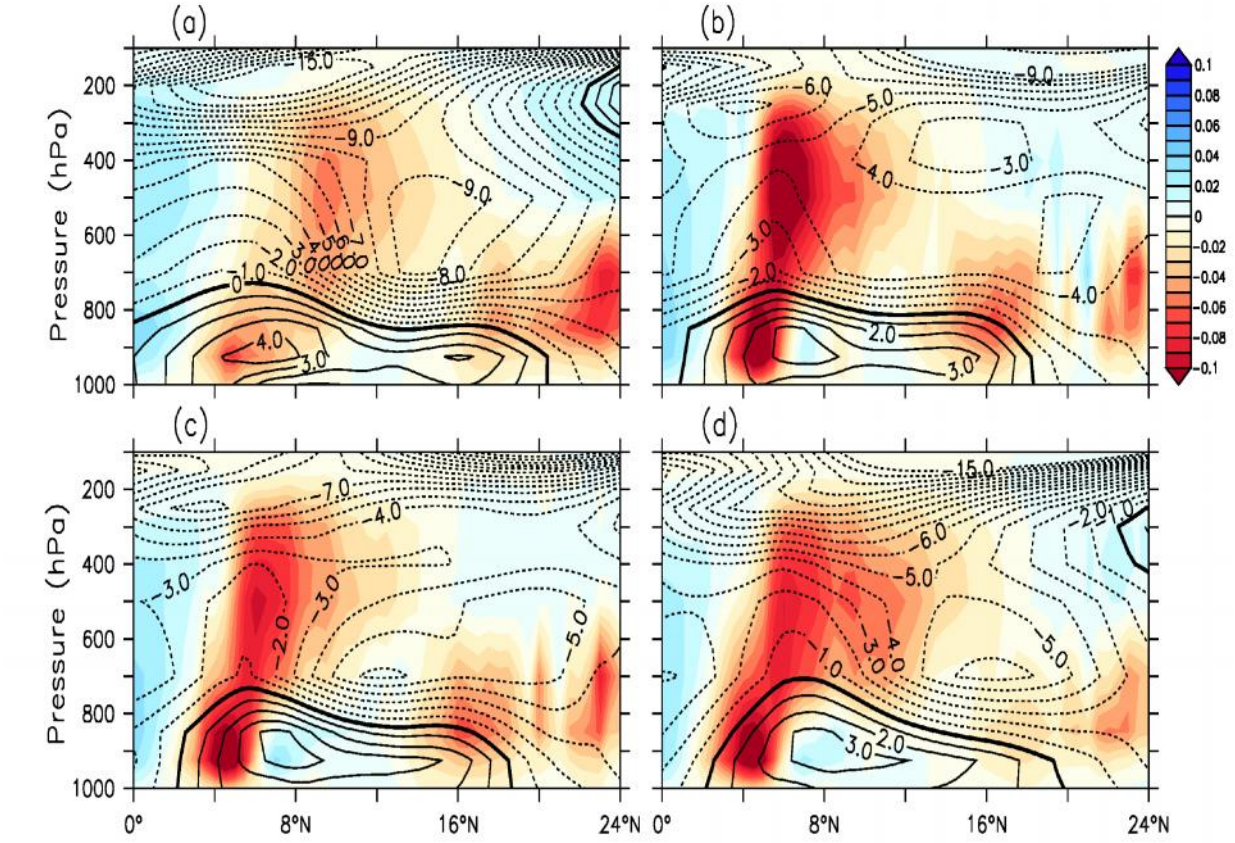

Fig. 4.11: The vertical structure of the zonal (m/s) averaged between 10°E and 10°W over West Africa in August for (a) Era-Interim observations (b) PRES (c) PRESd1 (d) *PRESd2* historical simulations. The shadings indicate the corresponding vertical component of the wind (ω, Pa/s).

The model simulates a narrow monsoon flow for **PRES**, **PRES*d1*** and **PRES*d2*** which begins at approximately 2°N and terminates at 17°N but only **PRES*d2*** reproduces the appearance of the Harmattan winds north of 20°N. The model underestimates the strength of the AEJ at 700 hPa (5 m s^{-1} in **PRES** and **PRES*d1***; 6 m s^{-1} in **PRES*d2***; 9m s^{-1} in Era-Interim) while the core of the jet is displaced northward (PRES centred at 20°N; **PRES*d1*** and **PRES*d2*** centred at 18°N; Era-Interim centred at 15°N). Similarly, the strength of the TEJ at 200 hPa is grossly underestimated by about 8-9 m s^{-1} (6 m s^{-1} in **PRES**; 7 m s^{-1} in **PRES*d1***; 13 m s^{-1} in **PRES*d2***; 15 m s^{-1} in Era-Interim) and displaced northward. Also, the core of the TEJ at 200 hPa is not distinctly captured in the model. The underestimated simulated AEJ and TEJ represent an important source of bias in the simulation of temperature and precipitation. However, the stronger vertical motions simulated in between 4°N and 10°N can be associated with the simulated broader maximum precipitation bands along this zone.

4.3 Projected Future Climate Change over West Africa

This section presents results of projected future climate change over West Africa as simulated by **FUTU**, **FUTU*d1*** and **FUTU*d2*** experiments. The differences obtained from the results of future and historical climate simulations (i.e., DJF, MAM, JJA and SON; 2030-2054 minus 1980-2004) gives an overview of the impact of greenhouse gases (GHG; RCP 4.5) on precipitation, temperature, winds, evapotranspiration, specific humidity, relative humidity and sensible heat flux over West Africa. The spatial distribution of the projected future changes in precipitation, temperature and winds across West Africa are non-homogeneous in all the seasons (Fig. 4.12, 4.13 and 4.14).

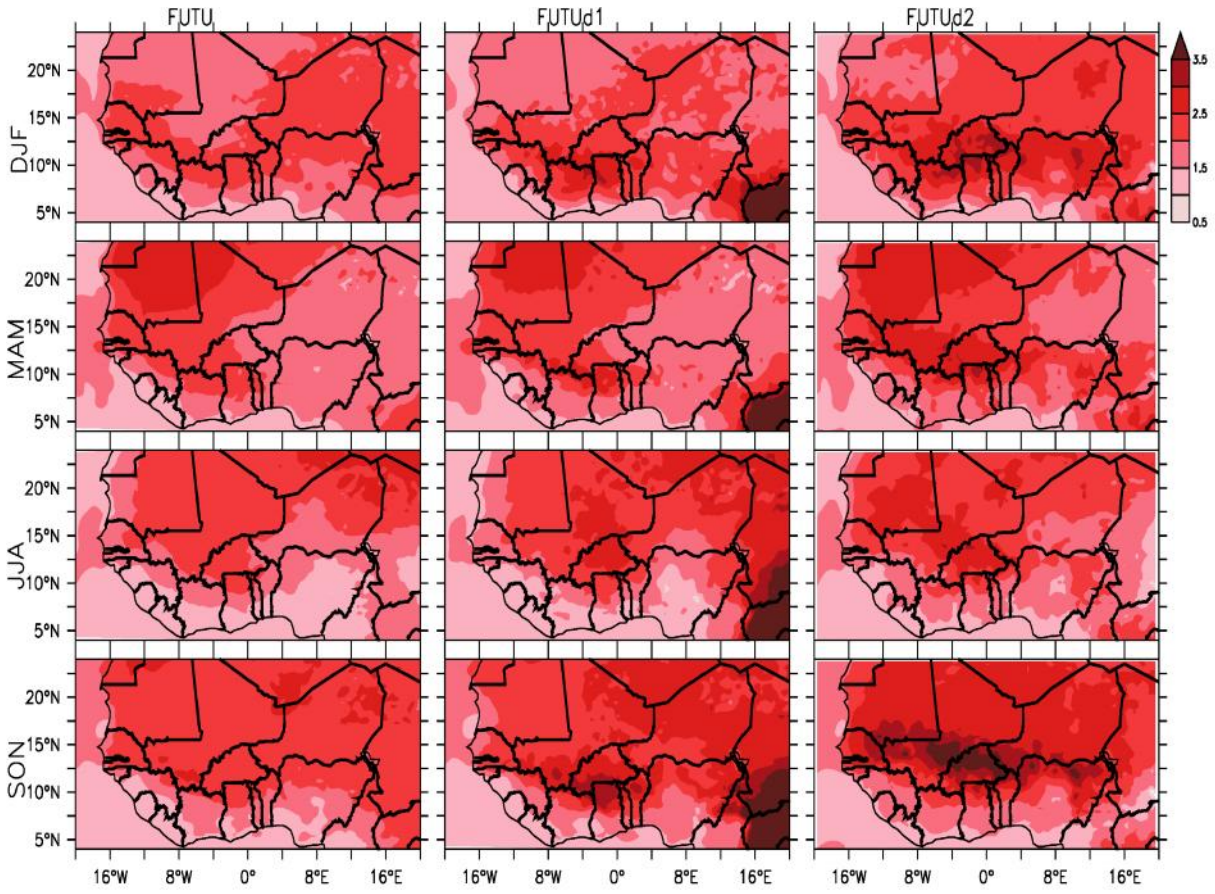

Fig. 4.12: Projected future (RCP 4.5; 2030-2054) changes in temperature (°C). First column shows the projection from RegCM4 prescribed vegetation; Second column is for RegCM4 dynamic vegetation projection; Third column shows RegCM4 dynamic vegetation CORDEX Africa domain projections.

Widespread warming is projected across most parts of West Africa in the three simulations which ranges from an increase of 0.5°C along the coastal and orographic regions (e.g. Guinea Mountains, Cameroon Mountain and Jos Plateau in Nigeria) in JJA to an increase of more than 1°C over the continent during DJF, MAM and SON season (Fig. 4.12). The coastal region manifestation of the least warming may be due to the influx of cool moist air from the Atlantic Ocean. Dynamic vegetation simulations (**FUTU*d1*** and **FUTU*d2***) project an increase of more than 2.5°C over Burkina Faso and some parts of Mali during the post-monsoon season (SON). However, the three simulations agree in the projection of a warmer (increase of 2°C) western Sahel from March to May (MAM).

FUTU, FUTU*d1* and FUTU*d2* project the greatest decrease in precipitation (greater than 3 mm/day) over most parts of Liberia and Sierra Leone in JJA and SON (Fig. 4.13). The other regions within West Africa are expected to have a positive/negative change in precipitation not exceeding 1 mm/day during the monsoon and post monsoon seasons. However, **FUTU** and **FUTU*d1*** agree in the projection of an increase precipitation (about 1 mm/day) over Mauritania, Niger, parts of northern Nigeria and Mali. The wet condition over these areas is associated with the enhancement of the westerlies north of 14°N in JJA (Fig. 4.14) but the drying condition appears not to correspond to the changes in the wind circulation over this region. This may suggest the influence of other local processes.

Further analysis which shows the latitude-time section of future changes in other surface variables (besides temperature and precipitation) is presented in Fig. 4.15. **FUTU** simulates warmer future climates in all months but the least warming occurs at latitude 10°N from July to September. With **FUTU*d1*** and **FUTU*d2***, the lowest warming of 1°C is found south of 8°N from January to December. The three simulations project a precipitation decrease greater than 2 mm/day over areas south of 8°N in March and October for **FUTU**, July to August for

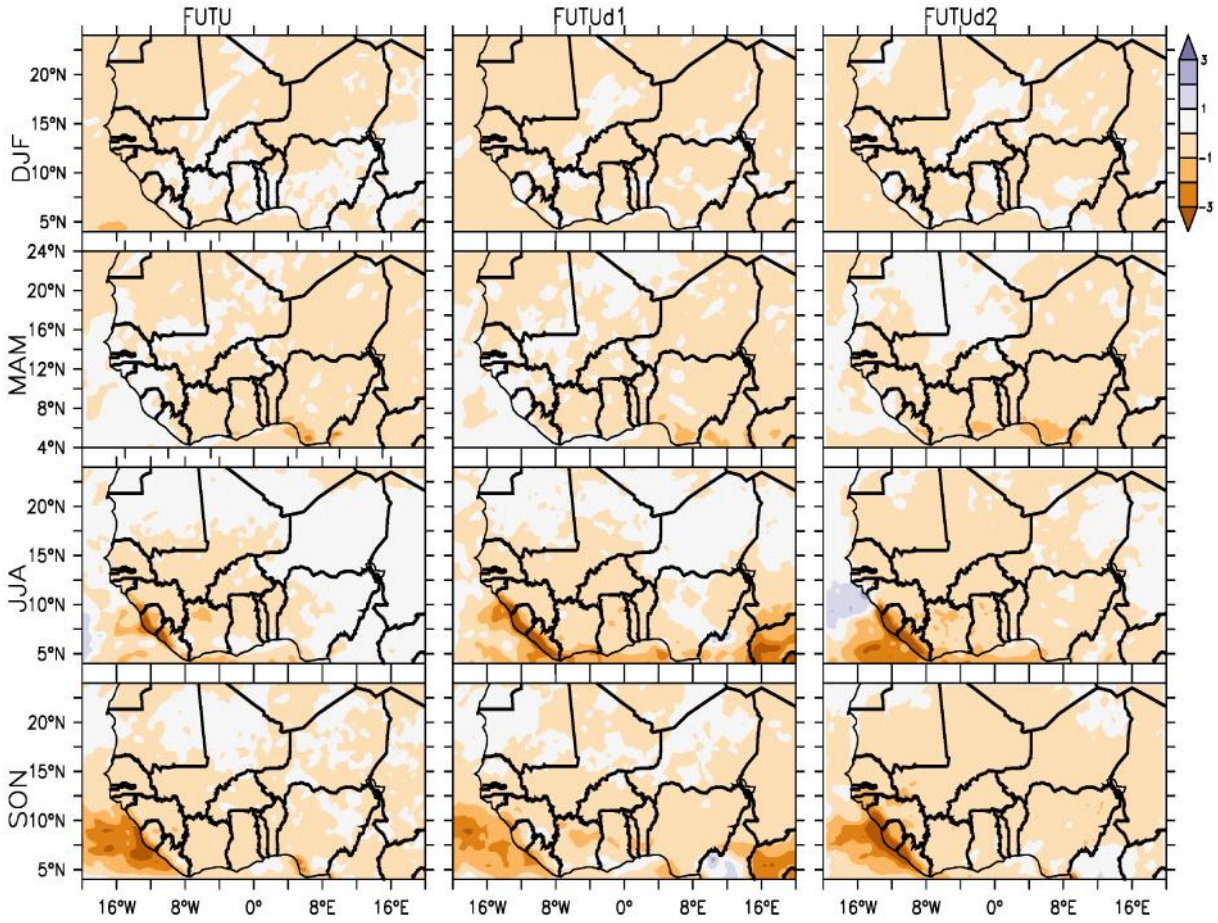

Fig. 4.13: Projected future (RCP 4.5; 2030-2054) changes in precipitation (mm/day). First column shows the projection from RegCM4 prescribed vegetation; Second column is for RegCM4 dynamic vegetation projection; Third column shows RegCM4 CORDEX domain dynamic vegetation projections.

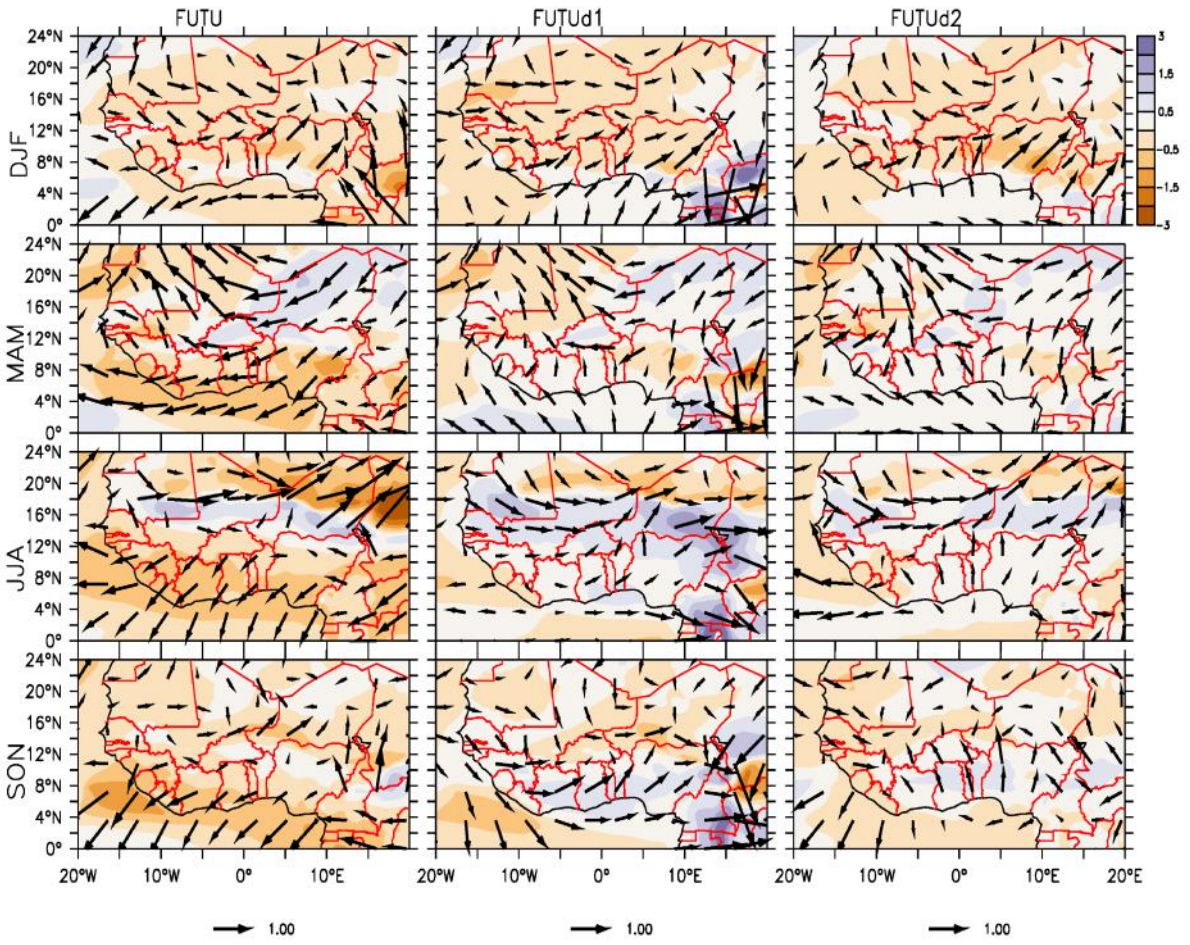

Fig. 4.14: Projected future (RCP 4.5; 2030-2054) changes in wind (m/s). The arrows indicate the wind direction and the colour shadings indicate the magnitude of the wind at 925 hPa. First column shows the projection from RegCM4 prescribed vegetation (PV), second column is for RegCM4 dynamic vegetation (DV) and third column is from RegCM4 CORDEX domain dynamic vegetation simulation (DV-CORDEX).

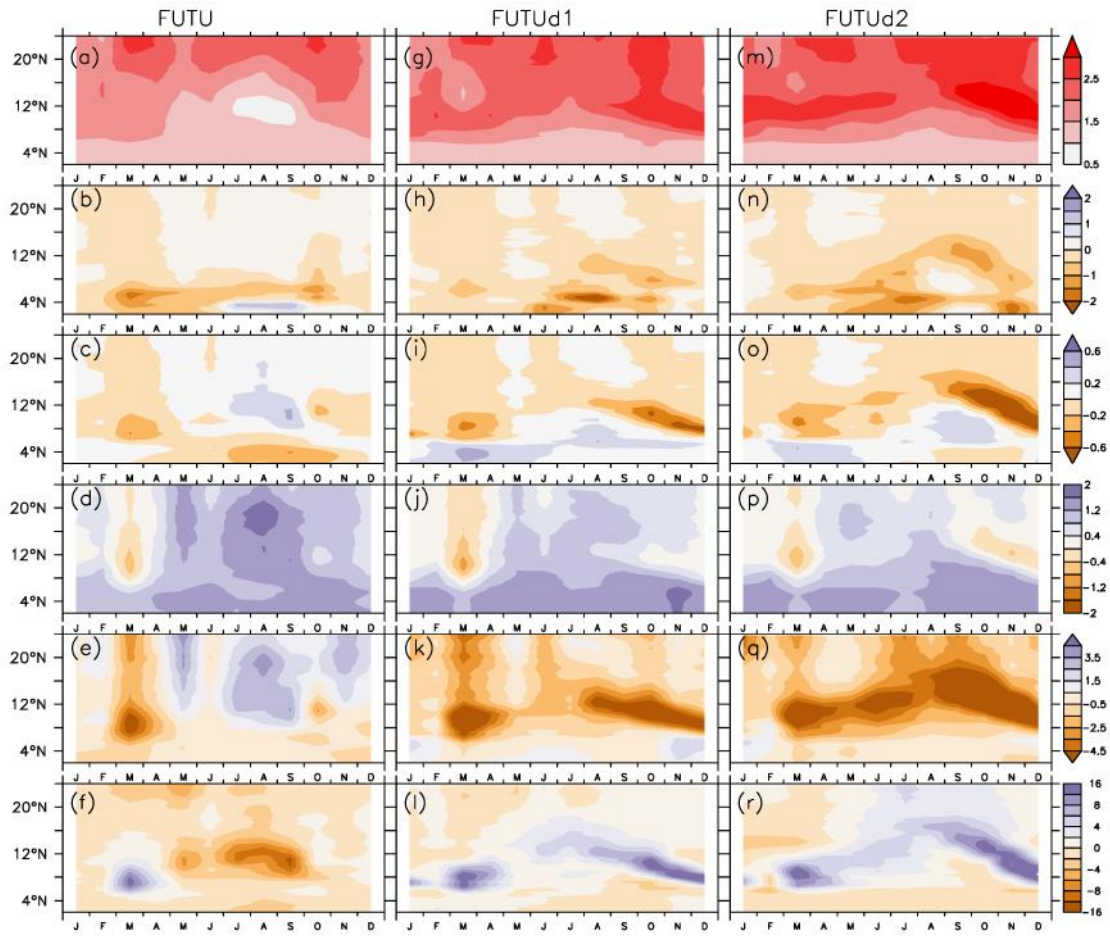

Fig. 4.15: Latitude–time section of future changes in surface (2 m) temperature (°C; a, g, m), precipitation (mm/day; b, h, n), evapotranspiration (mm/day; c, i, o), specific humidity (g/Kg; d, j, p) relative humidity (%; e, k, q) and sensible heat flux (W m-^{2}; f, l, r) due to increased greenhouse gas in future climate (2030–2054; RCP 4.5 scenario; The values are zonal averages between 10°E and 10°W over West Africa**.**

FUTU*d1* and **FUTUd2**. The magnitude and latitudinal distribution of changes in evapotranspiration vary among the three simulations. **FUTU** projects an increased rate of evapotranspiration within the range of 0.6 mm/day for areas between 6 °N and 14°N from July to September (Fig.4.15c).

The future warmer climate produces an increase in atmospheric moisture all year round (Fig. 4.15d) except in the month of March for areas south of latitude 8°N. The available moisture was insufficient to produce precipitation due to the projected decrease in relative humidity all year round (Fig. 4.15e). The three simulation show a good agreement of an increase in sensible heat flux in March but differs in other months for the dynamic vegetation. However, **FUTU*d1*** and **FUTU*d2*** exhibit similar pattern in the projected changes of sensible heat flux (Fig. 4.15f) in all months.

4.4 Impact of Agri-Silviculture on West Africa Future Climate

Computation of the impacts of agri-silviculture on the future climate of West Africa was accounted for by subtracting the result of future climate from each of the different future agri-silviculture experiments (i.e., **GUSAG** minus **FUTU**; **GUSAG*d1*** minus **FUTU*d1***; **GUSAG*d2*** minus **FUTU*d2***; **COAG** minus **FUTU**; **COAG*d1*** minus **FUTU*d1***). These provide information on the potential future climatic changes due to the practice of agri-silviculture over West Africa. This section focuses mainly on the impacts of agri-silviculture on the future climate (2030-2054) of West Africa.

The impact of the different simulated agri-silviculture options on the future climate of West Africa for each experiment was investigated. With **GUSAG** experiment, most areas along the agri-silviculture zone (e.g. Nigeria, Ghana, Cote d'Ivoire and Cameroon, Togo, Benin Republic and Ghana) has temperature reduction which ranges from 0.5 to 2°C in all seasons

(Fig. 4.16). The induced cooling enhances more precipitation over Togo, Benin, Ghana and coastal parts of Nigeria and Cote d'Ivoire during the onset of monsoon season (MAM) but during the peak of the monsoon (JJA) only Ghana is projected to experience increased precipitation that is greater than 1 mm/day (Fig. 4.17). On the contrary, **GUSAG** agri-silviculture induces warming of about 2°C in all seasons over most parts of Liberia and Sierra Leone in all seasons which intensifies the drying condition in these areas to about 1.8 mm/day. This suggests that with the specified fixed percentage cover of trees and crops along this zone, the intensity of the projected drying and warming over most parts of Liberia and Sierra Leone will be intensified. However, there exist no robust future changes in temperature and precipitation associated with **GUSAG** experiment for countries located outside the agri-silviculture zone.

Investigating the impact of the changing vegetation cover (trees and crop) with respect to the designed agri-silviculture experiment in **GUSAG*d1***, it was found that, there exist no pronounced changes in temperature along the agri-silviculture zone and over the entire West Africa region in all seasons (Fig. 4.16). The same effect is projected for precipitation except in JJA and SON which show increases in precipitation across some parts of Nigeria, Gambia, Senegal, coastal parts of Cote d'Ivoire, Guinea-Bissau, and Liberia during the peak of the monsoon season.

With the **GUSAG*d2*** experiment, some pronounced changes in temperature and precipitation occur both outside and within the agri-silviculture zone. The only difference between **GUSAG*d2*** and **GUSAG*d1*** agri-silviculture experiment is the domain size of the simulations. This shows that the influence of domain size plays a major role in altering the signal of the projected future climate due to agri-silviculture. Warming of about 0.5°C is enhanced over Senegal, Mauritania, Mali, Burkina Faso and some parts of Niger during JJA and SON season. On the other hand, **GUSAG*d2*** induces cooling within the range of 0.4 to 2°C over

Chad, Cameroon and Northeastern parts of Nigeria in all seasons (Fig. 4.16). The induced cooling only translates to increased precipitation (0.3 to 1.8 mm/day) during the peak and post-monsoon season (JJA and SON). However, during DJF and MAM seasons, **GUSAG*d2*** induces no pronounced changes in temperature and precipitation outside the agri-silviculture zone. Generally, widespread decreased precipitation (0.4 to 1.8 mm/day; Fig. 4.17) is found in areas located within 15°W and 10°E during JJA and SON. Therefore, the mitigation potential of **GUSAG*d2*** agri-silviculture experiment appears strong and favourable over Cameroon, North Eastern parts of Nigeria and Chad.

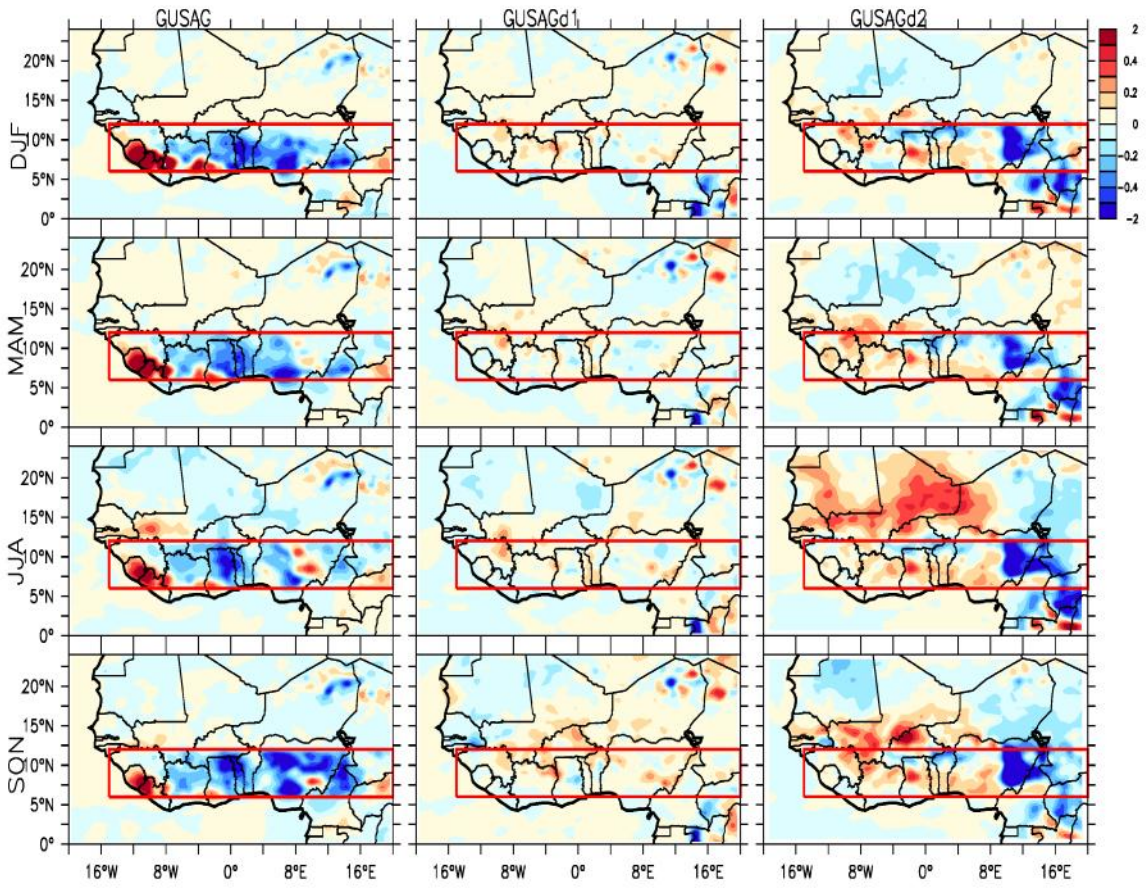

Fig. 4.16: Projected future (RCP 4.5; 2030-2054) changes in temperature (°C) over West Africa due to agri-silviculture practice along the Guinea Savanna zone from GUSAG, GUSAG*d1* and GUSAG*d2* experiments.

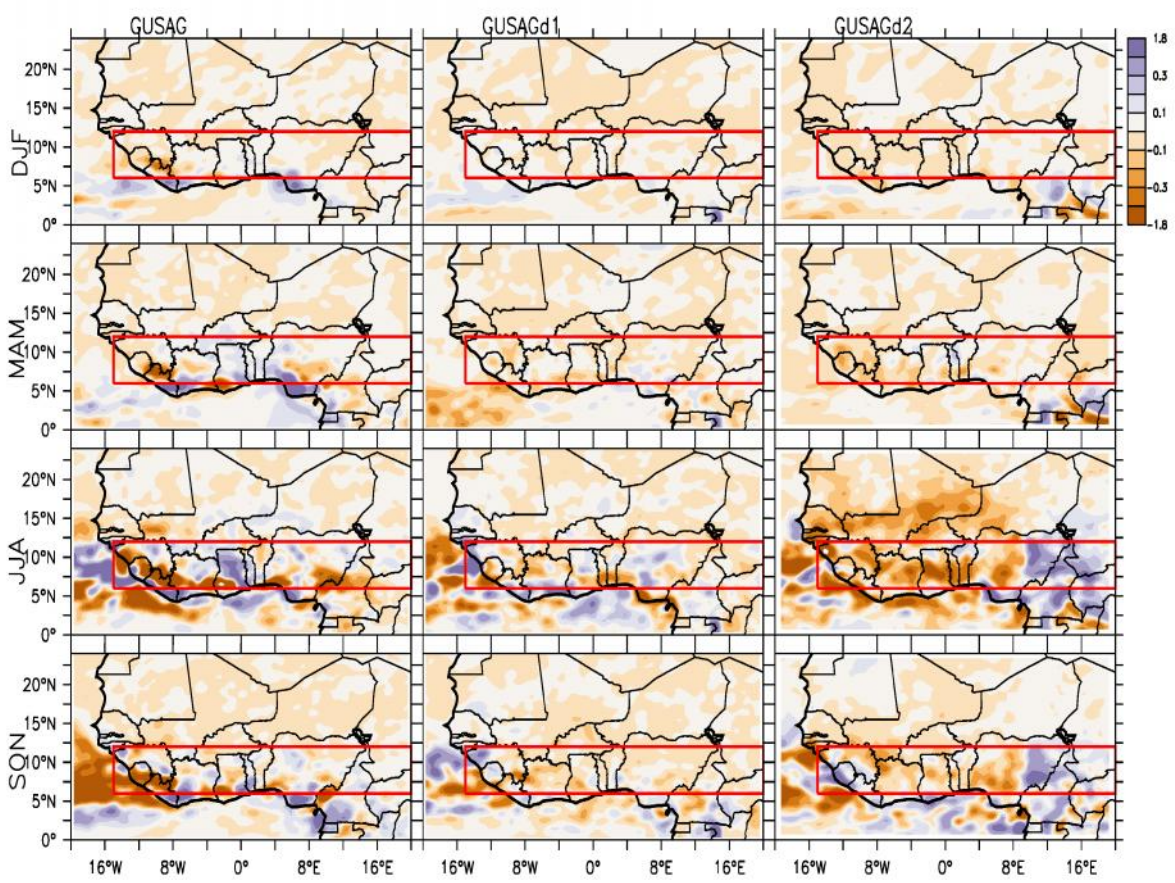

Fig. 4.17: Projected future (RCP 4.5; 2030-2054) changes in precipitation (mm/day) over West Africa due to agri-silviculture practice along the Guinea Savanna zone from GUSAG, GUSAG*d1* and GUSAG*d2* experiments.

Figure 4.18 shows the latitude-time section of future changes in temperature, precipitation, sensible heat flux, relative humidity and evapotranspiration due to **GUSAG**, **GUSAG*d1*** and **GUSAG*d2*** agri-silviculture experiments. The prescribed percentage cover of trees and grasses used in **GUSAG** experiment increases the sensible heat flux along the agri-silviculture zone (Fig. 4.18g). The resulting increased sensible heat flux causes the upward transfer of heat into the air which then induces surface cooling along the agri-silviculture zone (Fig. 4.18a). This is further confirmed by the increase in relative humidity (Fig. 4.18j) along the agri-silviculture zone in all months. On the other hand, with **GUSAG*d1*** experiment, which enables feedback between vegetation and climate, there are no pronounced future change in temperature, precipitation, sensible heat flux and relative humidity. However, when the same experiment was carried out using a larger domain as with **GUSAG*d2*** experiment, pronounced future change in temperature, relative humidity and evapotranspiration occur along the agri-silviculture zone. For instance, a slight cooling of about 0.25°C is induced in all months in areas along the agri-silviculture zone (Fig. 4.18c) but warming of the same magnitude occur in areas north of 12°N from June to October. The pattern of the projected future changes in temperature from June to December in **GUSAG*d2*** is in close agreement with the projected changes in relative humidity.

The changes in the vertical structure of temperature and precipitation associated with the three agri-silviculture options integrated along the Guinea Savanna zone is presented in Fig. 4.19. The figure re-emphasized that generally, agri-silviculture practices along the Guinea Savanna zone does not exacerbate the future warming or drying over West Africa. Rather, it enhances cooling, although no robust positive or negative changes is exerted on the precipitation regimes.

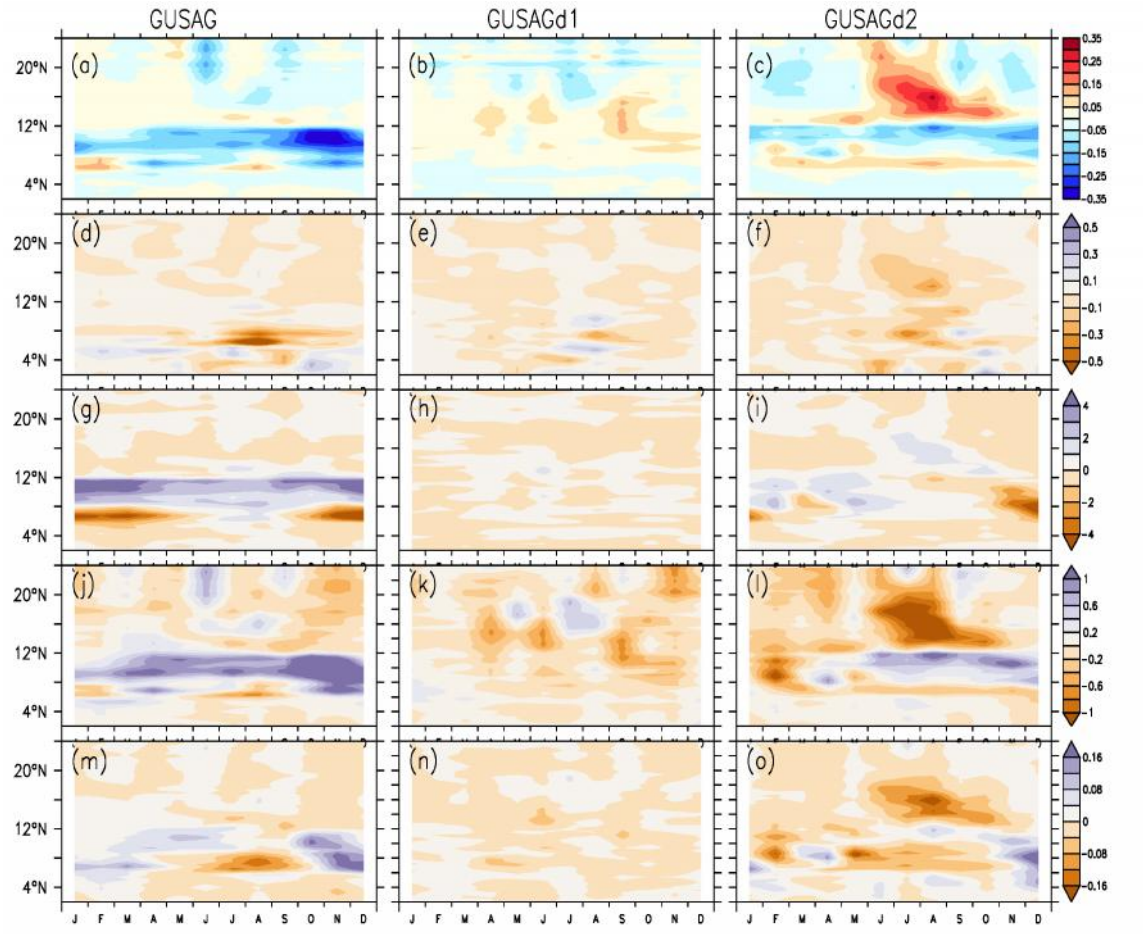

Fig. 4.18: Latitude–time section of future changes in surface (2 m) temperature (°C; a, b, c), precipitation (mm/day; d, e, f), sensible heat flux (W m^{-2}; g, h, i), relative humidity (%; j, k, l) and evapotranspiration (mm/day; m, n, o) due to agri-silviculture practice along the Guinea Savanna zone. First column shows the changes simulated by RegCM4 prescribed vegetation (GUSAG), second column is for RegCM4 dynamic vegetation (GUSAG*d1*) and third column is for RegCM4 CORDEX dynamic vegetation simulation (GUSAG*d2*). Zonal averages between 15°W and 15°E.

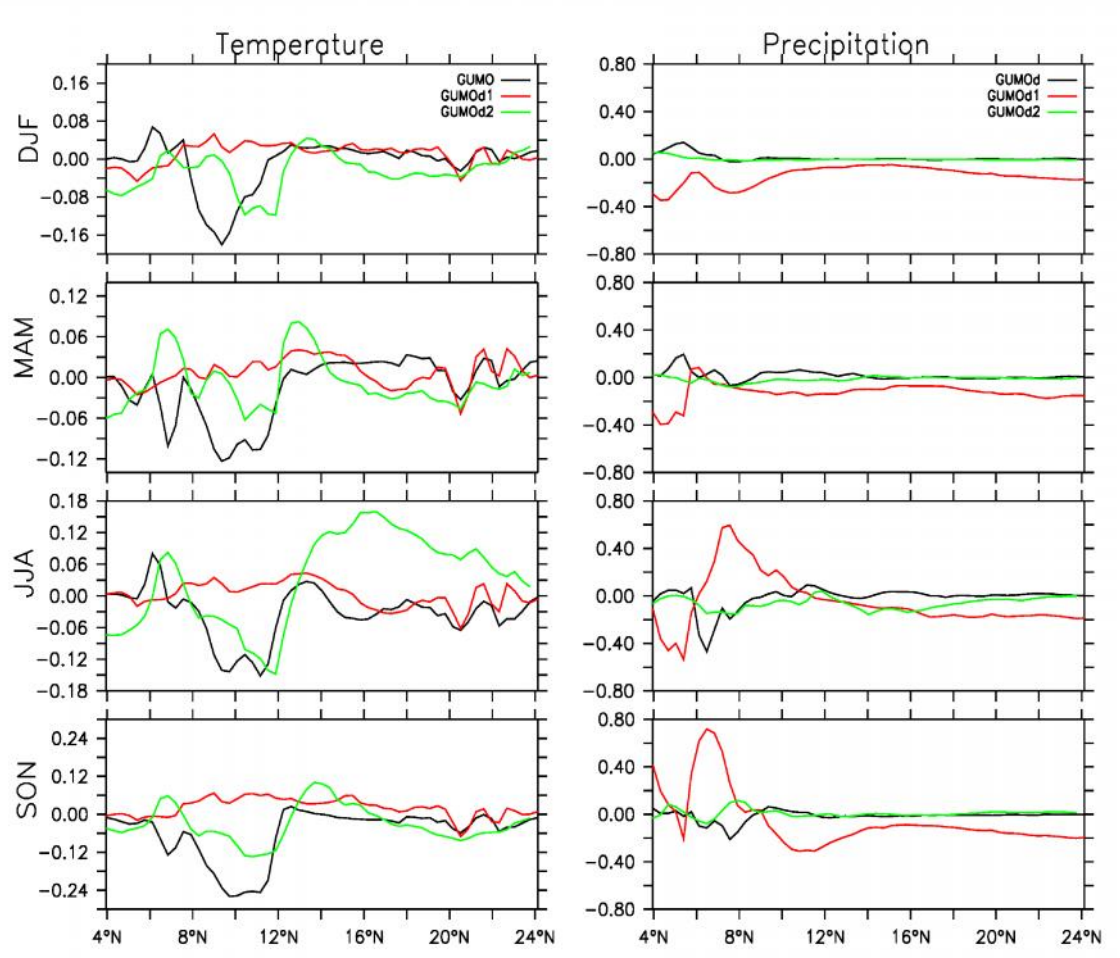

Fig. 4.19: Changes in the vertical structure of surface (2 m) temperature (°C; first column) and precipitation (mm/day; second column) due to agri-silviculture practice along the Guinea Savanna zone. These are averaged between 10°W to 10°E.

COAG and **COAG*d1*** experiments exert no robust positive or negative changes in future warming along the agri-silviculture zone (Fig. 4.20 and Fig. 4.21) in all seasons. However, both **COAG** and **COAG*d1*** experiments indicate a cooling of about -0.8°C over Northern parts of Niger while warming of the same magnitude is found over Northern parts of Chad in all seasons. The spatial distribution of the impacts of **COAG** and **COAG*d1*** experiments on future precipitation across West Africa is presented in Fig. 4.21. A wetter condition is projected for Gambia, Liberia, Guinea and Guinea Bissau in summer with **COAG** experiment while **COAG*d1*** projects increase precipitation (0.3 - 0.5 mm/day) over Liberia, Cote d'Ivoire, Cameroon, northern parts of Ghana and south-west Nigeria (Fig. 4.21). The latitude time section of the impacts of **COAG** and **COAG*d1*** on other surface variables besides temperature and precipitation is presented in Fig. 4.22. A similar pattern of cooling is projected north of 10 °N from July to September in both **COAG** and **COAG*d1*** experiments which correspond to decrease in relative humidity. Precipitation is also increased in August at latitude 8°N in both experiments.

Coastal agri-silviculture (**COAG** and **COAG*d1***) produces both negative and positive changes in temperature and precipitation (Fig. 4.23). In the region between 0 and 4°N, precipitation is reduced while it is enhanced in areas between 4°N and 7°N.

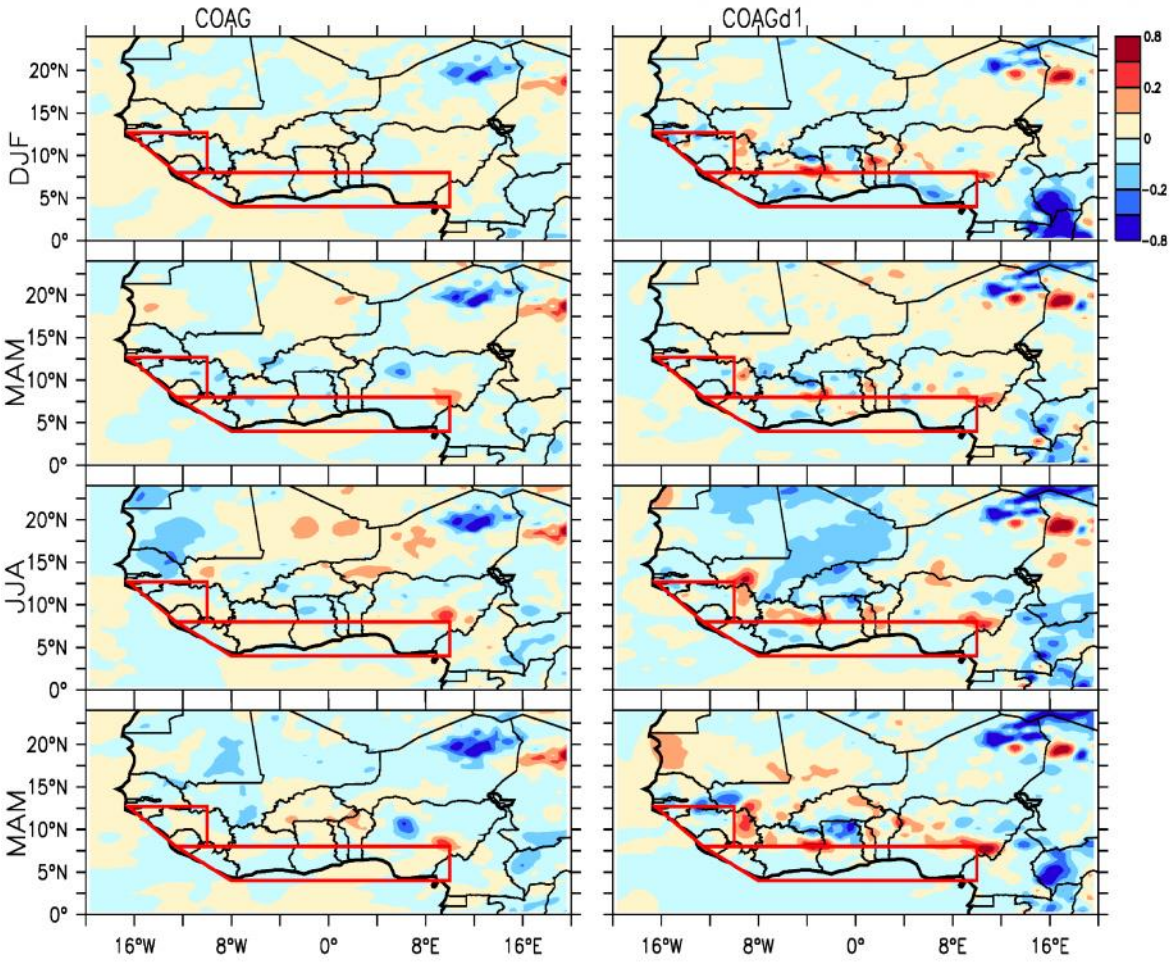

Fig. 4.20: Projected future (RCP 4.5; 2030-2054) changes in temperature (°C) over West Africa due to agri-silviculture practice along West Africa coasts from COAG and COAG*d1* experiment.

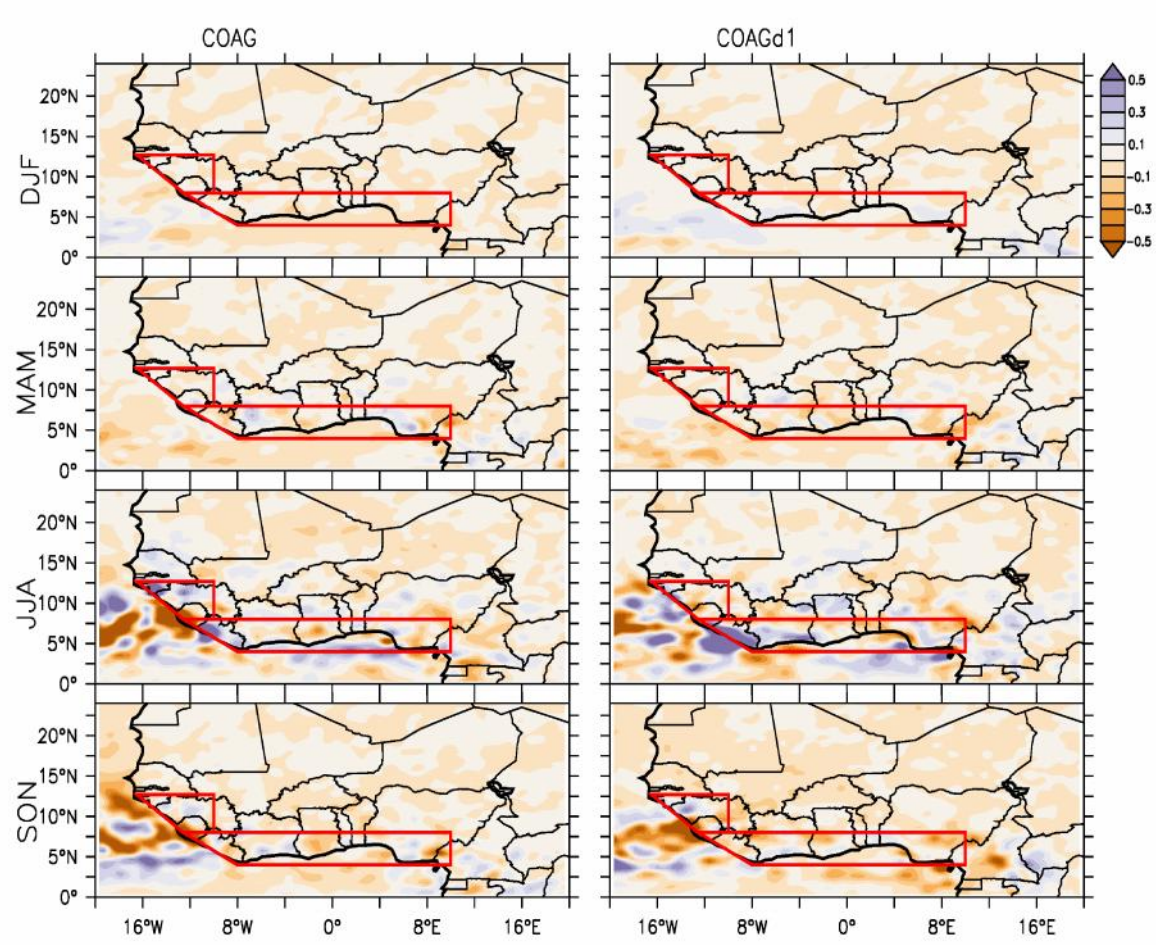

Fig. 4.21: Projected future (RCP 4.5; 2030-2054) changes in precipitation (mm/day) over West Africa due to agri-silviculture practice along West Africa coasts from COAG and COAG*d1* experiment.

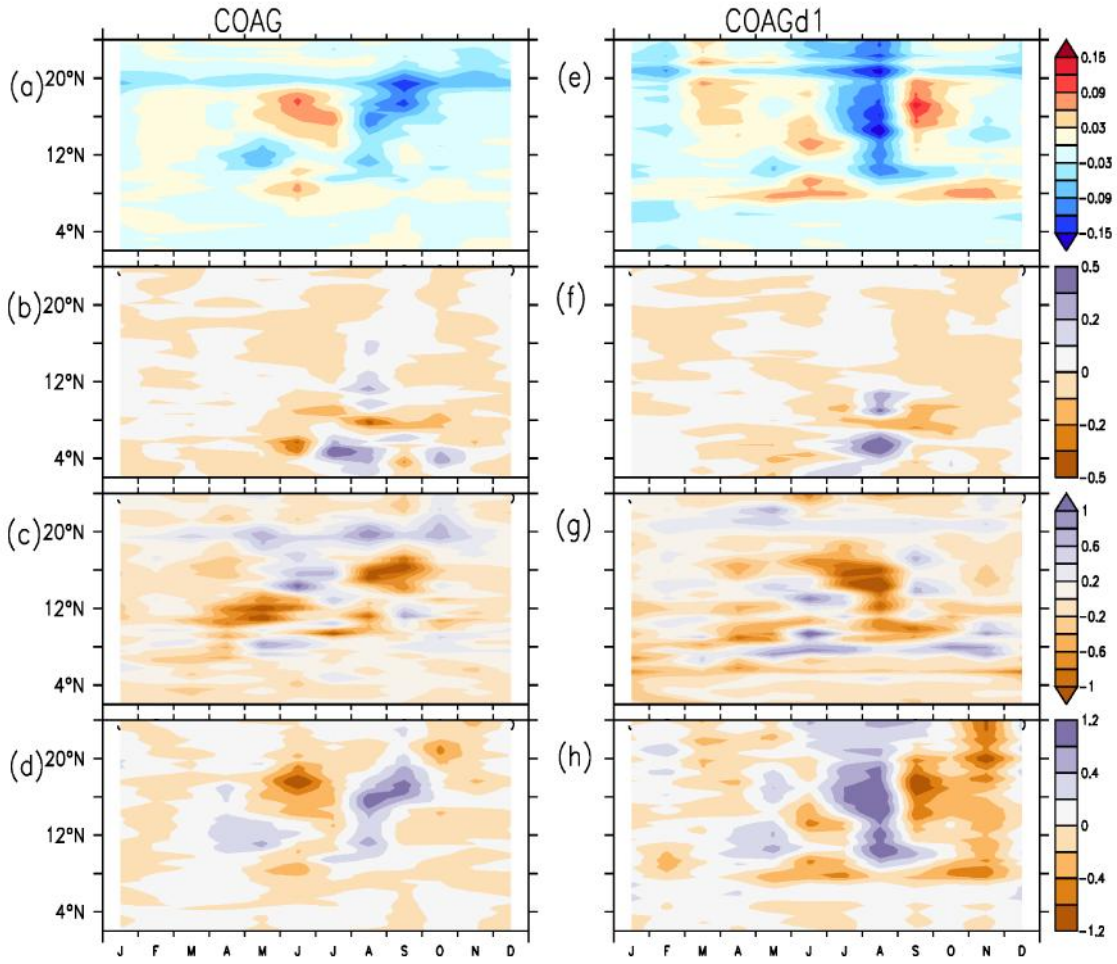

Fig. 4.22: Latitude–time section of future changes in (a) surface 2 m temperature (°C) (b) precipitation (mm/day) (c) sensible heat flux (W m^{-2}) (d) relative humidity (%) due to agri-silviculture practice along West Africa coasts. Zonal averages between 15°W and 15°E.

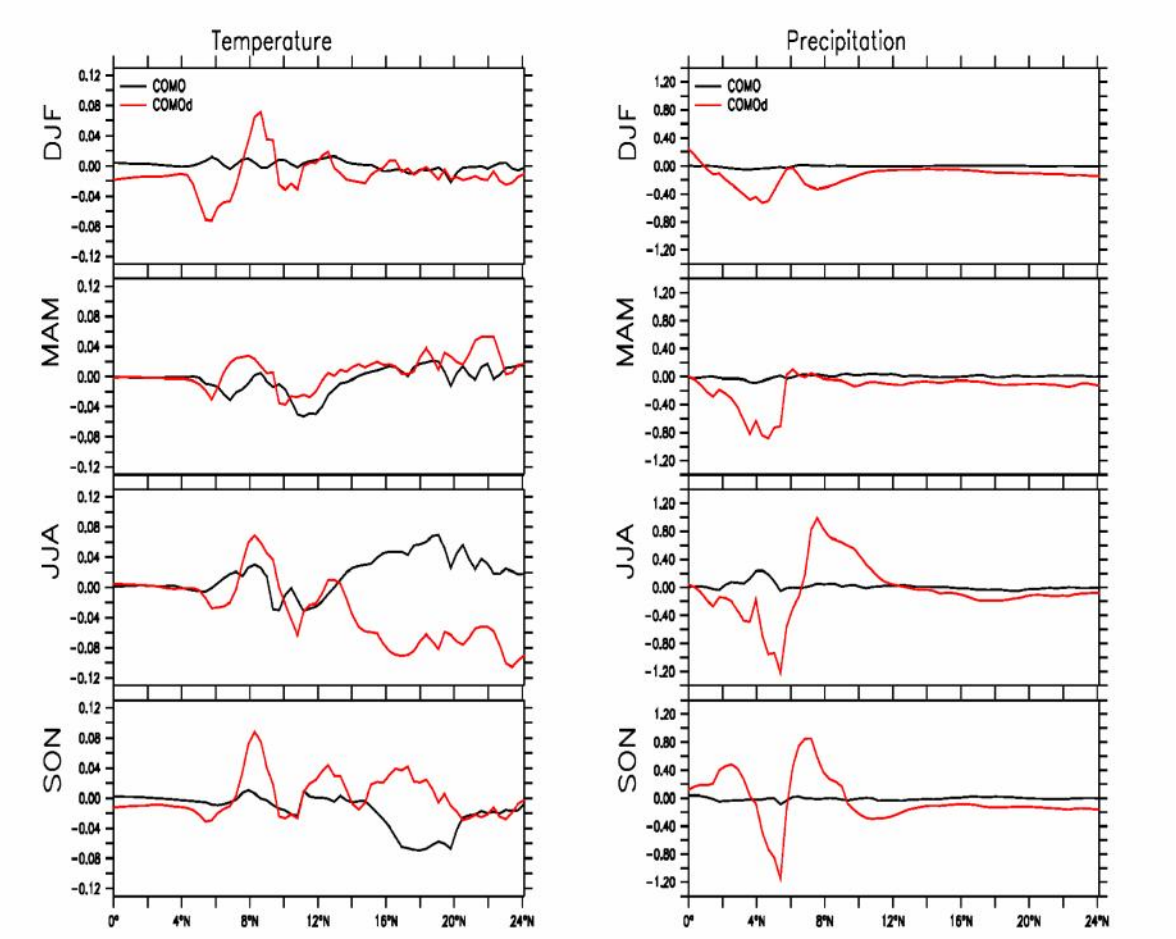

Fig. 4.23: Changes in the vertical structure of surface (2 m) temperature (°C; left column) and precipitation (mm/day; right column) due to agri-silviculture practice along the West African coast. These are averaged between 10°W to 10°E.

Tables 4.11 and 4.12 summarize and indicate the future climatic changes along the Guinea Savanna zone with or without agri-silviculture during JJA and MAM seasons. The projected future changes (without agri-silviculture) in the surface variables (e.g. temperature, precipitation, sensible heat flux, specific humidity evapotranspiration, wind and runoff are significant at 95% confidence level. The specific combination of trees and crops adopted in **GUSAG** experiment significantly increases the sensible heat flux, specific humidity and relative humidity along the Guinea Savanna zone during JJA (Table 4.11). On the other hand, temperature, precipitation, runoff, evapotranspiration and surface wind is slightly reduced along this zone in JJA. This suggests that with the fixed proportion of trees and crops utilized in **GUSAG** experiment produces slight but significant changes in the near future climate.

However, by considering the feedback from vegetation in the **GUSAG*d1*** experiment, the induced changes in temperature, precipitation, sensible heat flux, runoff, evapotranspiration and surface wind induced along the Guinea Savanna zone in JJA has an opposite signal from what is obtained when there is no feedback from vegetation (i.e, **GUSAG**). Hence, there is slight warming (an increase of 0.02°C), enhance precipitation (an increase of 0.01 mm/day) along the Guinea Savanna zone in the near future. The direction of the changes induced along the Guinea Savanna zone by the dynamic agri-silviculture experiment on a larger domain (**GUSAG*d2***) appears similar to **GUSAG** experiment in JJA for most of the climatic variables considered. However, only the changes in sensible heat flux, relative humidity and surface wind are significant during JJA season. During the onset of the monsoon season (MAM), the impact of **GUSAG** significantly increases precipitation, sensible heat flux and relative humidity while **GUSAG*d1*** only slightly increases the temperature and specific humidity. On the other hand, the **GUSAG*d2*** impact is significant only by decreasing specific humidity and increasing the surface wind.

The impact of **COAG** and **COAG*d1*** agri-silviculture experiment on most of the climate variables in the near future during MAM and JJA seasons are significant. However, the change signal induced on the future climate variables by **COAG** and **COAG*d1*** is the same except for temperature and precipitation. Agri-silviculture experiments designed along West Africa coasts significantly reduce the sensible heat flux and increases the relative humidity, specific humidity and evapotranspiration. However, **COAG** exerts no change in future temperature and surface wind along the Guinea Savanna zone in JJA. In contrast, during the onset of the monsoon season (MAM), **COAG*d1*** agri-silviculture experiment lowers temperature and sensible heat flux while **COAG*d2*** exerts no change in temperature but still reduces the sensible heat flux. The magnitude and direction of the changes induced by both **COAG*d1*** and **COAG*d2*** is approximately the same during MAM season

Table 4.11: The simulated mean and standard deviation (SD) of some climate variables over Guinea Savanna zone in JJA of the historical climate (PRES, PRESd1 and PRESd2), the projected future changes in the mean (FUTU, FUTUd1 and FUTUd2) and the impacts of the different forms of agri-silviculture practice (GUSAG, GUSAGd1, GUSAGd2, COAG and COAGd1) on future climate projections. The significant impacts at 95% confidence interval are in bold.

VARIABLES	PRESCRIBED VEGETATION SIMULATIONS					DYNAMIC VEGETATION SIMULATIONS								
	PRES					PRESd1					PRESd2			
	MEAN	SD	FUTU	GUSAG	COAG	MEAN	SD	FUTUd1	GUSAGd1	COAGd1	MEAN	SD	FUTUd2	GUSAGd2
Temp	25.37	2.87	**1.54**	**-0.06**	0.00	24.38	2.87	**1.98**	**0.02**	**-0.01**	23.17	2.51	**1.74**	-0.05
Prec	6.16	5.31	**-0.27**	**-0.07**	**-0.01**	6.79	4.96	**-0.70**	**0.01**	**0.03**	7.22	5.09	**-0.59**	-0.09
SHF	45.96	25.54	**-4.79**	1.**51**	**-0.09**	38.41	18.22	**2.10**	**-0.07**	**-0.66**	24.55	11.22	**1.28**	**0.41**
RH	64.23	17.56	**1.43**	**0.35**	**0.05**	72.42	14.81	**-2.79**	**0.11**	**0.38**	79.38	12.74	**0.03**	**0.29**
QAS	12.73	2.18	**1.30**	**0.03**	0.01	13.45	1.53	**0.97**	**0.01**	**0.04**	13.52	1.39	**1.05**	0.02
RO	0.51	1.37	**-0.08**	**-0.05**	0.00	1.03	0.05	**-0.22**	0.00	**0.09**	0.64	1.29	**-0.18**	-0.02
EVAP	2.91	1.03	**0.10**	**-0.02**	**0.02**	3.68	0.89	**-0.03**	**0.01**	**0.05**	3.42	0.89	0.01	-0.02
Wind	2.48	1.07	**-0.30**	**-0.08**	0.00	2.59	1.16	**0.25**	**0.03**	**0.03**	1.6	0.02	**0.06**	**0.04**

Note: The climate variables considered are temperature (Temp; °C), precipitation (Prec; mm/day), sensible heat flux (SHF; Wm^{-2}), relative humidity (RH; %), specific humidity (QAS; g/kg), surface runoff (RO; mm/day), evapotranspiration (EVAP; mm/day) and surface wind speed (Wind; m/s).

Table 4.12: The simulated mean and standard deviation (SD) of some climate variables over Guinea Savanna zone in MAM of the historical climate (PRES, PRESd1 and PRESd2), the projected future changes in the mean (FUTU, FUTU*d1* and FUTU*d2*) and the impacts of the different forms of agri-silviculture (GUSAG, GUSAG*d1*, GUSAG*d2*, COAG and COAG*d1*) experiments on future climate projections. The significant impacts at 95% confidence inter-val are in bold.

VARIABLES	PRESCRIBED VEGETATION SIMULATIONS					DYNAMIC VEGETATION SIMULATIONS								
	PRES					PRESd1					PRESd2			
	MEAN	SD	FUTU	GUSAG	COAG	MEAN	SD	FUTUd1	GUSAGd1	COAGd1	MEAN	SD	FUTUd2	GUSAGd2
Temp	28.46	2.90	**1.50**	-0.07	**-0.01**	27.15	3.08	**2.04**	**0.01**	**0.00**	26.37	2.82	**2.10**	0.00
Prec	1.99	1.81	**-0.11**	**0.02**	**0.02**	1.93	1.78	**-0.15**	0.00	**0.01**	1.95	1.67	**-0.26**	-0.04
SHF	68.90	26.09	**0.08**	**0.97**	**-0.20**	65.12	23.07	**2.96**	0.00	**-0.11**	57.24	21.52	**4.57**	*0.62*
RH	45.20	20.81	**-1.18**	**1.54**	**0.10**	49.96	21.43	**-3.35**	0.00	**0.11**	53.42	19.44	**-3.45**	-0.19
QAS	10.14	3.56	0.62	-7.5	**0.02**	10.39	3.36	**0.44**	**0.01**	**0.01**	10.73	2.99	**0.54**	**-0.04**
RO	0.10	0.27	**-0.02**	0.00	0.00	0.18	0.35	**-0.03**	0.00	0.00	0.11	0.20	**-0.03**	0.00
EVAP	2.05	1.41	**-0.09**	0.04	**0.37**	2.11	1.41	**0.14**	0.00	**0.01**	2.17	1.28	**-0.18**	0.78
Wind	2.13	0.03	**-0.23**	0.03	**0.36**	1.74	0.03	**-1.09**	0.00	**0.18**	1.31	0.02	**0.14**	**0.04**

Note: The climate variables considered are temperature (Temp; °C), precipitation (Prec; mm/day), sensible heat flux (SHF; W/m^2), relative humidity (RH; %), specific humidity (QAS; g/kg), surface runoff (RO; mm/day), evapotranspiration (EVAP; mm/day) and surface wind speed (Wind; m/s).

CHAPTER FIVE

CONCLUSIONS AND RECOMMENDATIONS

5.1 Summary and Conclusions

This study investigates the impacts of agri-silviculture on West African future climate, using a regional climate model (RegCM4). The study evaluated the performance of RegCM4 in simulating the West Africa Climate system using observed and reanalysis datasets. The model replicates all the features of West Africa climate system fairly well but not without some biases. The model also has the capability to provide feedback into the climate system with respect to dynamic and time-invariant vegetation. These options in RegCM4 are then fully deployed in simulating agri-silviculture using both prescribed vegetation and dynamic vegetation components of the model. However, the biases identified from the model validation must be considered while interpreting the future climate projections with or without agri-silviculture.

Agri-silviculture offers a win-win solution to the impacts of climate change in West Africa. However, there is limited information on its influence on regional climate vis-à-vis temperature, rainfall or wind. Its role as an adaptation and mitigation option to enhance food security and also contribute to the reduction of accumulated atmospheric greenhouse gases was examined in this study. This was achieved by simulating the impacts of different forms of agri-silviculture on West African climate using regional climate model. The results obtained from the study are hereby summarized.

5.1.1 Land Surface Schemes

Generally, all the land surface schemes reproduced the seasonal variation in the pattern of temperature, rainfall and wind quite well. However, The Biosphere-Atmosphere Transfer Scheme (BATS) grossly overestimate precipitation throughout the entire West Africa region in all months and by more than 2 mm/day during the peak of the summer monsoon. The four schemes underestimate temperature in all months but BATS has the greatest cold bias which is more than 1°C in all months. In contrast, the dynamic vegetation component of the Community Land Model Scheme version 4.5 simulates precipitation amount that matches closely with observation in all months. Therefore, the climate simulations carried out in this study utilizes both the time-invariant and dynamic vegetation component of the Community Land Model version 4.5 scheme coupled with RegCM4.

5.1.2 RegCM4 Validation

RegCM4 model simulations, driven by HadGEM2-ES reasonably simulated the spatial distribution of temperature and precipitation fields over West Africa. However, the model has a cold bias along West Africa coast which translates to overestimation of precipitation along this zone irrespective of the domain size used in the simulation. The observed dry bias further inland was reduced with the activation of the dynamic vegetation. The dry bias inland reduced drastically in all seasons when the dynamic vegetation was enabled using CORDEX-Africa recommended domain.

The essential features of the West African Climate System such as the Inter-tropical convergence zone, African Easterly Jet, Tropical Easterly Jet and the monsoon flow were fully captured by the model simulations. The north-south migration pattern of the ITCZ was well represented in the model. Similarly, the spatial distribution of the pattern of the low-level wind

in all seasons was captured in all historical simulations. However, the magnitude of the strength of the AEJ and TEJ were underestimated.

Generally, the model performance in simulating temperature, rainfall and wind fields when compared to CRU observations and Era-Interim reanalysis was good. Hence, despite the identified few weaknesses in the model's historical simulation over West Africa, the model was adequate to carry out the change in land cover sensitivity experiments done in this study.

5.1.3 Potential Future Climate Projection over West Africa

The model projected decreased precipitation over most parts of West Africa in the near future (2030-2054; RCP 4.5 scenario) with Liberia and Sierra Leone expected to experience the highest intensity of drying (more than 3 mm/day). The projected drying condition over Liberia and Sierra Leone prevail irrespective of the model domain size or vegetation state. However, during the peak of the monsoon, the projected change in precipitation in other countries within West Africa appears sensitive to domain size and vegetation state.

For instance, with time-invariant vegetation state, most parts of Niger, Cameroon, Chad and Mauritania and some parts of Nigeria were projected to experience enhanced precipitation not exceeding 1 mm/day during the peak of the summer monsoon. On the other hand, the dynamic vegetation simulation of the near future using similar domain size as the time-invariant vegetation simulation suggest enhanced precipitation of the same magnitude over Niger, Mauritania and northern parts of Mali. The influence of a larger domain size with dynamic vegetation simulations projects less precipitation during the peak of the summer monsoon throughout the entire West Africa region except for Chad.

5.1.4 Impact of Agri-silviculture on the Future Climate of West Africa

In all the seasons (DJF, MAM, JJA and SON), **COAG** and **COAG*d1*** experiment induces cooling of about 0.8°C over some parts of northern Niger while northern parts of Chad warms up by about 0.2 to 0.8°C. However, most areas located along and beyond the agri-silviculture zone has no pronounced changes in temperature. Similarly, agri-silviculture practice along the coast was able to slightly increase summer precipitation over Liberia and Gambia only by about 0.5 mm/day. Generally, agri-silviculture practice along the coast (with prescribed or dynamic vegetation) does not necessarily have a large-scale impact on temperature and precipitation over the entire West Africa region. Although agri-silviculture practice along the West African coast might not be sufficient to induce cooling or enhance precipitation over West Africa region, it will not exacerbate the projected warming or dryness along the region in the near future. This suggests that agri-silviculture practice along West Africa coasts can be effectively utilized to enhance food security and prevents deforestation due to agricultural expansion in the region without a negative impact on the future climate.

With fixed percentage cover of a broadleaf deciduous tree, C4 grass and C3 grass modified in **GUSAG** experiment, cooling up to about 2°C are induced over most countries along the agri-silviculture zone in all seasons. The resulting cooling translates to more precipitation only over Ghana in summer, while the projected drying over Liberia and Sierra Leone during the monsoon (JJA) and post-monsoon period (SON) were intensified. On the contrary, with the dynamic vegetation option (**GUSAG*d1***), there was no change in temperature over the entire West Africa region in the near future. However, simulation with a larger domain in **GUSAG*d2*** experiment suggests a cooling of about 2°C in areas located within 8°E and 16°E along the agri-silviculture zone in all seasons which translates to enhanced monsoon and

post-monsoon precipitation. Increased temperature of about 0.4 to 2°C was induced outside this area. Hence, the impact of agri-silviculture has a varying effect on the future climate of West Africa at different spatiotemporal scale. Therefore, the study has shown the capability of agri-silviculture to mitigate the projected future warming in some parts of West African countries.

5.2 Recommendations

It is recommended that similar agri-silviculture experiments with other regional climate models be carried out over the study area at a higher resolution. This will enable us to determine if the change signal induced with the agri-silviculture experiment are consistently reproduced in other regional climate models. It would also be necessary to downscale different global circulation models (GCMs) with RegCM4 over the study area so as to identify the most suitable GCM for RegCM4 over West Africa. This is to ascertain the sensitivity of such experiments to different boundary conditions and model uncertainties. This perhaps could reduce or partially eliminate some of the biases identified in the study.

Future agri-silviculture numerical experiments should incorporate tree-crop model to the atmospheric model in order to provide more robust information on the effect of agri-silviculture on the future climate of the region. Climate simulations which will consider the effect of agri-silviculture on the far future climate of West Africa may also be considered. Finally, agri-silviculture practices should be promoted as a conservation agriculture practices that can serve as environmental protection and enhance food security in the region.

REFERENCES

Abiodun, B.J., Pal, J.S., Afiesimama, E.A., Gutowski, W.J. and Adedoyin, A., 2008. Simulation of West African monsoon using RegCM3 Part II: impacts of deforestation and desertification. *Theoretical and Applied Climatology*, *93*(3-4), pp.245-261.

Abiodun, B.J., Adeyewa, Z.D., Oguntunde, P.G., Salami, A.T. and Ajayi, V.O., 2012. Modeling the impacts of reforestation on future climate in West Africa. *Theoretical and Applied Climatology*, *110*(1-2), pp.77-96.

Abiodun, B.J., Salami, A.T., Matthew, O.J. and Odedokun, S., 2013. Potential impacts of afforestation on climate change and extreme events in Nigeria. *Climate Dynamics*, *41*(2), pp.277-293.

Achard, F., Eva, H.D., Mayaux, P., Stibig, H.J. and Belward, A., 2004. Improved estimates of net carbon emissions from land cover change in the tropics for the 1990s. *Global Biogeochemical Cycles*, *18*(2).

Adeniyi, M.O., 2014. Sensitivity of different convection schemes in RegCM4. 0 for simulation of precipitation during the Septembers of 1989 and 1998 over West Africa. *Theoretical and applied climatology*, *115*(1-2), pp.305-322.

Ainsworth, E.A. and Long, S.P., 2005. What have we learned from 15 years of free-air CO_2 enrichment (FACE)? A meta-analytic review of the responses of photosynthesis, canopy properties and plant production to rising CO_2.*New Phytologist*, *165*(2), pp.351-372.

Ajayi, O.C., Akinnifesi, F.K., Sileshi, G. and Chakeredza, S., 2007, November. Adoption of renewable soil fertility replenishment technologies in the southern African region: Lessons learnt and the way forward. In *Natural Resources Forum* (Vol. 31, No. 4, pp.

306-317). Blackwell Publishing Ltd.

Albrecht, A. and Kandji, S.T., 2003. Carbon sequestration in tropical agroforestry systems. *Agriculture, ecosystems & environment*, *99*(1), pp.15-27.

Alo, C.A. and Wang, G., 2010. Role of dynamic vegetation in regional climate predictions over western Africa. *Climate dynamics*, *35*(5), pp.907-922.

Anthes, R.A., 1977. A cumulus parameterization scheme utilizing a one-dimensional cloud model. *Monthly Weather Review*, *105*(3), pp.270-286.

Asase, A., Wade, S.A., Ofori-Frimpong, K., Hadley, P. and Norris, K., 2008. Carbon storage and the health of cocoa agroforestry ecosystems in south-eastern Ghana. *Africa and the Carbon Cycle*, *131*.

Avila, F.B., Pitman, A.J., Donat, M.G., Alexander, L.V. and Abramowitz, G., 2012. Climate model simulated changes in temperature extremes due to land cover change. *Journal of Geophysical Research: Atmospheres (1984–2012)*,*117*(D4).

Barthe, C., Asencio, N., Lafore, J.P., Chong, M., Campistron, B. and Cazenave, F., 2010. Multi-scale analysis of the 25–27 July 2006 convective period over Niamey: Comparison between Doppler radar observations and simulations. *Quarterly Journal of the Royal Meteorological Society*, *136*(S1), pp.190-208.

Berenter, J., 2012. “Ground Truthing” Vulnerability and Adaptation in Africa [Busby, J.W. (ed.)]. Program on Climate Change and African Political Stability, Robert S. Strauss Center for International Security and Law, The University of Texas at Austin, Austin, TX, USA, 17 pp

Bergant, K., Belda, M. and Halenka, T., 2007. Systematic errors in the simulation of

European climate (1961–2000) with RegCM3 driven by NCEP/NCAR reanalysis. *International journal of climatology*, *27*(4), pp.455-472.

Bhaskaran, B., Jones, R.G., Murphy, J.M. and Noguer, M., 1996. Simulations of the Indian summer monsoon using a nested regional climate model: domain size experiments. *Climate Dynamics*, *12*(9), pp.573-587.

Biasutti, M., 2013. Forced Sahel rainfall trends in the CMIP5 archive. *Journal of Geophysical Research: Atmospheres*, *118*(4), pp.1613-1623.

Bonan, G.B., 1997. Effects of land use on the climate of the United States.*Climatic Change*, *37*(3), pp.449-486.

Bonan, G.B., 2008. Forests and climate change: forcings, feedbacks, and the climate benefits of forests. *science*, *320*(5882), pp.1444-1449.

Bonan, G.B., Lawrence, P.J., Oleson, K.W., Levis, S., Jung, M., Reichstein, M., Lawrence, D.M. and Swenson, S.C., 2011. Improving canopy processes in the Community Land Model version 4 (CLM4) using global flux fields empirically inferred from FLUXNET data. *Journal of Geophysical Research: Biogeosciences (2005–2012)*, *116*(G2).

Brink, A.B. and Eva, H.D., 2009. Monitoring 25 years of land cover change dynamics in Africa: A sample based remote sensing approach. *Applied Geography*, *29*(4), pp.501-512.

Canadell, J.G., Raupach, M.R. and Houghton, R.A., 2009. Anthropogenic CO 2 emissions in Africa. *Biogeosciences*, *6*(3), pp.463-468.

Castillo, C.K.G., Levis, S. and Thornton, P., 2012. Evaluation of the new CNDV option of the Community Land Model: effects of dynamic vegetation and interactive nitrogen on

CLM4 means and variability*. *Journal of Climate*, *25*(11), pp.3702-3714.

Charney, J.G., 1975. Dynamics of deserts and drought in the Sahel.*Quarterly Journal of the Royal Meteorological Society*, *101*(428), pp.193-202.

Chaudhry, M.A. and Silim, S., 1980. Agri-Silviculture in Uganda: A Case for Kachung Forest. *Unasylva*, *32*, pp.21-25.

Chen, G.S., Notaro, M., Liu, Z. and Liu, Y., 2012. Simulated Local and Remote Biophysical Effects of Afforestation over the Southeast United States in Boreal Summer*. *Journal of Climate*, *25*(13), pp.4511-4522.

Cook, K.H., 1997. Large-scale atmospheric dynamics and Sahelian precipitation. *Journal of climate*, *10*(6), pp.1137-1152.

Collins, J.M., 2011. Temperature variability over Africa. *Journal of climate*,*24*(14), pp.3649-3666.

Cook, K.H. and Vizy, E.K., 2013. Projected changes in East African rainy seasons. *Journal of Climate*, *26*(16), pp.5931-5948.

Cubasch, U., Wuebbles, D., Chen, D., Facchini, M.C., Frame, D., Mahowald, N., Winther, J.-G., 2013. *Introduction. In: Climate Change 2013: The Physical Science Basis. Contribution of Working Group I to the Fifth Assessment Report of the Intergovernmental Panel on Climate Change. Clim. Chang. 2013 Phys. Sci. Basis. Contrib. Work. Gr. I to Fifth Assess. Rep. Intergov. Panel Clim. Chang*. 119–158. doi:10.1017/CBO9781107415324.007

Davis, N., Bowden, J., Semazzi, F., Xie, L. and Önol, B., 2009. Customization of RegCM3 regional climate model for eastern Africa and a tropical Indian Ocean domain. *Journal*

of Climate, *22*(13), pp.3595-3616.

Dee, D.P., Uppala, S.M., Simmons, A.J., Berrisford, P., Poli, P., Kobayashi, S., Andrae, U., Balmaseda, M.A., Balsamo, G., Bauer, P. and Bechtold, P., 2011. The ERA-Interim reanalysis: Configuration and performance of the data assimilation system. *Quarterly Journal of the Royal Meteorological Society*, *137*(656), pp.553-597.

DeFries, R.S., Hansen, M.C., Townshend, J.R.G., Janetos, A.C. and Loveland, T.R., 2000. A new global 1-km dataset of percentage tree cover derived from remote sensing. *Global Change Biology*, *6*(2), pp.247-254.

Diallo, I., Sylla, M.B., Giorgi, F., Gaye, A.T. and Camara, M., 2012. Multimodel GCM-RCM ensemble-based projections of temperature and precipitation over West Africa for the early 21st century. *International Journal of Geophysics*, *2012*.

Dickinson, R.E., Kennedy, P.J. and Henderson-Sellers, A., 1993. *Biosphere-atmosphere transfer scheme (BATS) version 1e as coupled to the NCAR community climate model*. National Center for Atmospheric Research, Climate and Global Dynamics Division.

Diedhiou A, Janicot S, Viltard A, de Felice P, Laurent H. 1999. Easterly wave regimes and associated convection over West Africa and tropical Atlantic: results from NCEP/NCAR and ECMWF reanalyses. Climate Dynamics 15: 795–822.

Druyan, L.M., Feng, J., Cook, K.H., Xue, Y., Fulakeza, M., Hagos, S.M., Konaré, A., Moufouma-Okia, W., Rowell, D.P., Vizy, E.K. and Ibrah, S.S., 2010. The WAMME regional model intercomparison study. *Climate Dynamics*, *35*(1), pp.175-192.

Elguindi, N., Bi, X., Giorgi, F., Nagarajan, B., Pal, J., Solmon, F. and Giuliani, G., 2013. Regional Climate Model RegCM User Manual Version 4.4.*The Abdus Salam International Centre for Theoretical Physics, Strada Costiera, Trieste, Italy*

October, *21*(2013), p.54.

Emanuel, K.A., 1991. A scheme for representing cumulus convection in large-scale models. *Journal of the Atmospheric Sciences*, *48*(21), pp.2313-2329.

Emanuel, K.A. and Živkovic-Rothman, M., 1999. Development and evaluation of a convection scheme for use in climate models. *Journal of the Atmospheric Sciences*, *56*(11), pp.1766-1782.

Epstein, H.E., Gill, R.A., Paruelo, J.M., Lauenroth, W.K., Jia, G.J. and Burke, I.C., 2002. The relative abundance of three plant functional types in temperate grasslands and shrublands of North and South America: effects of projected climate change. *Journal of Biogeography*, *29*(7), pp.875-888.

FAO. 2001. State of the World's Forests 2001. Rome. ftp.fao.org/docrep/fao/003/y0900e/.

FAO, 2009. World's Forests 2007: Food and Agriculture Organization of the United Nations Rome, 2009. (http://www.fao.org/docrep/011/i0350e/i0350e00.htm)

FAO, 2010. Global forest resources assessment 2010 country report: Venezuela (available at http://www.fao. org/forestry/fra/67090/en/).

FAO, 2012. State of the World's Forests: Food and Agriculture Organization of the United Nations, 2012.http://www.fao.org/docrep/016/i3010e/i3010e.pdf

FAO, 2015. Global Forest Resources Assessment 2015: How have the world's forests changed? Rome, Italy.

Favreau, G., Cappelaere, B., Massuel, S., Leblanc, M., Boucher, M., Boulain, N. and Leduc, C., 2009. Land clearing, climate variability, and water resources increase in semiarid southwest Niger: A review. *Water Resources Research*, *45*(7).

Feddema, J.J., Oleson, K.W., Bonan, G.B., Mearns, L.O., Buja, L.E., Meehl, G.A. and Washington, W.M., 2005. The importance of land-cover change in simulating future climates. *Science*, *310*(5754), pp.1674-1678.

Fink, A.H., Vincent, D.G. and Ermert, V., 2006. Rainfall types in the West African Sudanian zone during the summer monsoon 2002. *Monthly weather review*, *134*(8), pp.2143-2164.

Flaounas, E., Bastin, S. and Janicot, S., 2011. Regional climate modelling of the 2006 West African monsoon: sensitivity to convection and planetary boundary layer parameterisation using WRF. *Climate Dynamics*, *36*(5-6), pp.1083-1105.

Forster, P., Ramaswamy, V., Artaxo, P., Berntsen, T., Betts, R., Fahey, D.W., Haywood, J., Lean, J., Lowe, D.C., Myhre, G. and Nganga, J., 2007. Changes in atmospheric constituents and in radiative forcing. Chapter 2. In *Climate Change 2007. The Physical Science Basis*.

Friedl, M.A., McIver, D.K., Hodges, J.C., Zhang, X.Y., Muchoney, D., Strahler, A.H., Woodcock, C.E., Gopal, S., Schneider, A., Cooper, A. and Baccini, A., 2002. Global land cover mapping from MODIS: algorithms and early results. *Remote Sensing of Environment*, *83*(1), pp.287-302.

Garnett, T., Appleby, M.C., Balmford, A., Bateman, I.J., Benton, T.G., Bloomer, P., Burlingame, B., Dawkins, M., Dolan, L., Fraser, D. and Herrero, M., 2013. Sustainable intensification in agriculture: premises and policies.*Science*, *341*(6141), pp.33-34.

Gbobaniyi, E., Sarr, A., Sylla, M.B., Diallo, I., Lennard, C., Dosio, A., Dhiédiou, A., Kamga, A., Klutse, N.A.B., Hewitson, B. and Nikulin, G., 2014. Climatology, annual cycle and interannual variability of precipitation and temperature in CORDEX

simulations over West Africa. *International Journal of Climatology*, *34*(7), pp.2241-2257.

Gianotti, R.L., Zhang, D. and Eltahir, E.A., 2012. Assessment of the regional climate model version 3 over the maritime continent using different cumulus parameterization and land surface schemes. *Journal of Climate*, *25*(2), pp.638-656.

Giorgi, F. and Mearns, L.O., 1999. Introduction to special section: Regional climate modeling revisited. *Journal of Geophysical Research: Atmospheres*,*104*(D6), pp.6335-6352.

Giorgi, F., Pal, J.S., Bi, X., Sloan, L., Elguindi, N. and Solmon, F., 2006. Introduction to the TAC special issue: The RegCNET network. *Theoretical and Applied Climatology*, *86*(1-4), pp.1-4.

Giorgi, F., Jones, C. and Asrar, G.R., 2009. Addressing climate information needs at the regional level: the CORDEX framework. *World Meteorological Organization (WMO) Bulletin*, *58*(3), p.175.

Giorgi, F., Coppola, E., Solmon, F., Mariotti, L., Sylla, M.B., Bi, X., Elguindi, N., Diro, G.T., Nair, V., Giuliani, G. and Turuncoglu, U.U., 2012. RegCM4: model description and preliminary tests over multiple CORDEX domains.*Climate Research*, *2*(7).

Gonzalez, P., Tucker, C.J. and Sy, H., 2012. Tree density and species decline in the African Sahel attributable to climate. *Journal of Arid Environments*, *78*, pp.55-64.

Grell, G.A., 1993. Prognostic evaluation of assumptions used by cumulus parameterizations. Monthly Weather Review, 121(3), pp.764-787.

Grell, G.A., Dudhia, J. and Stauffer, D.R., 1994. A description of the fifth-generation Penn

State/NCAR mesoscale model (MM5). NCAR Technical Note, NCAR/TN-398+STR

Grist, J.P., Nicholson and S.E., 2001. A Study of the Dynamic Factors Influencing the Rainfall Variability in the West African Sahel. J. Clim. 14, 1337–1359. doi:10.1175/1520-0442(2001)014<1337:ASOTDF>2.0.CO;2

Gockowski, J. and Asten, P.V., 2012. Agricultural intensification as a climate change and food security strategy for sub-Saharan Africa. *Climate Change Mitigation and Agriculture. Edited by Wollenberg E, Nihart A, Tapio-Bostro m ML, Grieg-Gran M. London-New York: ICRAF-CIAT*, pp.382-390.

Gonzalez, P., Tucker, C.J. and Sy, H., 2012. Tree density and species decline in the African Sahel attributable to climate. *Journal of Arid Environments*, *78*, pp.55-64.

Gu, H., Wang, G., Yu, Z. and Mei, R., 2012. Assessing future climate changes and extreme indicators in east and south Asia using the RegCM4 regional climate model. *Climatic Change*, *114*(2), pp.301-317.

Haensler, A., Saeed, F. and Jacob, D., 2013. Assessing the robustness of projected precipitation changes over central Africa on the basis of a multitude of global and regional climate projections. *Climatic Change*, *121*(2), pp.349-363.

Hagos, S.M. and Cook, K.H., 2007. Dynamics of the West African monsoon jump. *Journal of Climate*, *20*(21), pp.5264-5284.

Hansen, M.C., DeFries, R.S., Townshend, J.R.G., Carroll, M., Dimiceli, C. and Sohlberg, R.A., 2003. Global percent tree cover at a spatial resolution of 500 meters: First results of the MODIS vegetation continuous fields algorithm. *Earth Interactions*, *7*(10), pp.1-15.

Hartmann, D.J., Klein Tank, A.M.G., Rusticucci, M., Alexander, L. V, Brönnimann, S., Charabi, Y.A.-R., Dentener, F.J., Dlugokencky, E.J., Easterling, D.R., Kaplan, A., Soden, B.J., Thorne, P.W., Wild, M., Zhai, P., 2013. Observations: Atmosphere and Surface. Clim. Chang. 2013 Phys. Sci. Basis. Contrib. Work. Gr. I to Fifth Assess. Rep. Intergov. Panel Clim. Chang. 159–254. doi:10.1017/CBO9781107415324.008

Harris, I.P.D.J., Jones, P.D., Osborn, T.J. and Lister, D.H., 2014. Updated high-resolution grids of monthly climatic observations–the CRU TS3. 10 Dataset. *International Journal of Climatology*, *34*(3), pp.623-642.

Hastenrath, S., 1991. Climate Dynamics of the Tropics: Kluwer Academic.*Climate Dynamics of the Tropics: Kluwer Academic*.

Holtslag, A.A.M., De Bruijn, E.I.F. and Pan, H.L., 1990. A high resolution air mass transformation model for short-range weather forecasting. *Monthly Weather Review*, *118*(8), pp.1561-1575.

IBRD, 2011. Sahel and West Africa Program in Support of the Great Green Wall Initiative: to Expand Sustainable Land and Water Management in Targeted Landscapes and Climate Vulnerable Areas. Washington, DC: World Bank

IPCC, 2000. Land Use, Land-Use Change, and Forestry. Intergovernmental Panel on Climate Change. Cambridge University Press, Cambridge, UK.

IPCC, 2001. Climate Change 2001: The Scientific Basis. Contribution of Working Group I to The Third Assessment Report of the International Panel on Climate Change IPCC Cambridge. Cambridge University Press

IPCC, 2007a: Climate Change 2007: The Physical Science Basis. Contribution of Working Group I to the Fourth Assessment Report of the Intergovernmental Panel on Climate

Change, S. Solomon, D. Qin,M.Manning, Z. Chen,M.Marquis, K.B. Averyt,M.Tignor and H.L. Miller, Eds., Cambridge University Press, Cambridge, UK and New York, NY, USA

IPCC, 2007b. Climate change 2007: impacts, adaptation and vulnerability. In: Parry ML, Canziani OF, Palutikof JP, van der Linden PJ, Hanson CE (eds) Contribution of Working Group II to the Fourth Assessment Report of the Intergovernmental Panel on Climate Change. Cambridge University Press, Cambridge, pp 976

IPCC, 2007c. Climate change 2007: mitigation of climate change. In: Metz B, Davidson OR, Bosch PR, Dave R, Meyer LA (eds) Contribution of Working Group III to the Fourth Assessment Report of the Intergovernmental Panel on Climate Change. Cambridge University Press, Cambridge, pp 760

IPCC, 2013. Climate Change 2013: The Physical Science Basis. Contribution of Working Group I to the Fifth Assessment Report of the Intergovernmental Panel on Climate Change [Stocker, T.F., D. Qin, G.-K. Plattner, M. Tignor, S.K. Allen, J. Boschung, A. Nauels, Y. Xia, V. Bex and P.M. Midgley (eds.)]. Cambridge University Press, Cambridge, United Kingdom and New York, NY, USA, 1535 pp, doi:10.1017/CBO9781107415324.

Jalloh, A., Sarr, B., Kuiseu, J., Roy-Macauley, H. and Sereme, P., 2011. Review of climate in West and Central Africa to inform farming systems research and development in the sub-humid and semi-arid agroecologies of the region. *Central African Council for Agricultural Research and Development (CORAF/WECARD), CORAF/WECARD, Dakar, Senegal*.

Jalloh, A., Nelson, G.C., Thomas, T.S., Zougmoré, R.B. and Roy-Macauley, H. eds.,

2013. *West African agriculture and climate change: a comprehensive analysis*. Intl Food Policy Res Inst.

James, R. and Washington, R., 2013. Changes in African temperature and precipitation associated with degrees of global warming. *Climatic change*,*117*(4), pp.859-872.

Ji, Z., Wang, G., Pal, J.S. and Yu, M., 2015. Potential climate effect of mineral aerosols over West Africa. Part I: model validation and contemporary climate evaluation. *Climate Dynamics*, pp.1-17.

Jones, C., Giorgi, F. and Asrar, G., 2011. The Coordinated Regional Downscaling Experiment: CORDEX, an international downscaling link to CMIP5. *CLIVAR exchanges*, *16*(2), pp.34-40.

Jones, R., Hartley, A., McSweeney, C., Mathison, C. and Buontempo, C., 2012. Deriving high resolution climate data for West Africa for the period 1950–2100. *UNEP-WCMC technical report*.

Jose, S. and Bardhan, S., 2012. Agroforestry for biomass production and carbon sequestration: an overview. *Agroforestry Systems*, *86*(2), pp.105-111.

Kain, J.S. and Fritsch, J.M., 1990. A one-dimensional entraining/detraining plume model and its application in convective parameterization. *Journal of the Atmospheric Sciences*, *47*(23), pp.2784-2802.

Kain, J.S., 2004. The Kain-Fritsch convective parameterization: an update.*Journal of Applied Meteorology*, *43*(1), pp.170-181.

Kalame, F.B., Kudejira, D. and Nkem, J., 2011. Assessing the process and options for implementing National Adaptation Programmes of Action (NAPA): a case study from

Burkina Faso. *Mitigation and Adaptation Strategies for Global Change*, *16*(5), pp.535-553.

Kalapureddy, M.C.R., Lothon, M., Campistron, B., Lohou, F. and Saïd, F., 2010. Wind profiler analysis of the African Easterly Jet in relation with the boundary layer and the Saharan heat-low. *Quarterly Journal of the Royal Meteorological Society*, *136*(S1), pp.77-91.

Kalognomou, E.A., Lennard, C., Shongwe, M., Pinto, I., Favre, A., Kent, M., Hewitson, B., Dosio, A., Nikulin, G., Panitz, H.J. and Büchner, M., 2013. A diagnostic evaluation of precipitation in CORDEX models over southern Africa. *Journal of Climate*, *26*(23), pp.9477-9506.

Kahiluoto, H., Smith, P., Moran, D. and Olesen, J.E., 2014. Enabling food security by verifying agricultural carbon. *Nature Climate Change*, *4*(5), pp.309-311.

Kidd, C. and Pimentel, D., 1992. Integrated resource management: Agroforestry for Development: Academic. *San Diego, CA*.

Kiehl, J.T., Hack, J.J., Bonan, G.B., Boville, B.A. and Briegleb, B.P., 1996.*Description of the NCAR Community Climate Model (CCM3). Technical Note*(No. PB--97-131528/XAB; NCAR/TN--420-STR). National Center for Atmospheric Research, Boulder, CO (United States). Climate and Global Dynamics Div..

Kirtman, B., Power, S.B., Adedoyin, J.A., Boer, G.J., Bojariu, R., Camilloni, I., Doblas-Reyes, F.J., Fiore, A.M., Kimoto, M., Meehl, G.A. and Prather, M., 2013. Near-term climate change: projections and predictability. *Climate change*, pp.953-1028.

Klutse, N.A.B., Sylla, M.B., Diallo, I., Sarr, A., Dosio, A., Diedhiou, A., Kamga, A., Lamptey, B., Ali, A., Gbobaniyi, E.O. and Owusu, K., 2016. Daily characteristics of

West African summer monsoon precipitation in CORDEX simulations. *Theoretical and Applied Climatology*, *123*(1-2), pp.369-386.

Koteswaram, P., 1958. The Easterly Jet stream in the tropics*. *Tellus*, *10*(1), pp.43-57.

Koven, C.D., Riley, W.J., Subin, Z.M., Tang, J.Y., Torn, M.S., Collins, W.D., Bonan, G.B., Lawrence, D.M. and Swenson, S.C., 2013. The effect of vertically resolved soil biogeochemistry and alternate soil C and N models on C dynamics of CLM4. *Biogeosciences*, *10*(11), pp.7109-7131.

Krausmann, F., Erb, K.H., Gingrich, S., Haberl, H., Bondeau, A., Gaube, V., Lauk, C., Plutzar, C. and Searchinger, T.D., 2013. Global human appropriation of net primary production doubled in the 20th century.*Proceedings of the National Academy of Sciences*, *110*(25), pp.10324-10329.

Kutsch, W.L., Merbold, L., Ziegler, W., Mukelabai, M.M., Muchinda, M., Kolle, O. and Scholes, R.J., 2011. The charcoal trap: Miombo forests and the energy needs of people. *Carbon balance and management*, *6*(1), p.5.

Kueppers, L.M. and Snyder, M.A., 2012. Influence of irrigated agriculture on diurnal surface energy and water fluxes, surface climate, and atmospheric circulation in California. *Climate dynamics*, *38*(5-6), pp.1017-1029.

Lafore, J.P., Redelsperger, J.L. and Jaubert, G., 1988. Comparison between a three-dimensional simulation and Doppler radar data of a tropical squall line: Transports of mass, momentum, heat, and moisture. *Journal of the atmospheric sciences*, *45*(22), pp.3483-3500.

Lafore, J.P., Berre, L. and Fischer, C., 2006. Limited-area model error statistics over Western Africa: Comparisons with midlatitude results.*Quarterly Journal of the Royal*

Meteorological Society, *132*(614), pp.213-230.

Landsea, C.W. and Gray, W.M., 1992. The strong association between western Sahelian monsoon rainfall and intense Atlantic hurricanes. *Journal of Climate*, *5*(5), pp.435-453.

Lasco, R.D., Delfino, R.J.P., Catacutan, D.C., Simelton, E.S. and Wilson, D.M., 2014. Climate risk adaptation by smallholder farmers: the roles of trees and agroforestry. *Current Opinion in Environmental Sustainability*, *6*, pp.83-88.

Lawrence, P.J. and Chase, T.N., 2007. Representing a new MODIS consistent land surface in the Community Land Model (CLM 3.0). *Journal of Geophysical Research: Biogeosciences*, *112*(G1).

Le Barbé, L., Lebel, T. and Tapsoba, D., 2002. Rainfall variability in West Africa during the years 1950-90. *Journal of climate*, *15*(2), pp.187-202.

Lebel, T. and Ali, A., 2009. Recent trends in the Central and Western Sahel rainfall regime (1990–2007). *Journal of Hydrology*, *375*(1), pp.52-64.

Leblanc, M.J., Favreau, G., Massuel, S., Tweed, S.O., Loireau, M. and Cappelaere, B., 2008. Land clearance and hydrological change in the Sahel: SW Niger. *Global and Planetary Change*, *61*(3), pp.135-150.

Luedeling, E. and Neufeldt, H., 2012. Carbon sequestration potential of parkland agroforestry in the Sahel. *Climatic Change*, *115*(3-4), pp.443-461.

Machado, L.T., Duvel, J.P. and Desbois, M., 1993. Diurnal variations and modulation by easterly waves of the size distribution of convective cloud clusters over West Africa and the Atlantic Ocean. *Monthly Weather Review*,*121*(1), pp.37-49.

Majanen, T. and Scherr, S.J., 2011. Performance and Potential of Conservation Agriculture

for Climate Change Adaptation and Mitigation in Sub-Saharan Africa. Ecoagriculture Discussion Paper No. 6, Ecoagriculture Partners, Washington, DC, USA, 91 pp.

Mariotti, L., Coppola, E., Sylla, M.B., Giorgi, F. and Piani, C., 2011. Regional climate model simulation of projected 21st century climate change over an all-Africa domain: comparison analysis of nested and driving model results.*Journal of Geophysical Research: Atmospheres*, *116*(D15).

Martin, G.M., Bellouin, N., Collins, W.J., Culverwell, I.D., Halloran, P.R., Hardiman, S.C., Hinton, T.J., Jones, C.D., McDonald, R.E., McLaren, A.J. and O'Connor, F.M., 2011. The HadGEM2 family of met office unified model climate configurations. *Geoscientific Model Development Discussions*, *4*, pp.765-841.

Mathon, V., Laurent, H. and Lebel, T., 2002. Mesoscale convective system rainfall in the Sahel. *Journal of applied meteorology*, *41*(11), pp.1081-1092.

Mayaux, P., Pekel, J.F., Desclée, B., Donnay, F., Lupi, A., Achard, F., Clerici, M., Bodart, C., Brink, A., Nasi, R. and Belward, A., 2013. State and evolution of the African rainforests between 1990 and 2010. *Philosophical Transactions of the Royal Society of London B: Biological Sciences*,*368*(1625), p.20120300.

Mbow, C., Mertz, O., Diouf, A., Rasmussen, K. and Reenberg, A., 2008. The history of environmental change and adaptation in eastern Saloum–Senegal—Driving forces and perceptions. *Global and Planetary Change*, *64*(3), pp.210-221.

Mbow, C., Van Noordwijk, M., Luedeling, E., Neufeldt, H., Minang, P.A. and Kowero, G., 2014a. Agroforestry solutions to address food security and climate change challenges in Africa. *Current Opinion in Environmental Sustainability*, *6*, pp.61-67.

Mbow, C., Smith, P., Skole, D., Duguma, L. and Bustamante, M., 2014b. Achieving

mitigation and adaptation to climate change through sustainable agroforestry practices in Africa. *Current Opinion in Environmental Sustainability*, *6*, pp.8-14.

Meinshausen, M., Smith, S.J., Calvin, K., Daniel, J.S., Kainuma, M.L.T., Lamarque, J.F., Matsumoto, K., Montzka, S.A., Raper, S.C.B., Riahi, K. and Thomson, A.G.J.M.V., 2011. The RCP greenhouse gas concentrations and their extensions from 1765 to 2300. *Climatic change*, *109*(1-2), pp.213-241.

Meinke, I., Roads, J. and Kanamitsu, M., 2007. Evaluation of RSM-simulated precipitation during CEOP. *J Meteorol Soc Jpn 85*, pp.145-166.

Mertz, O., Mbow, C., Reenberg, A. and Diouf, A., 2009. Farmers' perceptions of climate change and agricultural adaptation strategies in rural Sahel. *Environmental management*, *43*(5), pp.804-816.

Minang, P.A., Duguma, L.A., Bernard, F., Mertz, O. and van Noordwijk, M., 2014. Prospects for agroforestry in REDD+ landscapes in Africa. *Current opinion in environmental sustainability*, *6*, pp.78-82.

Mohr, K.I. and Thorncroft, C.D., 2006. Intense convective systems in West Africa and their relationship to the African easterly jet. *Quarterly Journal of the Royal Meteorological Society*, *132*(614), pp.163-176.

Mohr, K.I., Famiglietti, J.S. and Zipser, E.J., 1999. The contribution to tropical rainfall with respect to convective system type, size, and intensity estimated from the 85-GHz ice-scattering signature. *Journal of Applied Meteorology*, *38*(5), pp.596-606.

Molden, D., Frenken, K., Barker, R., Fraiture, C.D., Mati, B., Svendsen, M., Sadoff, C., Finlayson, C.M., Attapatu, S., Giordano, M. and Inocencio, A., 2007. Trends in water and agricultural development.

Moncrieff, M.W., 1992. Organized convective systems: Archetypal dynamical models, mass and momentum flux theory, and parametrization.*Quarterly Journal of the Royal Meteorological Society*, *118*(507), pp.819-850.

Mora, C.F. and AG, R., Longman, RS Dacks, MM Walton, EJ Tong, JJ Sanchez, LR Kaiser, YO Stender, JM Anderson, CM Ambrosino, I. Fernandez-Silva, LM Giuseffi, and TW Giambelluca, 2013: The projected timing of climate departure from recent variability. *Nature*, *502*, pp.183-187.

Moss, R.H., Edmonds, J.A., Hibbard, K.A., Manning, M.R., Rose, S.K., Van Vuuren, D.P., Carter, T.R., Emori, S., Kainuma, M., Kram, T. and Meehl, G.A., 2010. The next generation of scenarios for climate change research and assessment. *Nature*, *463*(7282), pp.747-756.

Muthuri, C.W., Ong, C.K., Black, C.R., Mati, B.M., Ngumi, V.W. and van Noordwijk, M., 2004. Modelling the effects of leafing phenology on growth and water use by selected agroforestry tree species in semi-arid Kenya.*Land Use and Water Resources Research*, *4*, pp.1-11.

Nair, P.R., 1985. Classification of agroforestry systems. *Agroforestry systems*, *3*(2), pp.97-128.

Nair, P., 1993. Introduction to Agroforestry. Nairobi, Kenya: Kluwer Academic Publishers, published in collaboration with ICRAF.

Nair, P.K.R., Nair, V.D., 2003. Carbon storage in North American agroforestry systems, in Kimble, J., Heath, L.S., Birdsey, R. A., Lal, R. (eds.): The Potential of U.S. Forest Soils to Sequester Carbon and Mitigate the Greenhouse Effect. CRC Press, Boca Raton, FL, USA, pp. 333–346

Nair, P.K.R., Mohan Kumar, B. and Nair, V.D., 2009a. Agroforestry as a strategy for carbon sequestration. *Journal of plant nutrition and soil science*, *172*(1), pp.10-23.

Nair, P.R., Nair, V.D., Kumar, B.M. and Haile, S.G., 2009b. Soil carbon sequestration in tropical agroforestry systems: a feasibility appraisal.*environmental science & policy*, *12*(8), pp.1099-1111.

New, M., Hewitson, B., Stephenson, D.B., Tsiga, A., Kruger, A., Manhique, A., Gomez, B., Coelho, C.A., Masisi, D.N., Kululanga, E. and Mbambalala, E., 2006. Evidence of trends in daily climate extremes over southern and west Africa. *Journal of Geophysical Research: Atmospheres*, *111*(D14).

Niang, I., Ruppel, O.C., Abdrabo, M.A., Essel, A., Lennard, C., Padgham, J., Urquhart, P., 2014. Africa. Clim. Chang. 2014 Impacts, Adapt. Vulnerability - Contrib. Work. Gr. II to Fifth Assess. Rep. Intergov. Panel Clim. Chang. 1199–1265.

Nicholson, S.E., 1981. Rainfall and atmospheric circulation during drought periods and wetter years in West Africa. *Monthly weather review*, *109*(10), pp.2191-2208.

Nicholson, S.E. and Webster, P.J., 2007. A physical basis for the interannual variability of rainfall in the Sahel. *Quarterly Journal of the Royal Meteorological Society*, *133*(629), pp.2065-2084.

Nicholson, S.E., Barcilon, A.I., Challa, M. and Baum, J., 2007. Wave activity on the tropical easterly jet. *Journal of the atmospheric sciences*,*64*(7), pp.2756-2763.

Nicholson, S.E., 2009. A revised picture of the structure of the “monsoon” and land ITCZ over West Africa. *Climate Dynamics*, *32*(7-8), pp.1155-1171.

Nicholson, S.E., Nash, D.J., Chase, B.M., Grab, S.W., Shanahan, T.M., Verschuren, D.,

Asrat, A., Lézine, A.M. and Umer, M., 2013. Temperature variability over Africa during the last 2000 years. *The Holocene*, p.0959683613483618.

Nikulin, G., Jones, C., Giorgi, F., Asrar, G., Büchner, M., Cerezo-Mota, R., Christensen, O.B., Déqué, M., Fernandez, J., Hänsler, A. and van Meijgaard, E., 2012. Precipitation climatology in an ensemble of CORDEX-Africa regional climate simulations. *Journal of Climate*, *25*(18), pp.6057-6078.

Noble, I., Bolin, B., Ravindranath, N.H., Verardo, D.J. and Dokken, D.J., 2000. *Land Use, Land-Use Change, and Forestry*. Cambridge University Press.

Oguntunde, P.G., Abiodun, B.J. and Lischeid, G., 2015. A numerical modelling study of the hydroclimatology of the Niger River Basin, West Africa. *Hydrological Sciences Journal*, pp.1-13.

Oh, S.G., Park, J.H., Lee, S.H. and Suh, M.S., 2014. Assessment of the RegCM4 over East Asia and future precipitation change adapted to the RCP scenarios. *Journal of Geophysical Research: Atmospheres*, *119*(6), pp.2913-2927.

Oke, D.O. and Odebiyi, K.A., 2007. Traditional cocoa-based agroforestry and forest species conservation in Ondo State, Nigeria. *Agriculture, ecosystems & environment*, *122*(3), pp.305-311.

Oleson, K.W., Niu, G.Y., Yang, Z.L., Lawrence, D.M., Thornton, P.E., Lawrence, P.J., Stöckli, R., Dickinson, R.E., Bonan, G.B., Levis, S. and Dai, A., 2008. Improvements to the Community Land Model and their impact on the hydrological cycle. *Journal of Geophysical Research: Biogeosciences*, *113*(G1).

Oleson, K. W., Lawrence, D. M., Bonan, G. B., Drewniak, B., Huang, M., Koven, C. D., ... & Swenson, S. C. 2013. *Technical description of version 4.5 of the Community Land*

Model (CLM). Ncar Tech. Note NCAR/TN-503+ STR. National Center for Atmospheric Research, Boulder, CO, 422 pp. doi: 10.5065/D6RR1W7M.

Omotosho, J.B., 1984. Spatial and seasonal variation of line squalls over West Africa. *Archives for meteorology, geophysics, and bioclimatology, Series A*, *33*(2-3), pp.143-150.

Omotosho, J.B., 1985. The separate contributions of line squalls, thunderstorms and the monsoon to the total rainfall in Nigeria. *Journal of climatology*, *5*(5), pp.543-552.

Omotosho, J.B., 1992. Long-range prediction of the onset and end of the rainy season in the West African Sahel. *International Journal of climatology*,*12*(4), pp.369-382.

Omotosho, J.B. and Abiodun, B.J., 2007. A numerical study of moisture build-up and rainfall over West Africa. *Meteorological Applications*, *14*(3), pp.209-225.

Ong, C.K., Black, C. and Wilson, J. eds., 2015. *Tree-crop Interactions: Agroforestry in a Changing Climate*. CABI.

Paeth, H. and Thamm, H.P., 2007. Regional modelling of future African climate north of 15 S including greenhouse warming and land degradation.*Climatic Change*, *83*(3), pp.401-427.

Pal, J.S., Eltahir, E.A. and Small, E.E., 2000. Simulation of regional-scale water and energy budgets- Representation of subgrid cloud and precipitation processes within RegCM. *Journal of Geophysical Research*, *105*(D24), pp.29579-29594.

Pal, J.S., Giorgi, F., Bi, X., Elguindi, N., Solmon, F., Rauscher, S.A., Gao, X., Francisco, R., Zakey, A., Winter, J. and Ashfaq, M., 2007. Regional climate modeling for the developing world: the ICTP RegCM3 and RegCNET.*Bulletin of the American*

Meteorological Society, *88*(9), pp.1395-1409.

Patricola, C.M. and Cook, K.H., 2008. Atmosphere/vegetation feedbacks: A mechanism for abrupt climate change over northern Africa. *Journal of Geophysical Research: Atmospheres*, *113*(D18).

Patricola, C.M. and Cook, K.H., 2010. Northern African climate at the end of the twenty-first century: an integrated application of regional and global climate models. *Climate Dynamics*, *35*(1), pp.193-212.

Patricola, C.M. and Cook, K.H., 2011. Sub-Saharan Northern African climate at the end of the twenty-first century: forcing factors and climate change processes. *Climate dynamics*, *37*(5-6), pp.1165-1188.

Pielke Sr, R.A. and Niyogi, D., 2009. The role of landscape processes within the climate system. In *Landform-Structure, Evolution, Process Control* (pp. 67-85). Springer Berlin Heidelberg.

Ramankutty, N., Evan, A.T., Monfreda, C. and Foley, J.A., 2008. Farming the planet: 1. Geographic distribution of global agricultural lands in the year 2000. *Global Biogeochemical Cycles*, *22*(1).

Rauscher, S.A., Coppola, E., Piani, C. and Giorgi, F., 2010. Resolution effects on regional climate model simulations of seasonal precipitation over Europe. *Climate Dynamics*, *35*(4), pp.685-711.

Reij, C., Tappan, G. and Smale, M., 2009. *Agroenvironmental transformation in the Sahel: Another kind of" Green Revolution"* (Vol. 914). Intl Food Policy Res Inst.

Reij, C. 2011. Investing in trees to mitigate climate change. In: Nierenberg, D. and

Halliwell, B. (eds) State of the World: Innovations that Nourish the Planet. Worldwatch Institute, Washington, DC.

Reiter, E. R., 1969. *Tropospheric circulation and jet streams*. Climate of the Free Atmosphere, D. F. Rex, Ed., Vol. 4, World Survey of Climatology, Elsevier, 85–203.

Rhodes, E.R., Jalloh, A. and Diouf, A., 2014. Review of research and policies for climate change adaptation in the agriculture sector in West Africa. *Future Agricultures. Working Paper*, *90*.

Riehl, H., 1945. *Waves in the easterlies and the polar front in the tropics*. University of Chicago Press.

Rockel, B. and Geyer, B., 2008. The performance of the regional climate model CLM in different climate regions, based on the example of precipitation. *Meteorologische Zeitschrift*, *17*(4), pp.487-498.

Ruelland, D., Tribotte, A., Puech, C. and Dieulin, C., 2011. Comparison of methods for LUCC monitoring over 50 years from aerial photographs and satellite images in a Sahelian catchment. *International Journal of Remote Sensing*, *32*(6), pp.1747-1777.

Sanderson, M.G., Hemming, D.L. and Betts, R.A., 2011. Regional temperature and precipitation changes under high-end (≥ 4 C) global warming. *Philosophical Transactions of the Royal Society of London A: Mathematical, Physical and Engineering Sciences*, *369*(1934), pp.85-98.

Sarr, B. and Lona, I., 2009. Les fortes pluies et les inondations enregistrées au Sahel au cours de l'hivernage 2007: variabilité et/ou changement climatique. 14ème Colloque International. *SIFEE «Changement climatique et évaluation Environnementale» Outils et enjeux pour l'évaluation des impacts et l'élaboration des plans d'adaptation,*

Niamey, pp.26-29.

Seneviratne, S.I., N. Nicholls, D. Easterling, C.M. Goodess, S. Kanae, J. Kossin, Y. Luo, J. Marengo, K. McInnes, M. Rahimi, M. Reichstein, A. Sorteberg, C. Vera, and X. Zhang, 2012. Changes in climate extremes and their impacts on the natural physical environment. In: Managing the Risks of Extreme Events and Disasters to Advance Climate Change Adaptation. A Special Report of Working Groups I and II of the Intergovernmental Panel on Climate Change [Field, C.B., V. Barros, T.F. Stocker, D. Qin, D.J. Dokken, K.L. Ebi, M.D. Mastrandrea, K.J. Mach, G.-K. Plattner, S.K. Allen, M. Tignor, and P.M. Midgley (eds.)]. Cambridge University Press, Cambridge, UK and New York, NY, USA, pp. 109-230

Simmons, A., Uppala, S., Dee, D. and Kobayashi, S., 2007. ERA-Interim: New ECMWF reanalysis products from 1989 onwards. *ECMWF newsletter*,*110*(110), pp.25-35.

Smith, P., Martino, D., Cai, Z., Gwary, D., Janzen, H., Kumar, P., McCarl, B., Ogle, S., O'Mara, F., Rice, C., Scholes, B., Sirotenko, O., 2007. Agriculture. In climate change 2007: mitigation. In: Metz, B., Davidson, O.R., Bosch, P.R., Dave, R., Meyer, L.A. (Eds.), Contribution ofWorking Group III to the Fourth Assessment Report of the Intergovernmental Panel on Climate Change. Cambridge University Press, Cambridge, United Kingdom and New York, NY, USA.

Smith P., Bustamante, M., Ahammad, H., Clark, H., Dong, H., Elsiddig, E.A., Haberl, H., Harper, R., House, J., Jafari, M., Masera, O., Mbow, C., Ravindranath, N. H., Rice, C.W., Robledo Abad, C., Romanovskaya, A., Sperling, F., Tubiello, F., 2014. Agriculture, Forestry and Other Land Use (AFOLU). In: Climate Change 2014: Mitigation of Climate Change. Contribution of Working Group III to the Fifth Assessment Report of the Intergovernmental Panel on Climate Change [Edenhofer, O.,

R. Pichs-Madruga, Y. Sokona, E. Farahani, S. Kadner, K. Seyboth, A. Adler, I. Baum, S. Brunner, P. Eickemeier, B. Kriemann, J. Savolainen, S. Schlömer, C. von Stechow, T. Zwickel and J.C. Minx (eds.)]. Cambridge University Press, Cambridge, United Kingdom and New York, NY, USA

Stebbings E.P.,1935. The encroaching Sahara. Geogr Journal 86:509–510

Stott, P.A., Gillett, N.P., Hegerl, G.C., Karoly, D.J., Stone, D.A., Zhang, X. and Zwiers, F., 2010. Detection and attribution of climate change: a regional perspective. *Wiley Interdisciplinary Reviews: Climate Change*, *1*(2), pp.192-211.

Steiner, A.L., Pal, J.S., Rauscher, S.A., Bell, J.L., Diffenbaugh, N.S., Boone, A., Sloan, L.C. and Giorgi, F., 2009. Land surface coupling in regional climate simulations of the West African monsoon. *Climate Dynamics*, *33*(6), pp.869-892.

Sultan, B. and Janicot, S., 2003. The West African monsoon dynamics. Part II: The "preonset" and "onset" of the summer monsoon. *Journal of climate*,*16*(21), pp.3407-3427.

Sun, Y., Gu, L. and Dickinson, R.E., 2012. A numerical issue in calculating the coupled carbon and water fluxes in a climate model. *Journal of Geophysical Research: Atmospheres*, *117*(D22).

Swenson, S.C. and Lawrence, D.M., 2012. A new fractional snow-covered area parameterization for the Community Land Model and its effect on the surface energy balance. *Journal of Geophysical Research: Atmospheres*,*117*(D21).

Sylla, M.B., Gaye, A.T., Pal, J.S., Jenkins, G.S. and Bi, X.Q., 2009. High-resolution simulations of West African climate using regional climate model (RegCM3) with different lateral boundary conditions. *Theoretical and Applied Climatology*, *98*(3-4),

pp.293-314.

Sylla, M.B., Dell'Aquila, A., Ruti, P.M. and Giorgi, F., 2010a. Simulation of the intraseasonal and the interannual variability of rainfall over West Africa with RegCM3 during the monsoon period. *International Journal of Climatology*,*30*(12), pp.1865-1883.

Sylla, M.B., Gaye, A.T., Jenkins, G.S., Pal, J.S. and Giorgi, F., 2010b. Consistency of projected drought over the Sahel with changes in the monsoon circulation and extremes in a regional climate model projections.*Journal of Geophysical Research: Atmospheres*, *115*(D16).

Sylla, M.B., Giorgi, F., Coppola, E. and Mariotti, L., 2013a. Uncertainties in daily rainfall over Africa: assessment of gridded observation products and evaluation of a regional climate model simulation. *International Journal of Climatology*, *33*(7), pp.1805-1817.

Sylla, M.B., Diallo, I. and Pal, J.S., 2013b. West African monsoon in state-of-the-science regional climate models. *Climate Variability—Regional and Thematic Patterns*, *10*, p.55140.

Sylla, M.B., Pal, J.S., Wang, G.L. and Lawrence, P.J., 2016. Impact of land cover characterization on regional climate modeling over West Africa.*Climate Dynamics*, *46*(1-2), pp.637-650.

Takimoto, A., Nair, P.R. and Nair, V.D., 2008. Carbon stock and sequestration potential of traditional and improved agroforestry systems in the West African Sahel. *Agriculture, Ecosystems & Environment*, *125*(1), pp.159-166.

Tans, P., 2009. An Accounting of the Observed Increase in Oceanic and Atmospheric CO2 and the Outlook for the Future. *Oceanography*, 26-35

Taylor, K.E., Stouffer, R.J. and Meehl, G.A., 2012. *An overview of CMIP5 and the experiment design, B. Am. Meteorol. Soc., 93, 485–498, doi: 10.1175*. BAMS-D-11-00094.1.

Thorncroft, C.D. and Blackburn, M., 1999. Maintenance of the African easterly jet. *Quarterly Journal of the Royal Meteorological Society*, *125*(555), pp.763-786.

Tiedtke, M.I.., 1989. A comprehensive mass flux scheme for cumulus parameterization in large-scale models. *Monthly Weather Review*,*117*(8), pp.1779-1800.

Tougiani, A., Guero, C. and Rinaudo, T., 2009. Community mobilisation for improved livelihoods through tree crop management in Niger. *GeoJournal*,*74*(5), pp.377-389.

Torquebiau, E., 2013. Agroforestry and Climate Change, FAO Webinar, 5 February 2013, CIRAD - Agricultural Research for Development

Le Treut, H., Somerville, R., Cubasch, U., Ding, Y., Mauritzen, C., Mokssit, A., Peterson, T. and Prather, M., 2007. Historical overview of climate change. *Earth*, *Chapter 1*(October), 93–127. http://doi.org/10.1016/j.soilbio.2010.04.001

Tschakert, P., 2004. Carbon for farmers: Assessing the potential for soil carbon sequestration in the Old Peanut Basin of Senegal. *Climatic change*,*67*(2-3), pp.273-290.

Tschakert, P., 2007. Views from the vulnerable: understanding climatic and other stressors in the Sahel. *Global Environmental Change*, *17*(3), pp.381-396.

UNFCCC, 1995. United Nations Framework Convention on Climate Change. Treaty Series No. 28. New York

UNFCCC, 2014. Options for possible additional land use, land-use change and forestry activities and alternative approaches to addressing the risk of nonpermanence under the

clean development mechanism. Technical paper 2

Van Vuuren DP, Edmonds J, Kainuma MLT, Riahi K, Thomson A, Matsui T, Hurtt G, Lamarque J-F, Meinshausen M, Smith S, Grainer C, Rose S, Hibbard KA, Nakicenovic N, Krey V, Kram T 2011. Representative concentration pathways: An overview. Clim. Change, 109, 95–116. doi:10.1007/ s10584-011-0148-z

Verchot, L.V., Van Noordwijk, M., Kandji, S., Tomich, T., Ong, C., Albrecht, A., Mackensen, J., Bantilan, C., Anupama, K.V. and Palm, C., 2007. Climate change: linking adaptation and mitigation through agroforestry.*Mitigation and adaptation strategies for global change*, *12*(5), pp.901-918.

Vizy, E.K. and Cook, K.H., 2012. Mid-twenty-first-century changes in extreme events over northern and tropical Africa. *Journal of Climate*, *25*(17), pp.5748-5767.

Vizy, E.K., Cook, K.H., Crétat, J. and Neupane, N., 2013. Projections of a wetter Sahel in the twenty-first century from global and regional models.*Journal of Climate*, *26*(13), pp.4664-4687.

Ward, M. N., Cook, K., Diedhiou, A., Fontaine, B., Giannini, A., Kamga, A., Lamb, P. J., Ben Mohamed A., Nassor, A., Thorncroft, C., 2004. Seasonal-to-decadal predictability of West Africa climate. CLIVAR Exchanges 9(3): 14, 19–20.

Wang, Y., Leung, L.R., McGREGOR, J.L., Lee, D.K., Wang, W.C., Ding, Y. and Kimura, F., 2004. Regional climate modeling: progress, challenges, and prospects. *気象集誌*.

2 , *82*(6), pp.1599-1628.

Wang, M., Zhang, X. and Yan, X., 2013a. Modeling the climatic effects of urbanization in the Beijing–Tianjin–Hebei metropolitan area. *Theoretical and Applied*

Climatology, *113*(3-4), pp.377-385.

Wang, G., Yu, M., Pal, J.S., Mei, R., Bonan, G.B., Levis, S. and Thornton, P.E., 2016. On the development of a coupled regional climate–vegetation model RCM–CLM–CN–DV and its validation in Tropical Africa. *Climate Dynamics*, *46*(1-2), pp.515-539.

Wang, M., Yan, X., Liu, J. and Zhang, X., 2013b. The contribution of urbanization to recent extreme heat events and a potential mitigation strategy in the Beijing–Tianjin–Hebei metropolitan area. *Theoretical and Applied Climatology*, *114*(3-4), pp.407-416.

Woldemichael, A.T., Hossain, F., Pielke, R. and Beltrán-Przekurat, A., 2012. Understanding the impact of dam-triggered land use/land cover change on the modification of extreme precipitation. *Water Resources Research*, *48*(9).

World Bank, 2011. Africa Development Indicators, Washington DC: The World Bank

WMO. 2007. The role of climatological normals in a changing climate. WCDMP-No. 61, WMO-TD No. 1377, World Meteo- rological Organization, Geneva, Switzerland. http://www.wmo. int/datastat/documents/WCDMPNo61_1.pdf (accessed 2nd December 2015).

Xue, Y. and Shukla, J., 1993. The influence of land surface properties on Sahel climate. Part 1: desertification. *Journal of climate*, *6*(12), pp.2232-2245.

Xue, Y. and Shukla, J., 1996. The influence of land surface properties on Sahel climate. Part II. Afforestation. *Journal of Climate*, *9*(12), pp.3260-3275.

Xue, Y., 1997. Biosphere feedback on regional climate in tropical North Africa. *Quarterly Journal of the Royal Meteorological Society*, *123*(542), pp.1483-1515.

Yu, M., Wang, G. and Pal, J.S., 2015. Effects of vegetation feedback on future climate

change over West Africa. *Climate Dynamics*, pp.1-20.

Zeng, X., Zhao, M. and Dickinson, R.E., 1998. Intercomparison of bulk aerodynamic algorithms for the computation of sea surface fluxes using TOGA COARE and TAO data. *Journal of Climate*, *11*(10), pp.2628-2644.

Zeng, X., Zeng, X. and Barlage, M., 2008. Growing temperate shrubs over arid and semiarid regions in the Community Land Model–Dynamic Global Vegetation Model. *Global Biogeochemical Cycles*, *22*(3).

Zomer RJ, Trabucco A, Bossio DA, Vercot LV. 2008. Climate change mitigation: a spatial analysis of global land suitability for clean development mechanism afforestation and reforestation. Agriculture, Ecosystems and Environment 126(1–2): 67–80.

Zomer RJ, Trabucco A, Coe R, Place F. 2009. Trees on farm: analysis of global extent and geographical patterns of agroforestry. ICRAF Working Paper. Nairobi: World Agroforestry Centre (ICRAF).

POLICY BRIEF

SIMULATING THE IMPACT OF AGRI-SILVICULTURE ON THE FUTURE CLIMATE OF WEST AFRICA

Authors: Olusegun Christiana Funmilola, Oguntunde P.G., Gbobaniyi, E.O

Email: chrystali2002@gmail.com

Key Fact

Agri-silviculture practice is the deliberate incorporation of trees on agricultural lands and could be used to mitigate against the impacts of climate change, by enhancing food security and reducing deforestation associated with agricultural expansion.

Key Messages

- Agri-silviculture practice must be adopted as a land-based strategy to combat food insecurity, deforestation due to agricultural expansion and ameliorate the impacts of climate change in West Africa.
- Government at the local, national and regional level should support agri-silviculture practices by providing payment for environmental services (PES) as an incentive to farmers who retain 10 – 30% tree cover on their farmland in order to ensure diversified sources of income to farmers participating in climate-smart agricultural practices.

INTRODUCTION

Approximately ten percent of the total forest area in Africa was reported to have been converted to other uses such as agricultural purpose, wood fuel, building and construction between 1990 and 2010 (FAO, 2012). For instance, the rate of deforestation in Nigeria increased from 2.7 % in 1990 - 2000 to about 3.3 % in 2000 - 2005, with less than 12.2 % of forested land in the country left (FAO, 2009). Similarly, Ghana loses an average of 115, 000 hectares of forest annually, which correspond to 2.0 % of the country's land. The estimated rates of deforestation in Niger is 3.7 % annually as at the year 2000 while Burkina Faso has a lower deforestation rate of 0.2 %. Generally across West Africa, annual deforestation rate is estimated to be 1.17 % of its total land annually with about 12 million hectares of tropical forest in the last fifteen years (FAO, 2009). The estimates of deforestation rates for the period 2005-2010 in Togo, Nigeria, Ghana, Liberia, Benin, Guinea, Guinea Bissau, Liberia, Sierra Leone and Cameroon are 5.75 %, 4 %, 2.19 %, 0.68 %, 1.06 %, 0.54%, 0.49 %, 0.68 %, 0.70 % and 1.07 % respectively (FAO, 2010).

Although Africa continues to have the highest net loss of forest, the net emissions from African forest are reported to have decreased over the period 1990-2015 from an average of 3.9 to an average of 2.9 Gt of CO2 per year (FAO, 2010). This may be attributed partly to the large-scale planting of trees which increases substantially by about 5 million hectares per year during the period 2005-2010 (FAO, 2010). However, forestry projects executed in semi-arid regions like the Savanna often resulted in higher transpiration than the available precipitation. This causes the unsustainable use of groundwater and increased salinity. Hence, re-vegetation of West Africa landscape using plants that can adapt and mitigate against future climate disturbances in the region is highly important. Therefore, we hypothesized that agri-silviculture has the poten-

tial to reduce the vulnerability of West Africa future climate to actual or expected climate change impacts while also acting as a carbon sink. Hence, the need to investigate the impact of agri-silviculture on the future climate of West Africa. To address this question, a study was conducted which projects the future climate of West Africa with and without agri-silviculture. This brief contains two key messages options for policy action that emerged from the results of the study conducted.

TWO KEY MESSAGES

1. Agri-silviculture practice must be adopted as a land-based strategy to combat food insecurity, deforestation due to agricultural expansion and ameliorate the impacts of climate change in West Africa.

The interaction between water resources and agricultural practices is expected to become increasingly important as the climate changes. The increasing rates of deforestation and land degradation in West Africa have contributed immensely to increase in atmospheric concentration of greenhouse gases and food insecurity in the region. The need to address the challenge of food insecurity as well boost the economic situation of the region necessitate conversion of forests to agricultural lands for large-scale farming or for a developmental purpose such as urbanization. However, a combination of woody perennials (e.g. trees) and herbaceous plants (e.g. crops) on the same piece of land arranged in a spatial mixture or temporal sequence, a practice specifically referred to as agri-silviculture, is increasingly becoming more popular in the semi-arid and sub-humid region of West Africa.

Agri-silviculture has the potential to act as an adaptation and mitigation option to the impacts of climate change by drastically ameliorating some of the environmental problems introduced by deforestation and forest degradation. The incorporation of trees on agricultural land through agri-silviculture approach has the potential to enhance food security and combat the im-

pacts of climate change in West Africa. This is because trees on agricultural land will provide resilience to climate variability and mitigate against the impacts of climate change. The results obtained from agri-silviculture (30% tree cover and 70% crops) simulation along West Africa coastal zones carried out as part of this study suggested future cooling up to about 0.8 °C in all seasons in northern parts of Niger and Chad while summer precipitation over Liberia and Gambia is enhanced by 0.5 mm/day. Similarly, with fixed percentage cover of a broadleaf deciduous tree, C4 grass and C3 grass in the proportion of 30%, 60% and 10% respectively along West Africa Guinea Savanna zone, cooling up to about 2 °C is induced over most countries along the agri-silviculture zone in all seasons. The resulting cooling translates to more precipitation only over Ghana in summer, while the projected drying over Liberia and Sierra Leone during the monsoon (June -August) and post-monsoon period (September - October) was intensified.

2. Government at the local, national and regional level should support agri-silviculture practices by providing payment for environmental services (PES) which will serve as an incentive to farmers who retain 10 – 30% tree cover on their farmland to ensure diversified sources of income to farmers participating in climate-smart agricultural practices.

The government should provide instantaneous payment for environmental services to farmers who retain at least 10% tree cover on the farmland to encourage the integration of trees on farmlands. The payment will be for labor and cost incurred during planting and growth of the trees on a long-term scale. This is necessary to facilitate increased percentage cover of trees on agricultural land towards an improved future climate for West Africa. Similarly, all farmers in each agro-ecological zone should be trained on the benefits of trees on farms as well as the

appropriate management technique required for optimum crop yield under agri-silviculture practice.

ACKNOWLEDGEMENT

This is work was supported by the German Ministry of Education and Research (BMBF) through the West African Science Service Centre on Climate Change and Adapted Land Use (WASCAL).

REFERENCES

FAO, 2009. World's Forests 2007: Food and Agriculture Organization of the United Nations Rome, 2009. (http://www.fao.org/docrep/011/i0350e/i0350e00.htm)

FAO, 2010. Global forest resources assessment 2010 country report: Venezuela (available at http: //www.fao. org/forestry/fra/67090/en/).

FAO, 2012. State of the World's Forests: Food and Agriculture Organization of the United Nations, 2012.http://www.fao.org/docrep/016/i3010e/i3010e.pdf